Identification of ADORA1-PDE10A Complex Formation and Its Bidirectional Regulation of Intracellular Cyclic AMP Levels as a Novel Therapeutic Target for Treating Pulmonary Hypertension

MAX-PLANCK-GESELLSCHAFT

Inaugural Dissertation submitted to the

Faculty of Medicine in partial fulfillment

of the requirements for the degree of

Doctor of Human Biology in the Faculty

of Medicine of the Justus Liebig

University of Giessen

by

CHANIL VALASARAJAN

From Tellichery, Kerala, India

Gießen, 2020

From the Department of Internal Medicine

Director/Chairman: Prof. Dr. med. Werner Seeger
Universitätsklinikum Gießen und Marburg
Max Planck Institute for Heart and Lung Research

supervised by

Prof. Dr. Soni Savai Pullamsetti
Fachbereich Medizin der Justus-Liebig-Universität, Aulweg
130, 35392 Giessen, Germany

Gutachter 1: **Prof. Dr. Soni Savai Pullamsetti**

Gutachter 2: **Prof. Dr. Saverio Bellusci**

Disputation date: 22|09|2021

Dedicated to:

My Parents, Valasarajan and Bindhu...

TABLE OF CONTENTS

LIST OF FIGURES

LIST OF TABLES

List of abbreviations

AC - Adenylyl cyclase

ARs - Adrenergic receptors

AMP- Adenosine mono-phosphate

ADA- Adenosine deaminase

AChE - acetylcholinesterase

ATP - Adenosine triphosphate

ATF - Activating transcription factor

AKAPs - A-kinase anchoring proteins

ADO-Adenosine

ADORA1 - Adenosine receptor A1

ADORA2a - Adenosine receptor A2a

ADORA2b - Adenosine receptor A2b

ADORA3 - Adenosine receptor A3

AKAR - A Kinase activity reporter

APS - Ammonium persulfate

BSA - Bovine serum albumin

cAMP - 3´, 5´-cyclic adenosine monophosphate

cGMP - 3´, 5´-cyclic guanosine monophosphate

CREM - cAMP responsive modulator

CREB - cAMP-response element binding protein

CBP - CREB-binding proteins

CRE - cAMP-response elements

CaM - Calmodulin

CaN - Calcineurin

CNT - Concentrative nucleoside transporters

COPD - Chronic obstructive pulmonary disease

Co-IP - Co-immunoprecipitation

DPBS - Dulbecco's phosphate buffer saline

DAG - Diacylglycerol

DARPP - Dopamine- and cAMP-regulated phosphoprotein

DAPI - 4′,6-Diamidin-2-phenylindol

EPACs - Exchange proteins activated by cAMP

eNOS - Endothelial nitric oxide synthase

EGF - Epidermal growth factor

EPAC - Exchange protein activated by cAMP

ENT - Equilibrative nucleoside transporters

EL - Extracellular loops

ETRA - Endothelial receptor anatagonists

EDTA – Ethylenediaminetetraacetic acid

FCS - Fetal calf serum

FGF - Fibroblast growth factor

GPCRs - G-protein-coupled receptors

GF - Growth factors

HAT - Histone acetyltransferases

HDAC - Histone deacetylases

IL - Intracellular loops

IPAH - Idiopathic PAH

IP3 - Inositol 1,4,5-triphosphate

lncRNA - Long non-coding RNA

LV - Left ventricle

LVEF - Left ventricular ejection fraction

MAPK - Mitogen-activated protein kinase

MEF2 - Myocyte enhancer factor 2

miR - MicroRNAs

MCT - Monocrotaline

NO - Nitric oxide

PH - Pulmonary hypertension

PAH - Pulmonary arterial hypertension

PVOD - Pulmonary veno-occlusive disease

PAECs - Pulmonary artery endothelial cells

PASMCs - Pulmonary artery smooth muscle cells

PAAFs - Pulmonary artery adventitial fibroblast

PAP - Pulmonary arterial pressure

PVR - Pulmonary vascular resistance

PTMs - Post translational modifications

PPHN - Pulmonary hypertension of newborn

PDGF - Platelet derived growth factor

PDGFRs - PDGF receptors

PDE - Phosphodiesterase

PKA - cAMP dependent protein kinase

PLC - Phospholipase C

PKC - Calcium-dependent protein kinases

PGI2 - Prostacyclin

PAB - Pulmonary artery banding

PCLS - Precession cut lung slices

PDE - Phosphodiesterase

PLA - Proximity ligation assay

PVDF - Polyvinylidene fluoride

RV - Right ventricle

RVF - Right ventricular failure

Rim2 - Rab3-interacting molecule

RT-qPCR - Real time Quantitative Polymerase chain reaction

SD – Sprague Dawley

SOD - Superoxide dismutase

sGC - Soluble guanylyl cyclase

SDS-PAGE - SDS polyacrylamide gel electrophoresis

SEM - Standard Error of Mean

SmGM - Smooth muscle cell growth medium

TAC - Transverse aortic constriction

TF - Transcription factors

TD - Transmembrane domains

TEMED - N, N, N´, N´-Tetramethyl-1, 2-diaminomethane

VSMC - Vascular smooth muscle cells

VEGFR2 - Vascular endothelial growth factor receptor 2

VEGF - Vascular endothelial growth factor

WKY rats - Wistar Kyoto rats

1   INTRODUCTION

1.1   Pulmonary Circulation

The lung vasculature is comprised of both bronchial and pulmonary circulation. Being an integral part of systemic circulation, bronchial circulation is mainly involved in meeting the nutrient and oxygen demand of the lungs. In contrast, pulmonary circulation transports the deoxygenated blood from the heart and oxygenates it before dispersing it back into systemic circulation [1]. The pulmonary circulation can be divided into three anatomic compartments: the arterial tree, the venous tree, and the capillary bed. To facilitate the flow of blood in huge volumes, pulmonary circulation maintains a low pressure (15mmHg) in comparison to systemic circulation and low resistance by forming many capillaries running in parallel [2]. Furthermore, it ensures efficient gaseous exchange by providing a large surface area by forming a capillary network and a small diffusion distance through the thin capillary walls (0.3µm) [2, 3]. To perform these complex functions, the pulmonary vasculature requires a defined cellular composition. As such, the pulmonary artery is comprised of three defined layers: the intimal layer comprising endothelial cells, the medial layer comprising mainly smooth muscle cells, and the adventitial layer comprising fibroblast [4] (Figure 1.1). Apart from these cellular components, the vasculature is made up of various extracellular matrix components like collagen, elastin, fibronectin, and proteoglycans, which are required to maintain elasticity, tensile strength, and cell migration [5].
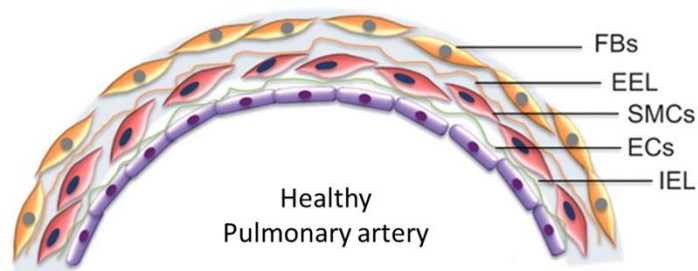
Figure 1.1. Pulmonary artery cellular arrangement (modified from ref [6]). FBs- fibroblasts, SMCs- smooth muscle cells, ECs- endothelial cells, EEL- external elastic lamina, IEL- internal elastic lamina.

A complex interplay between various dynamic processes mediates pulmonary vasculature's physiological response to various respiratory and metabolic demands. An unbalance in these events leads to the induction of pathophysiological conditions such as Pulmonary artery atresia, pulmonary artery aneurysm, and pulmonary hypertension [7]. This study focuses on one such disorder- pulmonary hypertension.

1.2   Pulmonary Hypertension

Pulmonary hypertension (PH) is a progressive and multifactorial disease of the pulmonary vasculature. Recently, the 6th World Symposium on Pulmonary Hypertension (WSPH) task force has recommended defining all forms of pre-capillary PH as the presence of mean pulmonary artery pressure (mPAP) >20mmHg, pulmonary capillary wedge pressure (PAWP)≤ 15, and pulmonary vascular resistance (PVR) ≥3 Wood units. PH groups are classified based on their similar clinical presentation, pathophysiological mechanism, hemodynamic characteristics, and therapeutic management (Table 1.1). PH consists of five major groups (G), G1: pulmonary arterial hypertension (PAH); G2: PH due to left heart disease; G3: PH due to lung disease and/or hypoxia; G4: PH due to pulmonary artery obstructions and G5: PH with unclear and/or multifactorial mechanisms [8].

Table 1.1: Clinical Classification of Pulmonary Hypertension [8]

1.   Pulmonary Arterial Hypertension (PAH)
1.1 Idiopathic PAH (IPAH)
1.2 Heritable PAH
1.3 Drug and toxin-induced PAH
1.4 PAH associated with:
1.4.1   Connective tissue disease
1.4.2   HIV infection
1.4.3   Portal hypertension
1.4.4   Congenital heart disease
1.4.5   Schistosomiasis
1.5 PAH long term responders to calcium channel blockers
1.6 PAH with overt features of venous/capillaries (PVOD/PCH) involvement
1.7 Persistent PH of the newborn syndrome
2.   PH due to left heart disease
2.1 PH due to heart failure with preserved LVEF
2.2 PH due to heart failure with reduced LVEF
2.3 Valvular heart disease

2.4 Congenital/acquired cardiovascular conditions leading to post-capillary PH
3. **PH due to lung diseases and/or hypoxia**
3.1 Obstructive lung disease
3.2 Restrictive lung disease
3.3 Other lung disease with mixed restrictive/obstructive pattern
3.4 Hypoxia without lung disease
3.5 Developmental lung disorders
4. **PH due to pulmonary artery obstructions**
4.1 Chronic thromboembolic PH
4.2 Other pulmonary artery obstructions
5. **PH with unclear and/or multifactorial mechanism**
5.1 Hematological disorders
5.2 Systemic and metabolic disorders
5.3 Others
5.4 Complex congenital heart disease

1.2.1 Pathophysiology of Pulmonary Hypertension

Irrespective of clinical classifications, every group of PH exhibits pulmonary vascular constriction, pathological remodeling of vessels, and right ventricular dilation.

1.2.1.1 Pulmonary vascular remodeling

The pathological remodeling of pulmonary vessels is mainly characterized by the muscularization of peripheral arteries, medial hypertrophy of muscular arteries, neointima formation, and plexiform lesion formation [9] (Figure 1.2). The events observed in the muscularization of peripheral arteries are usually preceded by the development of dysfunctional pulmonary artery endothelial cells (PAECs) and the differentiation of pericytes into smooth muscle cells (SMCs). Previous studies have demonstrated that PAECs isolated from IPAH patients have increased secretion of factors like serotonin and FGF2 which promote SMC proliferation [10, 11], as well as diminished production of factors like apelin which inhibits SMC proliferation [12]. The medial hypertrophy of muscular arteries and neo-intimal formation can be majorly driven by the hyperproliferation and migration of pulmonary artery smooth muscle cells (PASMCs) and pulmonary artery adventitial fibroblast

(PAAFs) [13]. Furthermore, in the later stage of the disease, aberrant vascular channels develop due to the monoclonal expansion of apoptosis-resistant endothelial cells leading to plexiform lesion formation [14]. Apart from the resident vascular cells, many inflammatory cells like macrophages, B cells, and T cells play critical roles in vascular remodeling, which is noteworthy [15].
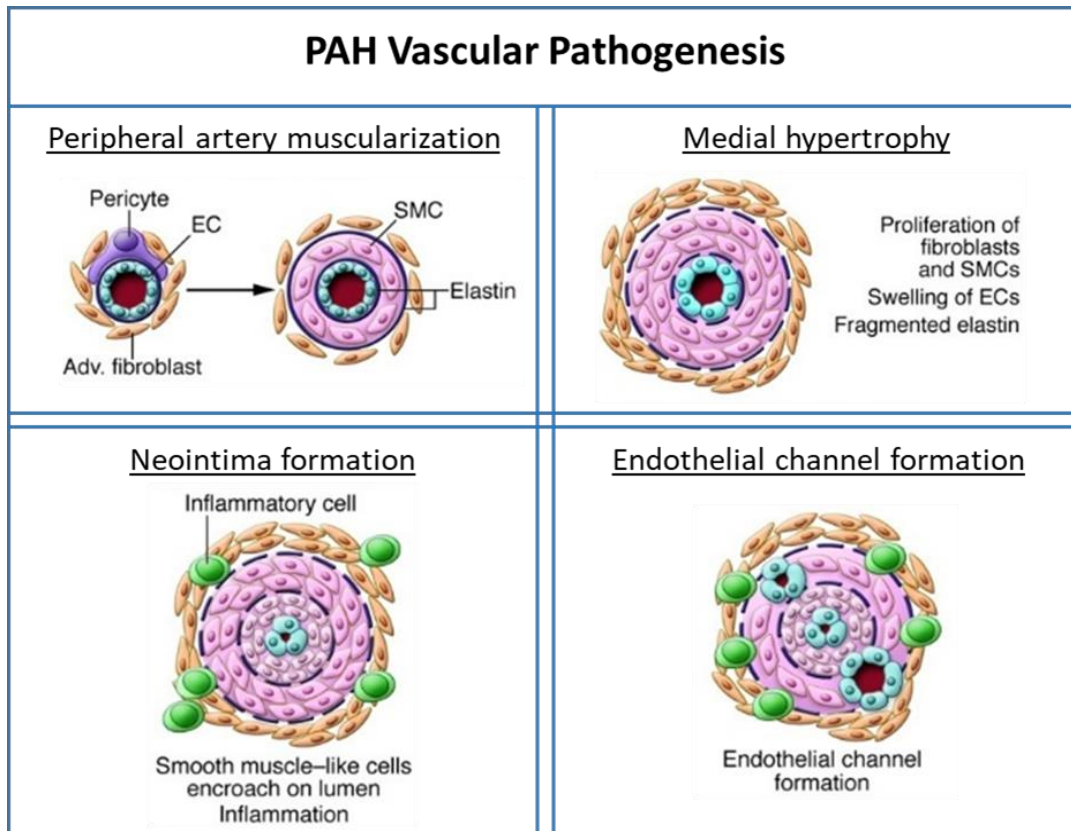
Figure 1.2. Pathological events in the remodeling of the vasculature (Modified from ref [9]): EC-Endothelial cells, SMC-Smooth Muscle Cells, Adv. - Adventitial.

1.2.1.2 Pulmonary vasoconstriction

Under physiological conditions, vasoconstriction is a controlled response to decreased alveolar oxygen levels and low oxygen partial pressure in pulmonary arterioles [16]. The increased PVR and mPAP that are observed in PH can also be partially caused by excessive vasoconstriction of the pulmonary vessels [17]. Endothelial cells play a major role in maintaining vascular tone under physiological conditions [18]. The vasoconstriction observed in high altitude-PH patients is an adaptive mechanism, as a result of hypoxia [19]. An increase in shear stress or endothelial dysfunction leads to excessive vasoconstriction due to an imbalance in the vasodilators and

vasoconstrictors composition in the vascular system (Figure 1.3). Previous studies have revealed that a reduction in the vasodilators like prostacyclin and an increase in the vasoconstrictors like thromboxane [20].
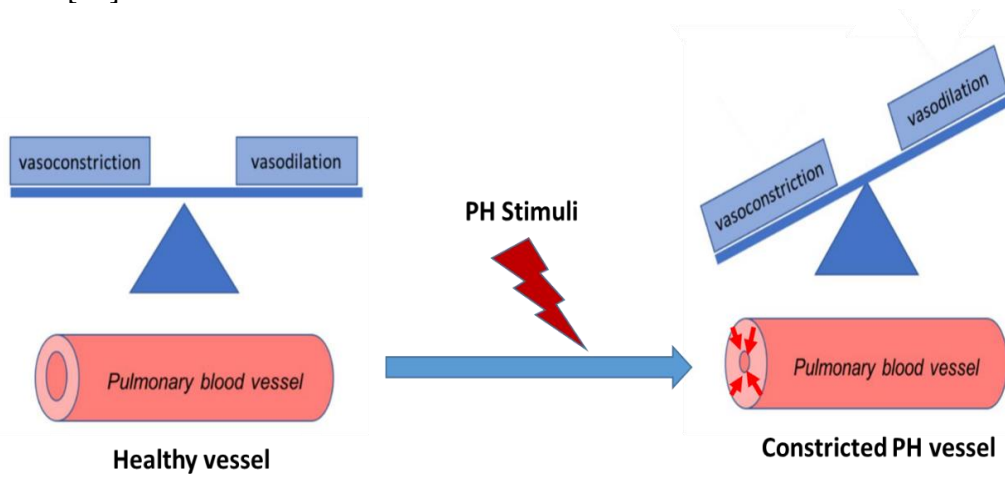
Figure 1.3. Vasoconstriction in pulmonary hypertension (Modified from ref [21])

1.2.1.3   Right ventricular failure

Patient survival in PH greatly depends on the response of the right ventricle (RV) to the increased afterload [22, 23]. Under physiological conditions, the RV maintains a crescentic geometry in comparison to the cone-like left ventricle (LV), and the RV is thin-walled in comparison to the thicker LV wall [24] (Figure 1.4). In PH, chronic pressure overload leads to RV hypertrophy and if persistent leads to RV failure (RVF). Right ventricle failure (RVF) is clinically defined as the inability of the RV to adequately perfuse the lung circulation to maintain LV filling [25]. Assessment of the RV function is based on both invasive like right heart catheterization and noninvasive methods like magnetic resonance and echocardiographic imaging [24]. At the cellular and molecular level, RVF results from increased cell death, fibrosis, and decreased angiogenesis due to inflammation, oxidative stress, metabolic dysfunction, and impaired calcium handling [26].
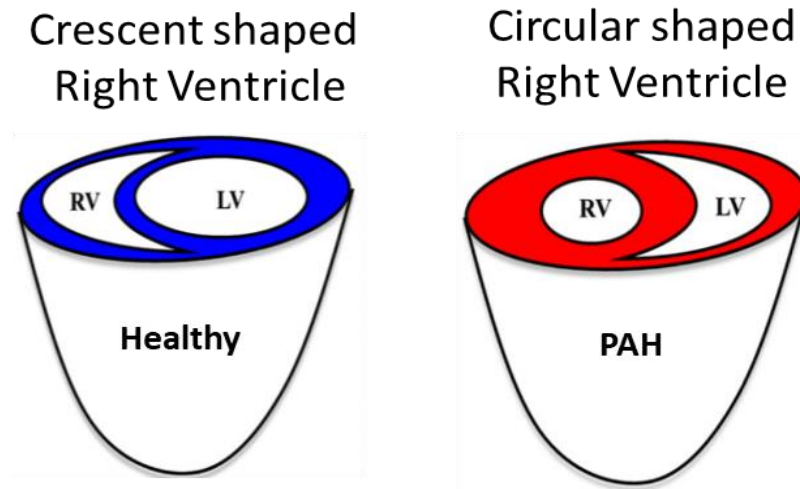
Figure 1.4. Right ventricular failure in pulmonary hypertension (modified from ref [27]): RV-right ventricle, LV- left ventricle, PAH- Pulmonary artery hypertension.

1.2.2   Molecular Modulators of PAH pathogenesis

The phenotypical alterations observed in PAH are mediated by various dysregulated signaling pathway modulators like transcription factors, growth factors, epigenetic modulators, metabolic regulators, and non-coding RNAs. Understanding these altered signaling pathways is important for exploring therapeutic options for treating PH.

1.2.2.1   Transcription factors

Transcription factors (TF) are DNA binding proteins that are capable of controlling the transcription process. Transcription factors are categorized as general transcription factors that are involved in basic transcription and regulatory or gene-specific TF which is involved in differential gene expression. Previous studies have demonstrated that TFs play an important role in mediating pathological events in PAH [28]. The TFs induce PH/PAH disease phenotypes includes hypoxia-inducible factor 1A (HIF1A), hypoxia-inducible factor 2A (HIF2A), single transducer and activator of transcription 3, nuclear factor-kappa B (NF-KB), twist basic helix-loop-helix transcription factor 1(TWIST1), GATA binding protein 6 (GATA-6) and octamer-binding transcription factor 4 (OCT4) [29-36]. The TFs that negatively regulate disease pathogenesis includes forkhead box protein 1 (FOXO1), tumor protein 53 (TP53), myocyte enhancer factor 2 (MEF2), kruppel like factor 4 (KLF4) and peroxisome proliferator activated receptor gamma 1 (PPARG1) [37-41].

Among these TFs, FOXO1 was discovered as one of the central players in regulating the hyperproliferative and apoptosis-resistant phenotype of the PASMCs, which is a pathological hallmark of PAH. FOXO1 inactivation due to hyperphosphorylation was observed exclusively in PASMCs in both, patients with PAH and experimental PAH models. Stimulation with growth factors and inflammatory cytokine led to the phosphorylation of FOXO1 at ser256 and Thr24 and exclusion from the nucleus, which suggests that FOXO1 acts as a central downstream molecule of pro-proliferative and pro-inflammatory PH stimuli. Importantly, *in vitro* and *in vivo* loss of FOXO1 specifically in SMCs was sufficient to induce PH. These results suggest that FOXO1 as a central player in PAH pathogenesis [38]. Thus, TFs-based therapeutic approaches can be an effective means for treating PAH.

1.2.2.2 Epigenetic modulators

Epigenetics is defined by the study of chemical modifications of DNA and its associated chromatin proteins without direct modifications of the sequence [42]. The epigenetic modifications can be *de novo* or may be inherited, it alters the chromatin organization and dictates the cell phenotype [43]. The known epigenetic modifications are DNA methylation, ATP-dependent chromatin remodeling, histone post-translational modifications, the replacement of canonical histones with variants, and altered 3D nuclear architecture [44, 45].

Recent studies have shown that aberrant DNA methylation in PH. Hypermethylation of the CpG Island in the promoter region of superoxide dismutase (SOD) 2 gene was observed in the lungs and PASMCs isolated from the fawn hooded rats, a spontaneous PH model, leading to the epigenetic silencing of the SOD2 gene. This silencing leads to an activation of HIF1 and the hyperproliferative phenotype [46]. Post-translational modifications (PTMs) of histones are also known to play important roles in PH pathogenesis, the most commonly known PTMs are acetylation and methylation. These PTMs regulate transcriptional regulation, chromatin condensation, and genetic imprinting [47]. The histone acetylation is tightly regulated by histone acetyltransferases (HAT) and histone deacetylases (HDAC). Increased acetylation of H3 and H4 at the promoter region of endothelial nitric oxide synthase (eNOS) has been observed in PAECs isolated from persistent pulmonary hypertension of newborn (PPHN) rat model. This study shows histone acetylation of eNOS plays an important role in the pathogenesis of PPHN [48]. It has also been observed that HDAC1, HDAC2, and HDAC3 were increased in the distal pulmonary arteries of chronically hypoxic hypertensive calves [49]. It has been observed that the activity of TF myocyte enhancer

factor 2(MEF2) was restored in PAECs derived from PAH patients upon inhibition of HDAC4 and HDAC5, leading to decreased cell migration and proliferation [40]. Several ongoing studies are currently exploring the therapeutic viability of targeting epigenetic modifiers in PH.

1.2.2.3   Growth factors

Growth factors (GF) are proteins that modulate cell survival, differentiation, proliferation, tissue repair, and inflammation. Several GFs like platelet-derived growth factor (PDGF), epidermal growth factor (EGF), and vascular endothelial growth factor (VEGF) have been shown to induce hyper-proliferation, migration, and apoptosis-resistance in pulmonary artery vascular cells (PAECs, PASMCs, PAAFs), which are phenotypical hallmarks of PAH pathology [50-53]. It has been observed that VEGF was highly expressed in PAECs found in the PAH patient's plexiform lesions [54]. Furthermore, in PAH lesions, EGF was observed to be colocalized with an extracellular matrix component tenascin C that is required for EGF dependent proliferation and migration of SMCs [55]. An increased expression of PDGF-A, PDGF-B, and PDGF receptors was observed in pulmonary arteries of IPAH patients, and treatment with tyrosine kinase inhibitor has shown beneficial effects in both rat PAH models and clinical trials [51, 56, 57].

1.2.2.4   Non-coding RNAs

Recent studies have shown that non-coding RNAs such as microRNAs (miR) and long noncoding RNA (lncRNA) play a major role in maintaining the physiological balance in several organs. Several miRNAs such as miR-21, miR-214, miR-130/301, and miR-125a were upregulated in pulmonary hypertension [58]. miR-130/301 family has to play an important role in PH by modulating the STAT3-miR-204 signaling in endothelial cells and apelin-miR424/503-FGF2 signaling in SMCs [59, 60]. LncRNAs are non-coding transcripts of more than 200 nucleotide length, they are studied in PH as molecular regulators, circulating biomarkers, and therapeutic targets [61]. LncRNAs such as MALAT1, MYOSLID, and TYKRIL was observed to be upregulated in pulmonary hypertension [62-64]. Several lncRNA such as MANTIS, MEG3, LISPR1, and CASC2 were down-regulated, and lncRNA H19 was found to be upregulated in patients with severe PH [64-68]. My recent work demonstrated that LncRNA TYKRIL regulates the proliferation and migration of both human PASMCs (hPASMCs) and lung pericytes by acting as a p53 decoy and by regulating the expression of PDGFRβ. It has been also shown that targeting

TYKRIL in *ex vivo* precision-cut lung slices derived from IPAH patients, reversed the vascular remodeling, suggesting it as a therapeutic option for the treatment of PH [64].

1.3   Cyclic adenosine 3´, 5´-monophosphate (cAMP) signaling pathway

The cAMP is a secondary messenger that aids in mediating cellular responses to various extracellular stimuli. Thus, it is important to tightly regulate cAMP levels to maintain the physiological state of cells [69].

1.3.1   cAMP production, regulation, and downstream signaling pathway

Intracellular cAMP levels are tightly regulated by two main enzymes, the rate of production is regulated by adenylyl cyclase (AC) and metabolism is regulated by phosphodiesterase (PDE) (Figure 1.5). Several isoforms of these enzymes regulate cAMP levels and mediate signaling in a more cell- and stimuli- specific manner [70].

The activation of AC is mostly dictated by downstream events upon the binding of the ligands to G-protein-coupled receptors (GPCRs). G_s- protein-coupled receptors mediate the activation of AC, whereas G_i-coupled receptors inhibit AC activity. The activation of AC results in increased intracellular cAMP levels due to the conversion of adenosine triphosphate (ATP) to cAMP and inorganic phosphate. Once produced the cAMP is degraded into adenosine monophosphate (5'AMP) by various cAMP targeting PDEs [71, 72].
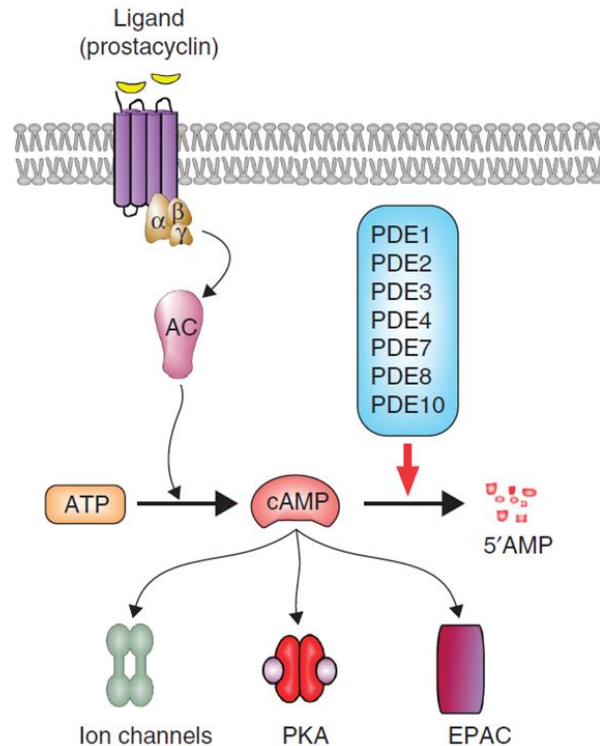
Figure 1.5. cAMP regulation and effectors (modified from ref [73]). AC- adenylyl cyclase, ATP- adenosine triphosphate, cAMP- 3', 5'-cyclic adenosine monophosphate, PDE-phosphodiesteraste, EPAC- exchange protein activated by cAMP, PKA-cAMP dependent protein kinase A.

The main effectors of intracellular cAMP are protein kinase cAMP-dependent protein kinase (PKA), exchange protein activated by cAMP (EPAC), and cyclic nucleotide-gated ion channels. PKA consists of two regulatory subunits (R) and two catalytic subunits (C), the cAMP binds to the R subunit of PKA which causes the dissociation of the C subunit [74]. The C subunit mediates the phosphorylation of various cytosolic and nuclear proteins. PKA is known to modulate various metabolic signaling like phosphorylating glycogen synthase, which leads to inhibition of glycogen synthesis and promotes glycogen breakdown by phosphorylating phosphorylase kinase. PKA is also known to mediate inhibitory effects in lipid synthesis by phosphorylating acetyl CoA carboxylase [75, 76]. PKA is also known to regulate transcription by directly phosphorylating transcription factors like cAMP-responsive modulator (CREM), activating transcription factor 1 (ATF1), and cAMP-response element binding protein (CREB) [76, 77]. The phosphorylation of CREB is crucial for its interaction with its coactivators CREB-binding proteins (CBP) and p300 that subsequently binds to the cAMP-response elements (CRE) found in target genes [78]. cAMP promotes the activation of small GTPases like Rap1 via EPAC1 leading to an increase of integrin

receptors and enhanced cell adhesion. Additionally, cAMP regulates insulin secretion via EPAC2, which was found to interact with Rab3-interacting molecule (Rim2) [79]. Another cAMP effector is the cyclic-nucleotide-gated ion channels, which are mainly non-selective cation channels for transporting calcium, sodium, and potassium which in turn alters the membrane potential of cells [76, 80].

1.3.2   cAMP microdomains and A-kinase anchoring protein complexes

Until recent times, cAMP stimulation and signaling were considered to be more uniform events throughout the cells. Recent studies have demonstrated that cAMP signaling can be confined within certain microdomains close to the site of synthesis, which leads to activation of effectors in close proximity [81]. First indirect proof of existing cAMP/PKA compartmentalization was observed in 1977 by Corbin et al. in the heart lysates [82]. The non-uniform localization of cAMP signaling mediating proteins like GPCRs, ACs, PDEs, PKA, and EPACs implicate the microdomain specific signaling within the cells [83-87]. Several studies have shown that the scaffolding protein A-kinase anchoring proteins (AKAPs) play an important role in mediating compartmentalized cAMP signaling. AKAP forms supercomplexes with several cAMP signaling proteins like PKA, receptors, ACs, PDEs, and phosphatases [88] (Table 1.2). For example, AKAP79 is known to anchor PKA, PKC, calmodulin, and calcineurin to the ion channels, such as L-type calcium channels, gamma-aminobutyric acid (GABA) receptors, glutamate receptors, and Kir 2.1 channel [89-93]. AKAPs also can dictate the localization of the cAMP microdomains, AKAP18α, AKAP18β and AKAP79 were found to be localized mostly in the plasma membrane [94-96], D-AKAP1 in mitochondria [97], AKAP350 in the nucleus [98] and in the cytoskeleton AKAPs, gravin and ezrin is localized [99].

Studies have shown that various AKAP complexes are important in maintaining the physiological functions and in the response to stress in the cardiovascular system. In the vasculature, AKAP79 is involved in the homeostasis of maintaining vascular tone by tight controlling of VSMC contraction and relaxation [100, 101] and, AKAP220 and gravin are involved in maintaining the vascular integrity [102, 103]. In the heart, AKAP Yotiao plays a role in cardiomyocyte repolarization followed by contraction and as a stress response, mAKAPβ and AKAPLbc induce cardiomyocyte hypertrophy [104-106].

Table 1.2. cAMP regulation and effectors [107]

Gene Name	Alternative Name	Cardiovascular Process
AKAP1	AKAP121/ AKAP149/AKAP84	Cardiac stress response
AKAP10	-	Cardiac repolarization
AKAP9	-	Endothelial barrier function
AKAP7	-	Excitation-contraction coupling
AKAP5	AKAP75/AKAP150	Vascular tone; Excitation-contraction coupling; β-AR desensitization/resensitization cycle
AKAP11	-	Endothelial barrier function
AKAP13	Brx-1/Proto-Lbc/ Ht31	Cardiac stress response
AKAP6	AKAP100	Excitation-contraction coupling; Cardiac stress response
AKAP9	GC-NAP	Cardiac repolarization
AKAP12	AKAP250	Endothelial barrier function; β-AR desensitization/resensitization cycle
SPHKAP	-	Cardiac stress response

These studies indicate that AKAP mediated cAMP microdomains play an important role in physiological and pathophysiological conditions. In PH it is observed that cAMP signaling significantly affects the pathogenesis of the disease, and targeting several cAMP modulators to increase intracellular cAMP levels has been proven to have beneficial effects [108, 109].

1.4   Adenosine signaling

Adenosine is a key extracellular signaling molecule that belongs to the purine family and, a building block of the genetic code and energy source adenosine triphosphate (ATP) [110, 111]. Therefore, it is also important to strictly maintain a desired concentration of adenosine under physiological conditions, adenosine is regulated at three levels- formation, degradation, and transport. Adenosine is usually produced by the conversion of ATP to adenosine monophosphate (AMP) by CD39 enzyme, followed by conversion of AMP to adenosine by CD73 [112, 113] (Figure 1.6). Adenosine transportation across the cell membrane by equilibrative nucleoside transporters (ENT) and concentrative nucleoside transporters (CNT) [114]. Adenosine levels can be reduced by adenosine deaminase (ADA) to inosine or phosphorylated into adenosine monophosphate by adenosine kinase [115]. These processes are orchestrated to fine tune the concentration of adenosine and it's signaling under physiological conditions.
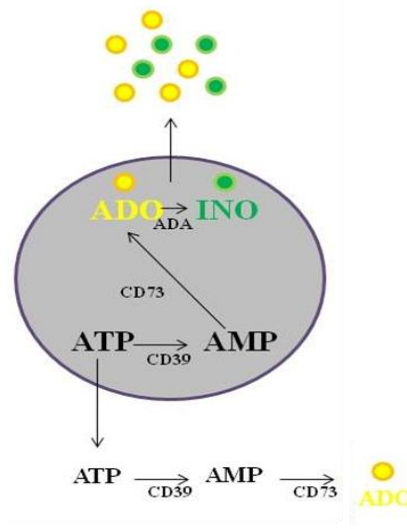
 Figure 1.6. Adenosine production and regulation (Modified from ref [116]). ADO-adenosine, ATP- adenosine tri-phosphate, AMP- adenosine monophosphate, INO-inosine, ADA-adenosine deaminase, CD73- ecto-5′-nucleotidase, CD39- Ectonucleoside triphosphate diphosphohydrolase-1 .

1.4.1   Adenosine receptors

Adenosine signaling is mainly mediated through the activation of four GPCRs, namely adenosine receptor A1 (ADORA1), adenosine receptor A2a (ADORA2a), adenosine receptor A2b (ADORA2b), and adenosine receptor A3 (ADORA3) [117]. The basic structure of these receptors is a seven core transmembrane domain (TD), an extracellular N-terminus, and an intracellular C-terminus that are connected by intracellular loops (IL) and extracellular loops (EL) of varying length [118]. The adenosine receptors are mainly characterized based on their adenosine requirement, adenosine concentration of 10nM-1μM is required for the activation of ADORA1, ADORA2a, and ADORA3, but ADORA2b requires a much higher concentration of adenosine (10μM) which is rarely observed under physiological conditions [119]. The receptors are further classified based on the G-protein coupling and downstream signaling, ADORA1 (lower adenosine requirement) and ADORA3 (higher adenosine requirement) couples with Gi proteins and inhibit the activity of ACs and impair the cAMP production. ADORA2a (lower adenosine requirement) and ADORA2b (higher adenosine requirement) couples with Gs proteins and increase the cAMP levels by inducing the AC activity [120, 121]. Thus, availability of adenosine receptor and adenosine levels can determine the activation of specific signaling pathways.

1.4.1.1   Adenosine receptor A1 (ADORA1)

ADORA1 consists of 326 amino acids, the transmembrane domain (TD) 3, TD7, and EL2 region affects the ligand binding [122, 123]. The main structural difference between ADORA1 and other adenosine receptors are 1) different confirmation of EL2 and 2) an alternative ligand binding pocket due to a bigger extracellular cavity [124]. These structural differences can play a major role in maintaining the ligand affinity of each receptor. ADORA1 is found to be expressed mainly in the brain, heart, lung, vasculature, kidney, and pancreas. In the vasculature, it is mainly present in the SMCs and ECs [125]. In the heart, it is highly expressed in the atria and less expressed in the ventricular myocardium [126]. The differential expression pattern also suggests a tightly regulated signaling system even with the organs, it mainly regulates the AC, phospholipase C beta (PLC- β), mitogen-activated protein kinase (MAPK) signaling, and ion channels (Figure 1.7). The main signaling mediated by ADORA1 is through the binding of Gi-protein and decreasing the intracellular cAMP level by inhibiting the AC activity. A reduction in cAMP leads to reduced CREB phosphorylation, ultimately resulting in reduced CREB mediated transcriptional activity. In

addition to this pathway, ADORA1 binding to the Gq proteins stimulates the phospholipase C (PLC)-β, resulting in increased diacylglycerol (DAG) and inositol 1, 4, 5-triphosphate (IP3). IP3 increases the intracellular calcium concentration and in turn activate the calcium-dependent protein kinases (PKC) [127]. Studies have also shown that activation of ADORA1 modulates the MAPK signaling [128]. Activation of ADORA1 induces the PKC-α pathway causing extracellular-signal regulated kinases (ERK) phosphorylation in the mouse coronary artery smooth muscle cells [129]. Moreover, ADORA1 was shown to contribute to atherosclerosis by inducing HIF-1 accumulation through increased p38 and AKT phosphorylation in the foam cells [130]. These studies show that ADORA1 mediated modulation of MAPK signaling occurs in different organs and under pathological conditions.
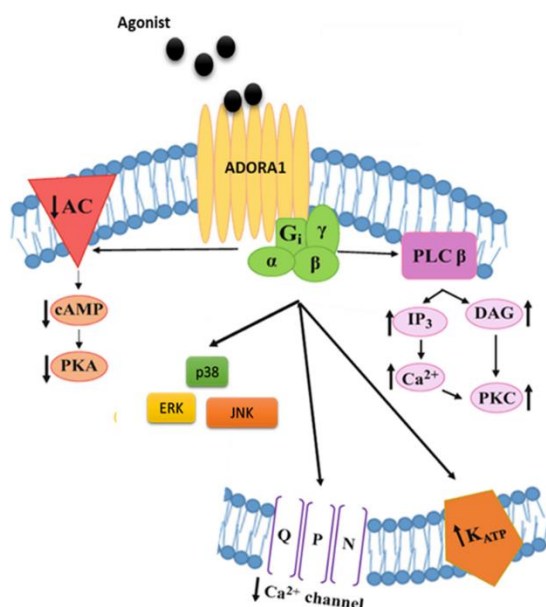
Figure 1.7. ADORA1 signaling pathways (modified from ref [131]). ADORA1- Adenosine receptor A1, AC-adenylyl cyclase, AC- adenylyl cyclase, cAMP- 3', 5'-cyclic adenosine monophosphate, PKA-cAMP dependent protein kinase A, IP3- inositol 1,4,5-triphosphate, DAG- diacylglycerol, PKC- calcium dependent protein kinase, ERK- extracellular signal regulated kinase, JNK- c-Jun N-terminal kinases.

1.4.1.2 Other adenosine receptors

ADORA2a consists of 412 amino acids, and its basic structure consists of 7TM with TM3 and EL2 made of cysteine residue forming disulfide bonds [132]. The main structural difference between the other subtypes is the presence of a long carboxy-terminal domain and an extra short TM8

domain present towards the cytoplasmic surface [132, 133]. The main phenomenon observed in the agonist binding to ADORA2a is the contraction of the agonist binding site due to rearrangements of TM3, TM5, TM6, and TM7 [122]. ADORA2a is present in the lungs, liver, and in both atria, ventricle, and in coronary vessels. Various cell types like lymphocytes, neutrophils, monocytes, macrophages, vascular smooth muscle, and endothelial cells express ADORA2a [134]. ADORA2a majorly signals by binding with Gs protein and stimulating AC activity, which leads to increased cAMP production and PKA phosphorylation. Some of the proteins that are phosphorylated and activated in ADORA2a/cAMP/PKA signaling are CREB, PDEs, and dopamine- and cAMP-regulated phosphoprotein (DARPP-32) [135]. ADORA2a mediated increase in cAMP, decreases the phosphorylation of p38, extracellular signal-regulated kinase (ERK), phosphoinositide 3-kinase (PI3K), hemopoietic cell kinase (HCK), and spleen associated tyrosine kinase (SYK) [136]. In hepatocyte, ADORA2a forms a part of the cAMP-responsive macro-complexes activated by adenosine, the membrane macro-complex consists of ADORA2a/AC6/AKAP79/PKA/PDE3A. These studies signify a spatiotemporal regulation of cAMP signaling within the cell in a receptor specific manner [137].

ADORA2b is made of 328 amino acids, the main regions involved in agonist and antagonist recognition are TM3, TM5, TM6, and TM7 [138, 139]. EL2 of ADORA2b is longer than other adenosine receptors and is crucial for ligand binding. The length of the EL2 of ADORA2b is responsible for its lower affinity of ligands compared to ADORA2a due to limiting the ligand access to the binding sites [140, 141]. It is present mainly in fibroblast, smooth muscle cells, endothelial cells, alveolar epithelial, and myocardial cells [139]. ADORA2b signals via Gs coupling leading to phosphorylation of PKA and recruitment of EPAC stimulated by cAMP. Additionally, coupling to Gq protein triggers PLC activation and modulates the ion channels via βγ subunits [137].

ADORA3 consists of 318 amino acids, in comparison to other adenosine receptors the desensitization process is very quick due to the lack of Ser and Thr residues at the C-terminus and presence of cys amino acids in the C-terminus tail. The desensitization and internalization process is important for βarr2 recruitment [142]. ADORA3 is widely expressed mostly in the coronary artery, carotid artery, and heart [117, 143]. ADORA3 mainly signals by inhibiting AC activity via Gi protein coupling, additionally, Gq coupling triggers PLC stimulation and increase intracellular

calcium [144, 145]. ADORA3 also regulates MAPK signaling by inducing ERK1/2 and in turn inducing cell proliferation [128].

1.4.2   Adenosine signaling in pulmonary hypertension

Adenosine is a well-known pulmonary vasodilator, it has been recommended as an alternative strategy in pulmonary vasoreactivity testing for identifying patients suitable for calcium channel blocker treatment [22, 146]. Studies has demonstrated that circulating adenosine levels are low in PAH patients, which is mostly due to the increased adenosine deaminase activity [147]. Studies have also shown that adenosine imparts beneficial effects in the heart [148]. One of the most limiting factors of using adenosine as a therapeutic option in PAH is its extremely short half-life and adverse non-selective activation of adenosine receptors, thus modulating specific adenosine receptors can have beneficial effects in PAH [149]. Previous studies have shown that under the physiological conditions the differential expression of adenosine receptors in various cell types in the lungs, imparting signaling in a cell specific manner. For example, in bronchial SMCs, ADORA2b is highly expressed, whereas ADORA1 and ADORA3 are hardly expressed in these cells [150]. Immunohistochemical analysis has revealed that ADORA2a and ADORA3 are only expressed in bronchial and alveolar epithelial cells, SMCs, and ECs [151]. Studies have shown that ADORA2a knock out mice exhibited PAH characteristics in terms of hemodynamics, histological and ultrastructural changes [152]. The spontaneous PAH development in knockout mice suggests an important role of ADORA2a in the pathogenesis of PAH. Salidroside has shown beneficial effects in chronic hypoxia induced PH and reversing pulmonary artery remodeling by increasing the expression of ADORA2a and enhancing ADORA2a mediated mitochondrial dependent apoptosis [153]. In the PH associated with lung fibrosis and chronic obstructive pulmonary disease (COPD), ADORA2b has been shown to play an important role in adenosine driven remodeling responses [154]. Attenuation of ADORA2b has shown to reduce the vascular remodeling in mouse models of PH related to lung fibrosis. The mechanism involved in the ADORA2b mediated vascular remodeling is the release of endothelin-1 and interleukin-6 from PAECs and PASMCs, respectively upon ADORA2b activation [155]. In COPD-associated PH it was observed that ADORA2b expression is upregulated and correlated to pulmonary artery pressures [156]. ADORA3 was shown to increase proliferation coronary SMCs via activation of PLC and MAPK, with the induction of early growth response gene 2 (EGR2) and 3 (EGR3) [157]. However, among the adenosine receptors, ADORA1 and ADORA3 are seldom studied in terms of PH.

1.5   Phosphodiesterase (PDE)

The intracellular secondary messenger molecules, cAMP and cGMP are tightly regulated by differentially distributed phosphodiesterase (PDEs) to induce localized and specific signaling pathways. PDEs, convert the 3´, 5´-cAMP/cGMP to 5´-AMP/GMP by hydrolysis of the 3´ cyclic phosphate bonds of adenosine/guanosine respectively (Figure 1.8).
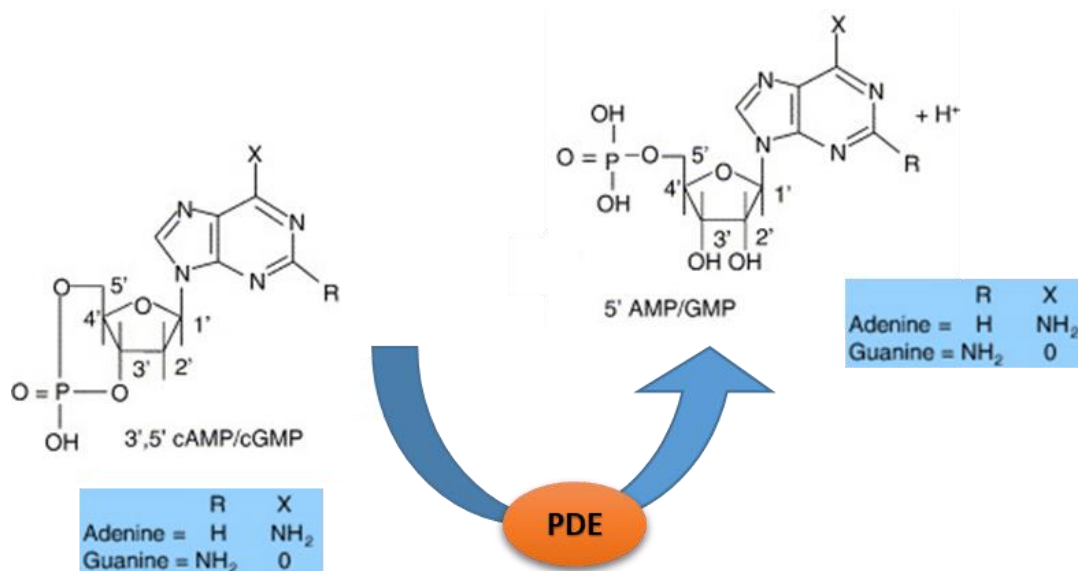
Figure 1.8. PDE hydrolysis of cyclic nucleotides (Modified from ref [158]). cAMP- 3', 5'-cyclic adenosine monophosphate, PDE- phosphodiesterase, cGMP- 3', 5'-cyclic guanosine monophosphate, AMP- adenosine monophosphate.

PDEs are modular proteins made up of a conserved core catalytic domain separating the divergent N-terminus regulatory region and targeting domains from the hydrophilic C-terminus [159, 160] (Figure 1.9).

Figure 1.9. Common structural pattern of PDEs (Modified from ref [161])

1.5.1   PDE Classification

PDEs superfamily consists of 11 gene families (PDE1 through PDE11), each containing 1-4 genes, and most of them forming a series of isoforms. PDEs are classified into 11 groups based on their differential regulatory and targeting domains in the N-terminal [162] (Figure 1.10).
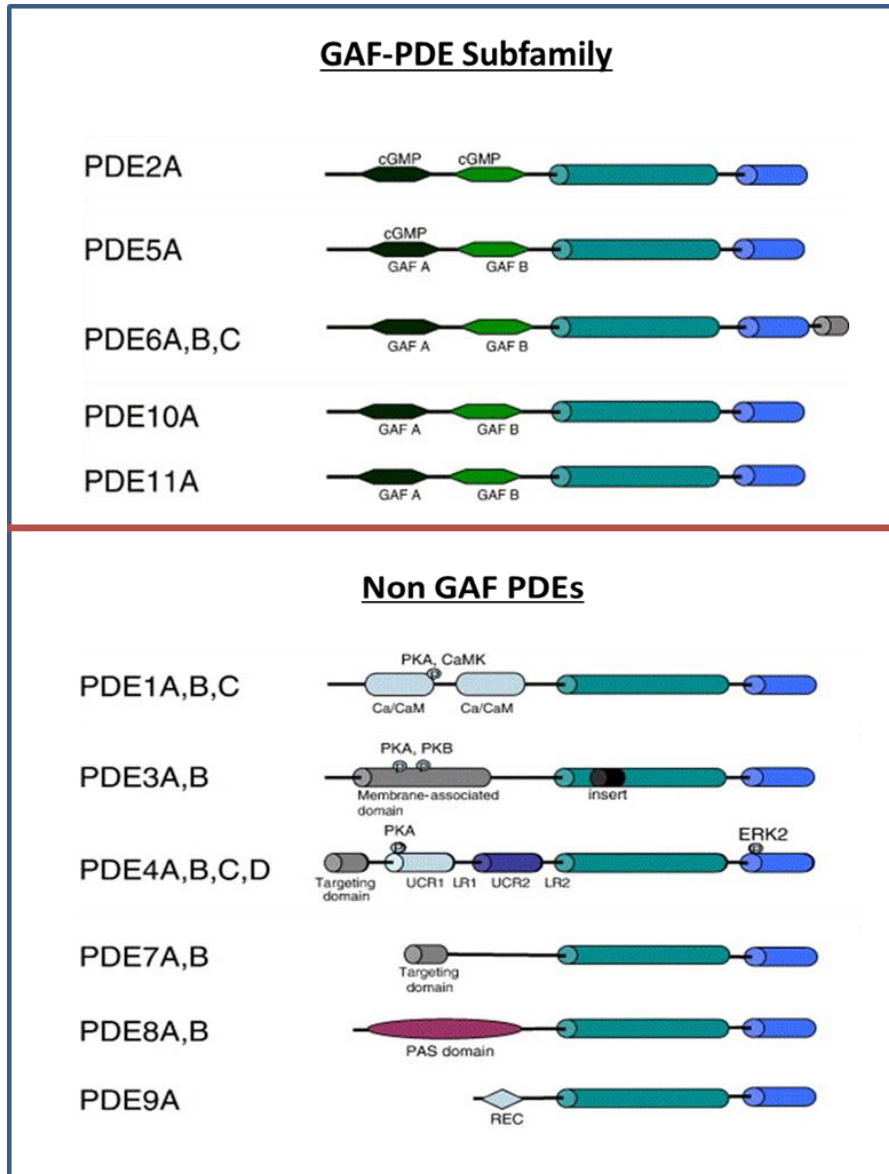
Figure 1.10. Structural classification of PDEs (Modified from ref [158]). GAF- cGMP-specific phosphodiesterases, adenylyl cyclases and FhlA, PAS- per-arnt-sim, REC- cheY-homologous receiver, cAMP- 3', 5'-cyclic adenosine monophosphate, PDE- phosphodiesterase, cGMP- 3', 5'-cyclic guanosine monophosphate, PKA-cAMP dependent protein kinase A, PKB- protein kinase B.

PDE1 consists of calmodulin binding sites in the regulatory domain and the presence of GAF domains for PDE2, PDE5, PDE6, PDE10, and PDE11 [163, 164] designated as GAF-PDE subfamily. The main function of GAF domains are cGMP binding mediated regulation and dimerization of GAF-PDEs and some of the GAF domains are known to bind cAMP. Other PDEs such as PDE1, PDE3, PDE4, PDE7, PDE8, and PDE9 are categorized as non-GAF PDE subfamily. PDE3 contains a transmembrane domain and PDE4 consists of UCRs (upstream conserved regions). The PDE8 consists of a response regulator receiver (REC) and a per-arnt-sim (PAS) domain. The PDE7 and PDE9 consist of no specific domains additionally to the catalytic domain [165]. PDEs are classified into three groups based on their substrate specificity are cAMP targeting PDEs (PDE7, PDE4 and PDE8), cGMP targeting PDEs (PDE9, PDE5 and PDE6) and dual cAMP/cGMP targeting PDEs (PDE1, PDE2, PDE10, PDE 11 and PDE3) (Figure 1.11).
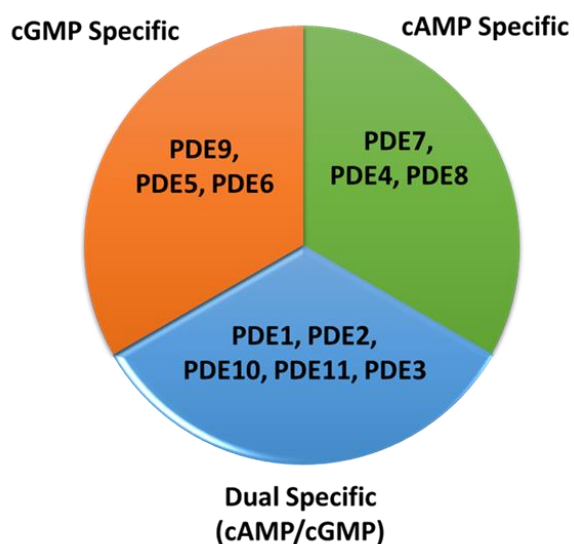
Figure 1.11. Substrate specific classification of PDEs (Modified from ref [166]). cAMP- 3', 5'-cyclic adenosine monophosphate, PDE- phosphodiesterase, cGMP- 3', 5'-cyclic guanosine monophosphate.

1.5.2   Phosphodiesterase 10 (PDE 10) Family

The PDE10 consists of only one gene in this family, PDE10A and, four variants PDE10A 1 to 4. PDE10A is made of 779 amino acids. Studies have shown that the PDE10 GAF domain shows specificity to cAMP rather than cGMP [167]. PDE10A is known to hydrolyze both cAMP and cGMP, it shows a higher affinity for cAMP than for cGMP, roughly Vmax of 2-5 fold lower for cGMP [168]. PDE10A has been shown to be highly expressed in several tissues, mRNA levels

were observed at higher levels in the striatal region of the brain and testis, and at a moderate level in the cerebellum, thalamus, hippocampus, and spinal cord [166]. PDE10A is the only PDE consisting of a catalytic domain in the C-terminus and two GAF domains in the N-terminus [167]. PDE10A1 and PDE10A3 variants are localized in the cytosolic fraction of the cell, PDE10A2 is found in the Golgi apparatus and membrane fractions [169]. The specific localization and substrate-specific regulations of PDE10 suggest its importance in maintaining the physiological conditions.

1.5.3   PDEs in pulmonary Hypertension

PDEs are involved in the pathogenesis of PAH by regulating the cyclic nucleotides signaling, several PDEs have been shown to have differential expression and activity in both experimental and human PAH. PDE1, PDE3, and PDE5 have been shown to be differentially regulated in the pulmonary vasculature of PAH [170, 171]. Inhibition of PDE1 and PDE5 by 8MM-IBMX and sildenafil respectively by stabilizing the cAMP/cGMP signaling and vascular remodeling [172-174]. In the MCT rat PAH model, inhibition of PDE3 and PDE4 shows a partial reduction of vascular remodeling [175, 176]. PDE10A is upregulated in the vasculature of IPAH patient lung samples and MCT rat PAH models. PDE10A inhibition has been shown to increase intracellular cAMP concentration and reversal of vascular remodeling in the MCT rat PAH model [177].

1.6   Current therapeutic options in pulmonary hypertension

Current FDA approved therapeutic options available for PAH target three main pathways namely prostacyclin (PGI2), nitric oxide (NO), and endothelin-1 focusing on endothelial function, vasodilation, and anti-proliferation [166]. The prostacyclin analogs like epoprostenol, treprostinil, iloprost, and Slexipeg targets IP receptors and increase the intracellular cAMP levels leading to vasodilation and anti-proliferative effects [178-181] (Figure 1.12). Treatment with prostacyclin analogs is the most sorted therapy for advanced PAH patients. The routes of administration are intravenous infusion (Epoprostenol and treprostinil), subcutaneous infusion (Treprostinil), inhalations (Treprostinil and iloprost), and oral administration (Selexipeg) [166].
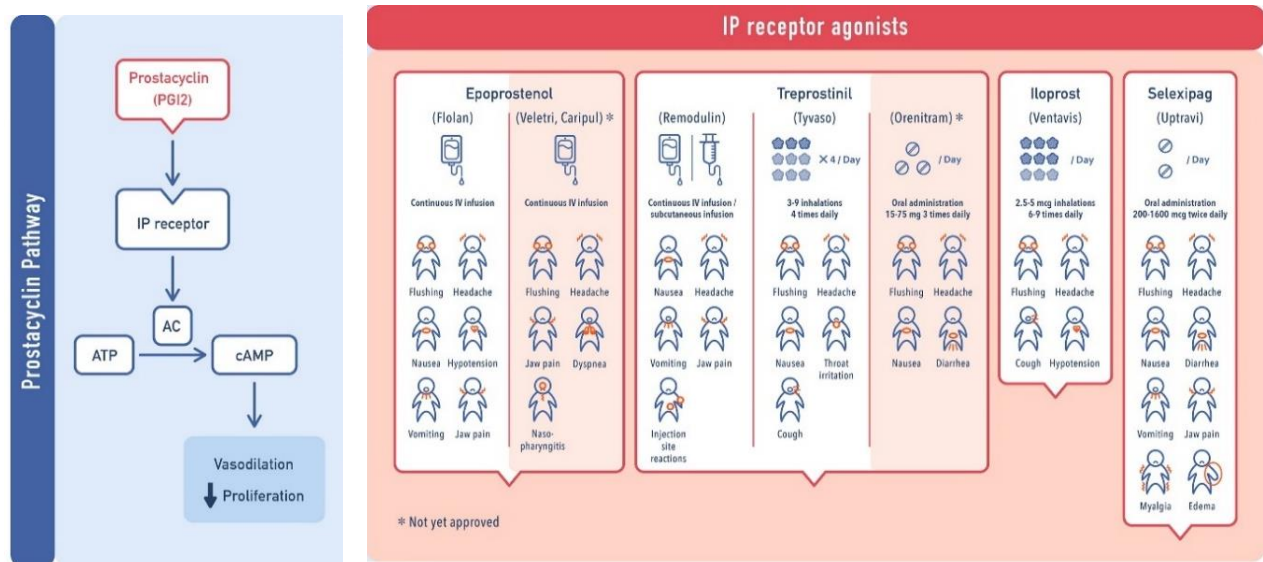
Figure 1.12. Prostacyclin treatment in pulmonary hypertension (Modified from ref [166]). ATP- adenosine triphosphate, cAMP- 3', 5'-cyclic adenosine monophosphate, IP- prostacyclin receptor, PGI2- prostacyclin.

Bosentan and ambrisentan are the endothelial receptor antagonists (ETR) approved by the FDA for the treatment of Group 1 PAH. These antagonists via blocking both endothelin receptors (ETRA, ETRB) and a single endothelin receptor, ETRA reduces the vasoconstriction and proliferation [182, 183] (Figure 1.13). Oral administration of ETRA is preferred in treating PAH patients [166].
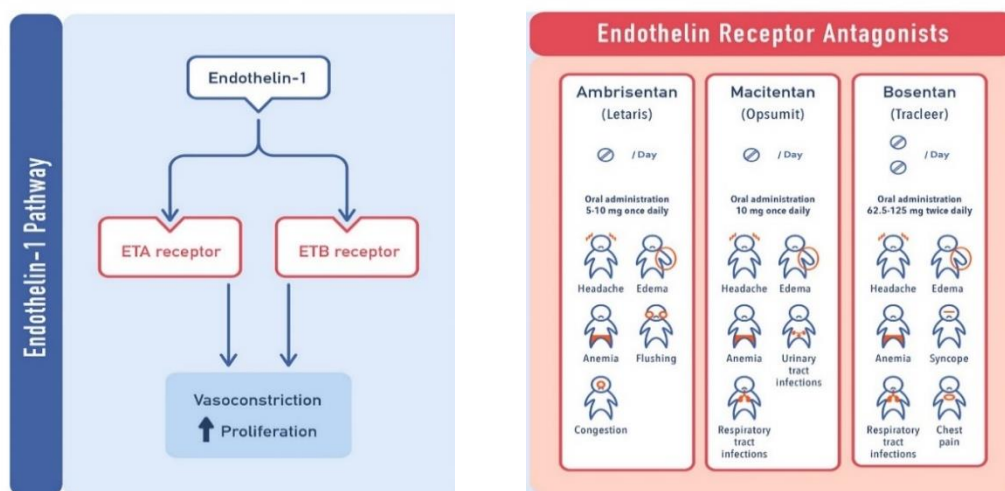
Figure 1.13. ETRA treatment in pulmonary hypertension (Modified from ref [166]). ETA- endothelin receptor A, ETB- endothelin receptor B.

The NO-sGC-cGMP pathway is targeted in PAH by soluble guanylyl cyclase (sGC) stimulators and PDE-5 inhibitors. Currently, Sildenafil and Tadalafil are the two PDE5 inhibitors available for the treatment of PAH [184, 185] (Figure 1.14). These inhibitors inhibit the activity of PDE5 and in turn increase the intracellular cGMP levels, leading to increased vasodilatory effects. The approved sGC stimulator for PAH and CTEPH treatment is Riociguat, which stimulates the sGC activity leading to increased conversion of GTP to cGMP [186, 187]. The sGC stimulators and PDE5 inhibitors are administered orally to the patients [166].
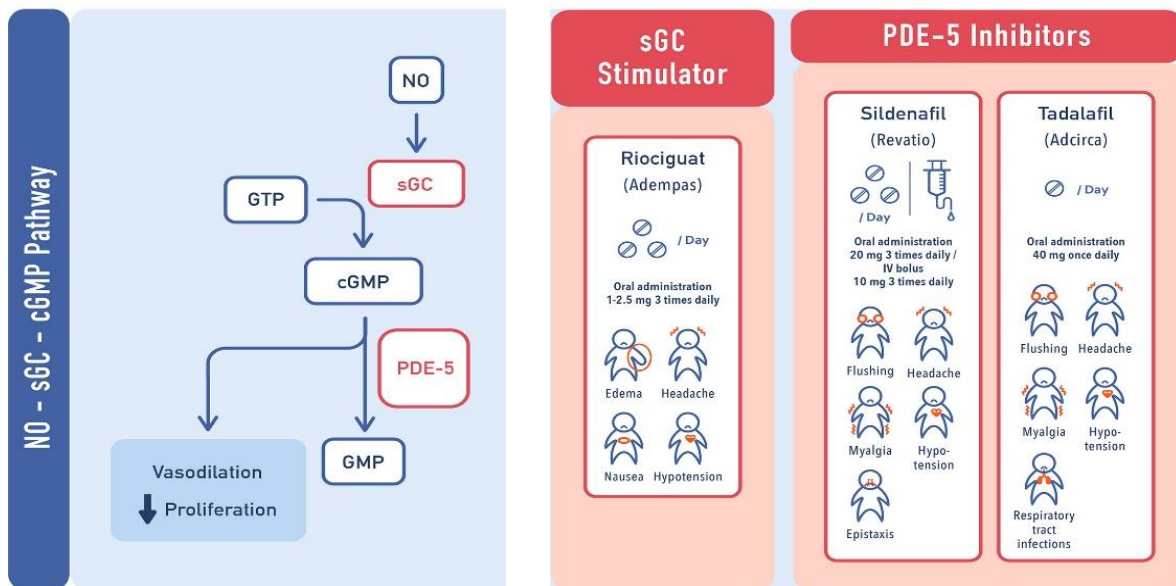
Figure 1.14. Targeting the NO-sGC-cGMP pathway in pulmonary hypertension (Modified from ref [166]). sGC- soluble guanyly cyclase , GTP- guanosine triphosphate, cGMP- cyclic guanosine monophosphate, PDE5- phosphodiesterase 5, NO- nitric oxide.

Although various drugs have been approved for the treatment of PAH, class specific side-effects are reported and mortality remains high [188]. Apart from PAH and CTEPH, there are almost no drugs available for treating other forms of PH. Thus, there is a necessity and urgency to identify novel therapeutic targets to fulfill the unmet medical needs in PH.

2   AIM OF THE STUDY

Pulmonary arterial hypertension (PAH) is a multifactorial disease that is characterized by increased pulmonary vascular pressure due to vasoconstriction and the pathological inward remodeling of the vessels. The persistent pressure in the pulmonary artery leads to pressure overload and ultimately leads to right ventricular failure. Several pathways are found to be dysregulated in the PAH patients, among which cAMP and cGMP, a secondary messenger signaling pathways have shown to be dysregulated at various levels, this implies that cAMP/cGMP pathways significantly affect the disease progression. Several drugs targeting cAMP/cGMP axis have been approved for the treatment of PAH, yet an optimal outcome in terms of curing the disease is need to be achieved. In parallel, several studies propose the existence of a compartmentalized cAMP signaling that can determine spatiotemporal regulation of cAMP downstream signaling and phenotypic outcome. However, the existence of such compartmentalized cAMP signaling is not delineated in PAH so far. Moreover, the regulation of cAMP levels and cAMP modulating enzymes and their influence on phenotypic modulation of pulmonary vascular cells is sparsely studied. Hence, in this study, I would like to investigate the regulation of cAMP modulating enzymes and their role in modulating compartmentalized cAMP signaling in PAH. After identifying those novel cAMP modulator/s, I aim to target them genetically ad pharmacologically to explore whether they can provide novel therapeutic strategies for PAH.

Objectives:

1) Identification of a novel molecular target/s to enhance intracellular cAMP levels in PAH condition

2) Investigate the role of cAMP modulator/s in mediating a compartmentalized cAMP signaling

3) *In vitro* studies in pulmonary vascular cells isolated from PAH patient lungs to investigate the phenotypical outcome of targeting the cAMP modulator/s employing genetic and pharmacological tools

4) *In vivo* studies in in experimental models of PAH to investigate the therapeutic potential and reverse-remodeling potential of cAMP modulator/s employing pharmacological tools

3 MATERIALS AND METHODS

3.1 Materials

Table 3.1. Reagents and Chemicals

Reagent	Company
4′,6-Diamidin-2-phenylindol (DAPI)	Invitrogen, USA
Acetone	Carl Roth, Germany
Acrylamide solution (30%)	Sigma Aldrich, USA
Ammonium Persulfate (APS)	Sigma Aldrich, USA
Bovine serum albumin (BSA)	Carl Roth, Germany
Bromophenol blue	Roche, Germany
BSA solution (2mg/ml)	BioRad, USA
Chloroform	Carl Roth, Germany
Dimethyl sulfoxide	Sigma Aldrich, USA
Diphenylacetohydroxamic acid	Sigma Aldrich, USA
Di-sodium hydrogen phosphate	Carl Roth, Germany
Ethanol absolute	Carl Roth, Germany
Ethylenediamine-Tetraceticacid (EDTA)	Carl Roth, Germany
Fluorescence mounting medium	Dako, USA
Glycerol	Sigma Aldrich, USA
Glycine	Sigma Aldrich, USA
Halt™ protease and phosphatase inhibitor cocktail	Thermo Scientific, USA
Hydrochloric acid	Carl Roth, Germany
Isopropanol	Carl Roth, Germany

iTaq™ Universal SYBR® Green Supermix	BioRad, USA
Lipofectamine 3000	Invitrogen, USA
Magnesium chloride	Carl Roth, Germany
Mayer's Hematoxylin Solution	Sigma Aldrich, USA
Methanol	Carl Roth, Germany
Milk powder	Carl Roth, Germany
N,N,N´,N´-Tetramethyl-1,2-diaminomethane (TEMED)	Sigma Aldrich, USA
Paraformaldehyde	Carl Roth, Germany
Ponceau S Solution	Sigma Aldrich, USA
Potassium chloride	Carl Roth, Germany
Potassium dihydrogen phosphate	Carl Roth, Germany
Proteinase K	Peqlab, Germany
Rainbow protein molecular weight marker	AmershamBiosciences, USA
RIPA lysis Buffer	Thermo Scientific, USA
RNase Away	Invitrogen, USA
Sodium bicarbonate	Carl Roth, Germany
Sodium chloride	Carl Roth, Germany
Sodium dodecylsulfate (20% w/v)	Carl Roth, Germany
Sodium hydroxide	Carl Roth, Germany
Stripping Buffer	Thermo Scientific, USA
Tris 0.5 M (pH 6.8)	Amresco, Germany
Tris 1.5M (pH 8.9)	Amresco, Germany
Tris base	Sigma Aldrich, USA

Triton X-100	Carl Roth, Germany
Trizol reagent	Invitrogen, USA
Tween 20	Sigma Aldrich, USA
Xtreme gene siRNA transfection reagent	Roche, Germany
Xylol	Carl Roth, Germany
β mercaptoethanol	Sigma Aldrich, USA

Table 3.2. Kits used

Names	Company
High Capacity cDNA synthesis kit	Applied Biosystems, USA
DC Protein assay kit	BioRad, USA
BrdU Incoportation assay kit	Roche, Germany
In situ cell death detection kit	Roche, Germany
Supersignal West Femto maximum sensitivity substrate kit	Thermo Scientific, USA
Duolink™ In Situ Red Starter kit	Sigma Aldrich, USA
Cyclic AMP EIA kit	Cayman Europe, Estonia
DAB substrate kit	Vector, USA
ImmPRESS kit	Vector, USA
NovaRED substrate kit	Vector, USA
Vectastain kit	Vector, USA
Vector VIP substrate kit	Vector, USA

Table 3.3. Cell Culture medium and reagents

Names	Company
Dulbecco's Phosphate Buffer saline (DPBS)	Sigma, USA
Fetal calf serum (FCS)	PAA, USA
Human Pulmonary arterial smooth muscle cells (PASMCs)	Lonza, USA
Idiopathic pulmonary arterial smooth muscle cells (IPAH-PASMCs)	Biobank, University of Gießen
OptiMEM	Gibco, Germany
Penicillin/Streptomycin	Lonza, USA
Smooth Muscle Cell Growth Medium 2	PromoCell, Germany
Smooth muscle cell medium (SmGM)	Lonza, USA
Trypsin/EDTA	Lonza, USA

Table 3.4 Equipment and Miscellaneous

Names	Company
Bruker Biospin	Pharmascan, Germany
Cell culture incubator, Hera cell	Heraus, Germany
Centrifuge	Life Technologies, Germany
CFX96 tm Real-Time PCR detection system	BioRad, USA
Leica DM6000	Leica, Germany
ImageQuant™ LAS 4000	Fujifilm, Japan
Hypoxia Chamber - The Clean Spot	Coy Lab products, USA
Homeothermic plate	AD Instruments, Germany
MiniVent 845	Hugo Elektronik, Germany
Body temperature probe unit	AD instruments, Germany

1.4F Micromanometer/Mikro-Tip Pressure catheter	Millar Instruments, USA
LabChart v7	AD Instruments, Australia
Microplate reader Infinite 200	TECAN, Germany
NanoDrop2000 Sprectrophotometer	Thermo Scientific, USA
PCR thermocycler	Eppendorf, USA
Power supply	BioRad, USA
Qmass	Medis, Netherlands
Vaporizer	Visualsonics, Canada
Water bath (cell culture)	Heraus, Germany
Western blot chambers	BioRad, USA
Zeiss confocal microscope LMS 710	Carl Zeiss, Germany
Amicon Ultra centrifugal filter units	Millipore, USA
Cell scrapers	BD Falcon, USA
Cell culture dishes (10cm, 6cm, 6well, 48well, 96well)	Greiner bio-one, Germany
Centrifugal protein concentrators	Millipore, USA
Gel blotting paper	Whatman, USA
Microcentrifuge tubes	Eppendorf, USA
Polyvinylidene fluoride (PVDF) membrane	Carl Roth, Germany
Polypropylene tubes (15ml, 50ml)	Greiner bio-one, Germany

Table 3.5 Animal used for PAH model

Names	Company
Sprague Dawley® rat	Charles River Laboratories, Germany
Wistar Kyoto (WKY) rats	Charles River Laboratories, Germany

3.2   Methods

3.2.1   Human Pulmonary Arterial Smooth Muscle Cells isolation and culturing

The ethics committee (Ethik Kommission am Fachbereich Humanmedizin der Justus Liebig Universität Giessen) approved the study protocol for tissue donation of the University Hospital Giessen (Giessen, Germany) in accordance with national law and with Good Clinical Practice/International Conference on Harmonization guidelines. Written informed consent was obtained from each patient or the patient's next of kin (AZ 31/93).

Human explanted lung tissues from subjects with IPAH or control donors were obtained during lung transplantation. Samples of donor lung tissue were taken from the lung that was not transplanted. Pulmonary arterial smooth muscle cells (PASMCs) isolated from healthy controls and patients with IPAH were obtained after an isolation procedure from the Giessen lung Biobank. The isolated hPASMCs were cultured in a 10cm Petridish containing 8ml of PASMC growth media. The cells were maintained in a humidified chamber at 37°C and 5% CO_2. The cells were passaged at 90-95% confluency in the ratio 1:2. The cells were taken for performing various experiments in passage 6. For passaging the cells, the culture dishes were rinsed using 8ml of DPBS followed by incubation with 3ml of Trypsin/EDTA for 3-4mins. The plates were viewed under the microscope to confirm the detachment of the cells from the culture dishes. The effect of Trypsin/EDTA was neutralized by adding an equal volume of growth media. The cells are transferred to 50ml falcon tubes and centrifuged at 1350rpm for 7mins. Following the centrifugation, the supernatant was removed and the 1ml of PASMC growth media was added to the cell pellet. The cell pellet was gently suspended in the PASMC growth media and seeded into the new culture dishes.

The hPASMCs obtained at P2 from the biobank were usually frozen in the liquid after passage 4 for further use. For freezing the hPASMCs, the cell pellets following trypsinization and centrifugation were suspended in 1ml of FCS with 5% DMSO for each 10cm culture dish. 500µl cell suspension was aliquoted into 1ml cryovials and 500µl of growth media was added to it. The cryovials are placed in the isopropanol freezing box at -80°C overnight and then transferred into liquid nitrogen storage tanks. Snap thawing of the frozen cells was done by plunging the cryovials taken out from liquid nitrogen tanks into the 37°C bead bath. Once thawed the cryovial contents were transferred into the culture dish containing PASMC growth media in a dropwise manner. After overnight culturing, growth media was changed to remove the traces of DMSO.

3.2.2 Cell death detection assay

The cell death in donor and IPAH hPASMCs measurements were performed using *in situ* cell death assay kit based on the quantitative sandwich-enzyme-immunoassay principle, it employs antibody against histones and nicked DNA. The assay works mainly by the detection of cleaved nucleosome fragments formed prior to the plasma membrane disintegration, which is a hallmark of apoptosis. The cells were cultured in 48 well plates for cell death assay experiments, 15000cells were seeded in each well. After 24hrs of seeding, the cells are either transfected using siRNAs or treated with inhibitors. Following the defined period of treatment duration, the cells were centrifuged for 10mins at 200g. Following the centrifugation, the media was removed and 100µl of 1X lysis buffer was added to each well and incubated for 30mins at RT. The plates were centrifuged for 10mins at 300g; 40µl of lysate was pipetted into the streptavidin-coated microplate. The anti-histone (biotin-labeled) and anti-DNA (HRP-labelled) were mixed in the ratio 1:1:10 with 1X incubation buffer and 80µl of the immunoreagent mix is pipetted into the microplate. The microplate was incubated in the 2hrs at 300rpm, following the incubation the plates were washed thrice using the incubation buffer and incubated in 100µl of substrate solution until the color develops. The plates were measured at 405nm with reference at 409nm using the ELISA plate reader.

3.2.3 Cell Proliferation measurement Assay

The cell proliferation was quantitatively measured in both donor and IPAH PASMCs using the colorimetric based BrdU incorporation assay kit. It works on the principle of incorporation of 5-bromodeoxyuridine into DNA during the synthesis phase of the cell cycle, which is detected using the antibody conjugated with peroxidase enzyme against the incorporated BrdU. The rate of cell proliferation was measured against the rate of DNA synthesis.

The cells were cultured in 96 well plates for cell proliferation experiments, 6000cells were seeded in each well. After 24hrs of seeding, the cells are either transfected using siRNAs or treated with inhibitors. Following the defined period of treatment duration, the cells are incubated in the BrdU labeling solution for 2hrs. The media was removed and cells were fixed for 30mins at room temperature using 200µl of FixDenat solution for each well. After the fixation, the cells are incubated for 3hrs in anti-BrdU-POD at RT, the wells were washed thrice using wash buffer. The plate was incubated in 100µl of substrate solution until the color develops. The plates were measured at 370nm with reference at 492nm using the ELISA plate reader.

3.2.4   cAMP measurement Assay

The intracellular cAMP concentration of hPASMCs was measured using a competitive non-acetylated EIA assay, according to the manufacturer's instructions. The assay is based on competition between cAMP-acetylcholinesterase (AChE) conjugated tracer and free cAMP to bind to the limited number of cAMP specific antibody. The concentration of the cAMP-tracer and the cAMP specific antibody remains the same while the free cAMP concentration varies, thus the amount of cAMP-tracer bound to the antibody will be inversely proportional to the free cAMP concentration present. The amount of cAMP tracer bound to the antibody is determined by the amount of enzymatic product formed from adding the substrate solution for AChE, which can be measured at 412nm. Thus, the absorbance measured at 412nm is directly proportional to the amount of cAMP-tracer bound to the well, which is inversely proportional to the amount of free cAMP present.

To perform the cAMP assay, hPASMCs were seeded in the 6well plate followed by transfection of siRNA or inhibitor treatment. After the specific treatment period, the cells were washed twice with DPBS and lysed with 0.1 M HCl for 15mins at RT. The cell lysates were collected and centrifuged at 12000rpm at 4ºC for 30mins. The supernatant was transferred to new tubes and stored at -80ºC. The standard solutions were prepared according to the manufacturer's instructions in 0.1M HCl. In the pre-coated secondary anti-rabbit antibody microplates, 50µl of standards or sample solutions were pipetted along with 50µl of tracer and 50µl of cAMP specific rabbit antibody. The blank wells were prepared by pipetting only 50µl of cAMP specific antibody into the wells without the free cAMP and cAMP-tracer. The microplates were incubated in overnight at 4ºC with gentle shaking. Following the overnight incubation, the wells were washed five times using the wash buffer and incubated with the Ellman's reagent for 90mins at RT with gentle shaking. The plates were measured at 412nm using the ELISA plate reader and concentrations of free cAMP were determined directly from the Magellan software by plotting against the standard curve. The concentration thus obtained was normalized to the total protein concentration of the sample determined using the Dc protein estimation method, thus the final concentration obtained is denoted by pmol/mg of total protein.

3.2.5 RNA isolation from cells

The RNA isolation from cells was performed using the TRIzol™ reagent. The cells were cultured in 6 well plates for RNA isolation. The culturing media was removed from the wells and washed with 2ml of DPBS, 250µl of TRIzol™ reagent was added to each well and incubated at RT for 10mins. After incubation, the lysates were transferred into the autoclaved 1.5ml tubes and 50µl of chloroform was added to it. The tubes were vortexed thoroughly and samples were incubated at RT for 30mins. The tubes were then centrifuged at 13000rpm for 30mins at 4°C. The upper aqueous phase was carefully transferred into the fresh autoclaved 1.5ml tubes and add 125µl of isopropanol to each tube. The tubes were slowly mixed and incubated for 30mins at RT. The tubes were then centrifuged at 13000rpm for 30mins at 4°C. The supernatant was removed and 1ml of ice-cold 80% ethanol was added to the pellet. The pellet was dislodged and centrifuged at 10000rpm for 15mins. The ethanol was removed and the washing was repeated one more time. After the second wash, the pellet was dried under the chemical hood and the pellet was dissolved in 14µl of DNase/RNase free water at 60°C for 10mins. The RNA concentration and purity were analyzed using a Nanodrop2000 spectrophotometer.

3.2.6 cDNA preparation from isolated RNA

The cDNA was synthesized from the isolated RNA using the high capacity cDNA synthesis kit according to the manufacturer's instructions. For the cDNA synthesis, 1000ng of RNA was used as a template and made up the volume to 10µl using DNase/RNase free water. The RNA template was incubated in 10µl of 2xRT master mix at 25°C for 10mins, followed by incubation at 37°C for 2hrs to perform the annealing and reverse transcription. Finally maintained at 85°C for 5mins for the inactivation of reverse transcriptase function. The primer mix composition is shown in the table below (Table 3.6).

Table 3.6. Master Mix composition for cDNA preparation for each sample

Components	Volume (µl)	Final Concentration
10X RT Buffer	2	1X
25X dNTP mix, 100mM	0.8	4mM
10X Random primers	2	1X
Ribonuclease inhibitor	0.5	10U

MultiScribe reverse transcriptase	1	50U
RNase/DNase free water	3.7	-

3.2.7   Real time Quantitative Polymerase chain reaction (RT-qPCR)

The expression of various genes was quantified using the RT-qPCR, it is based on simultaneous polymerase dependent amplification using specific primers (the primer list are shown in appendix table 9.2) and quantification based on the incorporation of SYBR green into the double stranded products formed from the amplification. The primer mix composition is shown in the table below (Table 3.7).

Table 3.7. RT-qPCR master mix composition for each sample

Components	Volume (µl)
Forward Primer	0.5
Reverse Primer	0.5
iTaq Universal SYBR Green Supermix	7
RNase/DNase free water	10

In 96 well PCR plate, 18µl of the master mix and 2µl of cDNA template was pipetted into each well and centrifuged at 3000rpm for 2mins. The amplification and quantification were performed using the CFX96 real time PCR system. The program setup for RT-qPCR is shown in the table below (Table 3.8).

Table 3.8. Program setup used for RT-qPCR

Process	Temperature (°C)	Time	Cycles
Initial denaturation	95	3min	1
Denaturation	95	10sec	
Annealing	60	30sec	40
Elongation	72	30sec	
Denaturation	95	10sec	1
Melting curve	65-95	Increment of 0.5 °C for every 5sec	1

3.2.8   Protein isolation from cells

To perform the expression studies, RIPA buffer containing protease-phosphatase inhibitor cocktail (PPi) was used to isolate protein from the cells. The hPASMCs were seeded in 6cm dishes and treatments were performed. After the specified treatment period, the media was removed and washed with 4ml of DPBS. The cells were lysed by adding 150µl of RIPA buffer and incubating the 6cm dishes at 4°C for 10mins. After the incubation, the plates were scratched using cell scrapers and the lysates were transferred to the autoclaved 1.5ml tubes. The tubes were then centrifuged at 13000 rpm for 30mins at 4°C and the supernatants were transferred into new 1.5ml tubes. The supernatants can be stored at -80°C or taken directly for protein quantification.

3.2.9   Total protein quantification and normalization

The total protein estimation was performed using the colorimetric assay based Bio-Rad DC protein assay kit. The assay works on the principle of Lowry's method where the protein reacts with the copper in an alkaline medium and reacts with Folin reagent to produce a blue coloured product with a maximum absorbance at 750nm. The standards were prepared using the BSA in the range of 2, 1, 0.5, 0.25, and 0.125 mg/ml. The protein was pre-diluted in a 1:5 ratio to fit into the standard curve, 5µl of both the samples and standards are pipetted into the wells of 96 well microplates. The reaction mix was prepared by adding 25µl of reagent S to 1ml of reagent A from the kit and 25µl of this reaction mix was pipetted into each well. 100µl of the reagent B was added into the wells and incubated for 10mins at RT. The plates were then measured for absorbance at 750nm using the ELISA plate reader. The exact concentration of the samples was determined from the standard curve using the Magellan software. The protein samples were normalized to the least protein concentration among the samples. The 5X loading buffer was prepared as shown in the table below (Table 3.9).

Table 3.9. 5X loading buffer preparation components

Components	Final Concentration
Tris-HCl (2M,pH 6.8)	375mM
SDS	10% (w/v)
Glycerol	50% (v/v)
β-mercaptoethanol	12.5% (v/v)

Bromophenol blue	0.02% (w/v)
Autoclaved water	Makeup to the final volume

The normalized proteins were then mixed with the 5X gel loading buffer (4:1 ratio) and denatured at 95⁰C for 10mins. The samples were either taken directly for the western blotting process or stored in -20⁰C until further experiments.

3.2.10 Western Blotting for studying specific protein expression

The expression pattern of specific proteins was studied using the western blotting technique. This involves three different steps: SDS polyacrylamide gel electrophoresis, electrophoretic transfer, and antibody based probing of specific proteins.

3.2.10.1 SDS polyacrylamide gel electrophoresis (SDS-PAGE)

The normalized and denatured proteins were separated based on their molecular weights using a SDS-PAGE. The system uses a stacking gel and a resolving gel for optimal protein separation. The protein samples and the molecular weight marker were loaded into the wells of the polyacrylamide gels and were run in the vertical electrophoretic assemblies using the 1X running buffer. In the initial phase, the voltage is set to 80V for 30mins for the protein sample and marker to migrate through the stacking gel, and then it was increased to 100V. The buffers and gels were prepared as per the tables below (Table 3.10-3.12)

Table 3.10. Components for preparing staking gel

Components	Final Concentration
Tris-HCl (0.5M,pH 6.8)	125mM
Acrylamide/Bis-acrylamide	6%
SDS 10% (w/v)	0.1%
APS 10% (w/v)	0.05%
TEMED	0.1%
Autoclaved water	Makeup to the final volume

Table 3.11. Components for preparing to resolve gels

Components	Final Concentration
Tris-HCl (1.5M,pH 6.8)	375mM
Acrylamide/Bis-acrylamide	10%
SDS 10% (w/v)	0.1%
APS 10% (w/v)	0.05%
TEMED	0.1%
Autoclaved water	Makeup to the final volume

Table 3.12. Components for preparing 1X SDS running buffer

Components	Final Concentration
Tris	25mM
Glycine	250mM
SDS 10% (w/v)	0.1%
Autoclaved water	Makeup to the final volume

3.2.10.2 Electrophoretic transfer of proteins

After molecular weight based transfer of proteins in SDS-PAGE, the proteins were transferred on to the polyvinylidene fluoride (PVDF) membrane by electrophoretic transfer. The membrane was activated in methanol for at least 1min before preparing the blotting sandwich (Figure 3.1). The blotting sandwich was prepared as shown in the figure below. The transfer was performed in the blotting chamber using the transfer buffer for 1hr at 100V. The buffers were prepared as per the table below (Table 3.2.8).
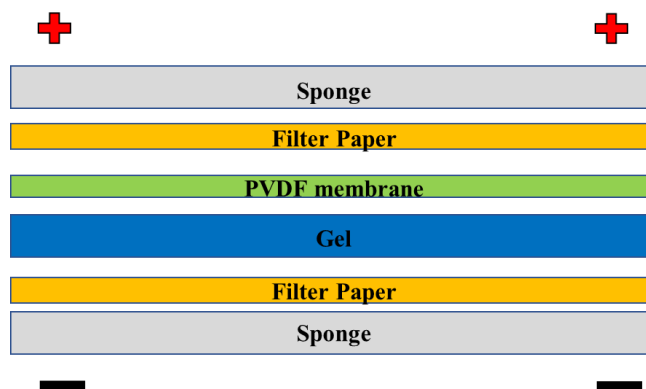
Figure 3.1. Western blotting stack preparation

Table 3.13. Components for preparing 1X transfer buffer

Components	Final Concentration
Tris	25mM
Glycine	192mM
Methanol	20% (v/v)
Autoclaved water	Makeup to the final volume

3.2.10.3 Antibody based probing of specific proteins

After the transfer, the PVDF membranes were incubated in the blocking buffer (5% non-fat dry milk dissolved in 1X TBST buffer) for 1hr at RT. The primary antibody required for probing was diluted in the blocking (the primary antibody dilutions are shown in appendix table 9.3) and incubated overnight with the membrane at 4⁰C with gentle shaking. After primary antibody incubation, the membranes were washed thrice for 15mins in 1X TBST buffer with shaking at RT. The membranes were then probed using HRP conjugated secondary antibodies (the secondary antibody dilutions are shown in appendix table 9.4) for 2hrs at RT. After secondary antibody incubation, the membranes were washed thrice for 15mins in 1X TBST buffer with shaking at RT. The membranes were then incubated in the Supersignal West Femto maximum sensitivity substrate and then imaged using the western blotting imager for signal detection. The time of exposure was based on the signal intensity. The buffers were prepared as per the table below (Table 3.14).

Table 3.14. Components for preparing 1X TBST buffer

Components	Final Concentration
Tris	20mM
Sodium chloride	137mM
Tween 20	0.1% (v/v)
HCl	For setting pH to 7.4
Autoclaved water	Makeup to the final volume

3.2.11 Immunohistochemistry of lung tissue

The lung paraffin sections of 4µm thickness were incubated at 65⁰C for 30mins and subsequently, the slides were dipped for 10mins in xylene for deparaffinization. After the deparaffinization, the

slides were rehydrated by a series of grade decreasing ethanol treatment. The slides were then washed using PBS for 5mins, the antigen retrieval was performed by boiling the slides in the 10mM citrate buffer (pH 6.0) for 20mins. The slides were then slowly cooled to the RT and washed thrice in PBS for 5mins. The slides were then blocked using the blocking buffer (5% BSA+0.1% triton in PBS) for 1 hr at RT and then the slides were incubated in the primary antibody diluted in the blocking buffer (the primary antibody dilutions are shown in appendix table 9.3) overnight at 4°C. The slides were washed thrice in PBS after overnight incubation and then incubated in the secondary antibody diluted in the blocking buffer (the secondary antibody dilutions are shown in appendix table 9.4) for 2hrs at RT. The slides were washed thrice in PBS and then incubated in DAPI diluted in PBS (1:1000) for 5mins at RT for nuclear staining. Subsequently, the slides were washed in PBS and covered by placing the coverslip over the anti-fade mounting medium. The slides were stored in dark at 4°C until imaging. The images were obtained using the Zeiss LSM700 confocal microscope using the Zen black software.

3.2.12 siRNA transfection of hPASMCs

Knockdowns of ADORA1 and PDE10A were performed using siRNA smart pool technology from dharmacon and a lipid based transfection reagent, Lipofectamine 3000, was used to transport the siRNAs into the cells. The scrambled siRNA was used as a negative control throughout the study. The knockdown studies were performed by seeding 150,000 cells/well in 6well plates and culturing for 24hrs. After 24hrs, the media was removed and cells are replenished with the transfection media (50% Opti-MEM+50% basal SMC media+ 0.1% FCS) and incubated for 30mins. The transfection master mix containing 250µl of Opti-MEM with 1.5µg of siRNA (siRNA smart-pool sequences are provided in appendix table 9.1) and 7.5µl of lipofectamine 3000 was prepared for each siRNA and was incubated at RT for 30mins for complex formation. The transfection master mix was added in the dropwise manner to the wells containing transfection media and the plates were incubated in the CO_2 incubator for 6hrs. After the incubations, the transfection media was discarded and replenished with the PASMCs growth media and cultured in the CO_2 incubator. The RNA is isolated 24hrs after transfection and the protein is isolated after 48hrs. For performing Proliferation and apoptosis assay, the cells were trypsinized, recounted, and reseeded into the 96- and 48well plates after 24hrs of transfection. The proliferation and apoptosis were measured 72hrs after transfection.

3.2.13 Inhibitor treatment of hPASMCs

The inhibitor studies were performed using ADORA1 antagonist, PDE10A inhibitor, and a novel dual inhibitor against both ADORA1/PDE10A. The cells were seeded according to the experimental needs and cultured for 24hrs in the PASMCs growth media. After 24hrs, the cells were washed using DPBS, and then the cells were cultured in serum starvation media (PASMCs basal media + 0.1% FCS) for another 24hrs. Following the serum starvation, the cells were treated with the inhibitors in PASMCs growth media. The Proliferation and apoptosis were performed after 24hrs of treatment, the cAMP studies were performed 30mins after treatment, and protein isolation was done after 6hrs and 24hrs of treatment.

3.2.14 Immunocytochemistry in hPASMCs

For performing immunocytochemistry, hPASMCs were seeded in the eight well chamber slides (15000/well) for 24hrs. After the defined period, the cells were washed with PBS and fixed with acetone: methanol (1:1) for 20mins at 4ºC. The fixation solution was discarded and the fixed cells were washed three times with PBS. The cells were blocked in blocking solution (5% BSA, 5% goat serum, 0.1% Triton X100 in PBS) for 1hr at RT. After blocking, the cells were incubated in the primary antibody diluted in the blocking buffer (the primary antibody dilutions are shown in appendix table 9.3) overnight at 4ºC. Following the overnight incubation, the cells are washed three times in PBS and then incubated in the secondary antibody diluted in the blocking buffer (the secondary antibody dilutions are shown in appendix table 9.4) for 2hrs at RT. Subsequently, the cells were washed with PBS and the nucleus was stained using DAPI diluted in PBS (1:1000) for 5mins at RT. The cells were then washed in PBS and covered by placing the coverslip over the anti-fade mounting medium. The slides were stored in dark at 4ºC until imaging. The images were obtained using the Zeiss LSM700 confocal microscope using the Zen black software.

3.2.15 Co-Immunoprecipitation of protein complexes

The Co-immunoprecipitation (Co-IP) was performed to study protein-protein interactions; in this technique, the specific protein is immunoprecipitated and is probed using an antibody for its interacting partners. The cells are cultured in 10cm dishes for Co-IP experiments, the lysis buffer was prepared by dissolving one tablet of mini protein protease inhibitor cocktail (Roche) in 1ml of Pierce IP-lysis buffer from ThermoFisher scientific, and 1mM sodium orthovanadate was also added to it. For each plate of 1ml of the lysis, the mixture was added and incubated at 4ºC for

10mins. The cells were scratched using cell scrapers and transferred into a sterilized 1.5ml tubes. The lysates were centrifuged at 13000rpm for 15mins at 4°C and supernatant was pipetted out into low binding tubes. The protein concentration was measured using the Bio-Rad DC protein assay kit and 500µg of protein was taken for each condition. The volume was made up to 1ml using the IP-lysis buffer and pre-clearing was performed for 1h at 4°C after adding protein G-sepharose beads. After pre-clearing, the tubes were centrifuged at 2500rpm at 4°C for 5mins and the supernatant was collected into the new low binding tubes. The supernatant, 10µg of specific antibody (the antibody concentration is provided in appendix table 9.3), or an equal amount of IgG controls were added to the supernatant and incubated overnight at 4°C with rotation. Following day, the samples were incubated with G-sepharose beads for 3hrs to allow capturing of the immune complex and then centrifuged at 2500rpm for 5mins at 4°C. The supernatants were removed and the beads were washed using IP wash buffer for 5times. After washing, 50µl of 2X sample buffer was added to the beads. The beads were then incubated at 95°C for 10mins and then the western blotting was performed. The buffers were prepared as per the table below (Table 3.15).

Table 3.15. Components for preparing IP wash buffer

Components	Final Concentration
Tris-HCl (pH 7.4)	50mM
EDTA	15mM
TritonX-100	0.1% (v/v)
NaCl	100mM
Autoclaved water	Makeup to the final volume

3.2.16 Proximity ligation assay

The proximity ligation assay was performed using Duolink® *In situ* PLA kit from Sigma. The assay works on the proximity ligation assay principle and combines with the rolling circle amplification-based detection system. A combination of oligonucleotide labeled secondary antibodies (PLA probes) generates an amplified signal only when the probes are in close proximity (i.e. <400nm).

For performing the proximity ligation assay, the hPASMCs were seeded in the 8 well chamber slides for 24hrs. The following day, the cells were washed using DPBS and fixed with ice cold acetone: methanol (1:1) for 10mins at 4°C. After fixation, the cells were then washed using DPBS

and were blocked using 5% BSA in 1X PBST for 30mins in RT. The blocking solution was removed and the primary antibody diluted in the antibody diluent (the primary antibody dilutions are shown in appendix table 9.3) overnight at 4°C. The following day, the cells were washed three times using DPBS and incubated with the PLA probes (1:5) for 1hr at 37°C. The cells were then washed two times in wash buffer and incubated with the ligation reagent (1:5) for 30mins at 37°C followed by amplification using polymerase solution. Finally, the cells were incubated with dapi (1:1000) for 10mins at RT. The cells were then washed using wash buffer and covered by placing the coverslip over the anti-fade mounting medium. The slides were stored in dark at 4°C until imaging. The images were obtained using the Zeiss LSM700 confocal microscope using the Zen black software. The detection was made at the Texas-red detection range.

3.2.17 *In vivo* PAH rat models

The rats used in this study were purchased from Charles River Laboratories (Sulzfeld, Germany). All the experiments were performed in accordance with the National Institute of Health guidelines on the use of laboratory animals. The study protocol (Zeichen nr: V54-19c20/15-B2/1079) was approved by both the University Animal care committee and the Federal authorities of animal research of the Regierungsprasidium Darmstadt (Hessen, Germany). The in vivo studies were performed on Monocrotaline induced PAH and Su5416+Hypoxia induced PAH rat models.

3.2.17.1 Monocrotaline induced PAH rat model (MCT-PAH model)

The Sprague-Dawley rats (250-300g body weight) were taken for the study. Alkaloid Monocrotaline (MCT) was dissolved in 1mol/L HCl and the pH was adjusted to 7.4 and the resulting solution was 20mg/ml. Rats were subcutaneously injected with 60mg/kg MCT to induce pulmonary hypertension and the disease was developed for 3weeks. After 3 weeks, the rats were randomized into two groups, a placebo group, and a treatment group. The treatment group was given 10mg/kg of Dual inhibitor (C21) and the placebo group was given the nitrocellulose solution, both through oral gavage. After 2weeks of treatment, the rats were taken for cardiac MRI, hemodynamic studies, and organ harvest (Figure 3.2).
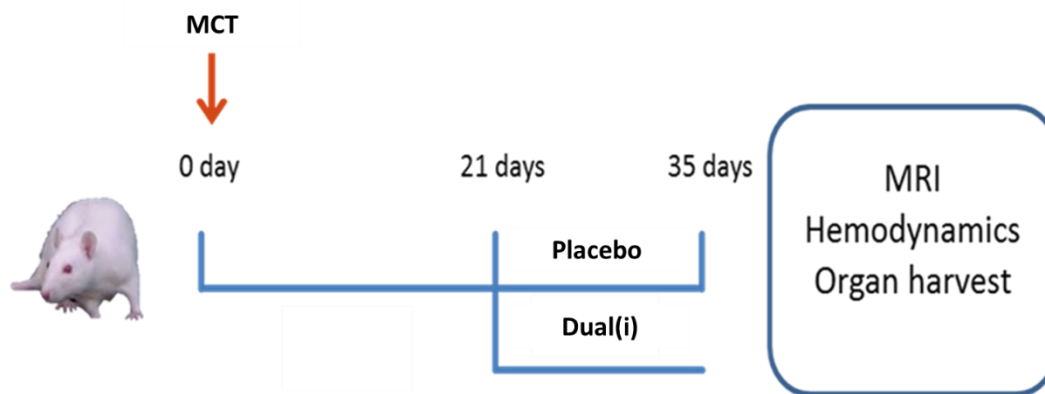
Figure 3.2. Experimental plan for dual inhibitor treatment on MCT-PAH rat model. Dual (i) - dual inhibitor, MRI- Magnetic resonance imaging.

3.2.17.2 Sugen hypoxia induced rat PAH model (SuHx-PAH rat model)

The Wister Kyoto rats weighing 250-300g body weight were used for the SuHx model, the Su5416 was dissolved in DMSO at a concentration of 25mg/ml. The Su5416 was injected subcutaneously on the neck and was put in a hypoxia chamber (10% O_2) for 3weeks. After 3 weeks, the rats were moved to normoxic conditions (room condition), and the rats were randomized into two groups, a placebo group, and a treatment group. The treatment group was given 10mg/kg of Dual inhibitor (C21) and the placebo group was given the nitrocellulose solution, both through oral gavage. After 2weeks of treatment, the rats were taken for cardiac MRI, hemodynamic studies, and organ harvest (Figure 3.3).
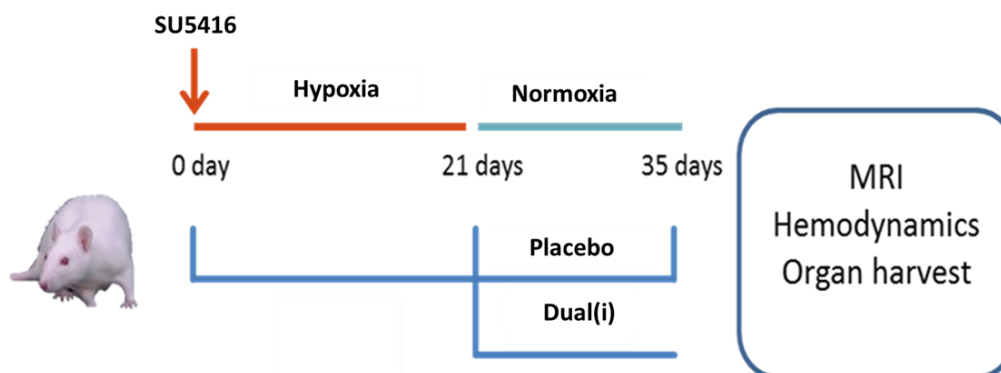

Figure 3.3. Experimental plan for dual inhibitor treatment on SuHx-PAH rat model. Dual (i) - dual inhibitor, MRI- Magnetic resonance imaging.

3.2.18 Hemodynamic Measurements of rats

After the treatment duration, the rats were anesthetized by intraperitoneal injection of ketamine (9mg/kg body weight) and medetomidine (100µg/kg body weight), followed by intramuscular injection of heparin. A tracheotomy was performed on the anesthetized rats and was ventilated at 60 breaths/min frequency. A catheter (PE 50 tube) was inserted through the right jugular vein to measure the right ventricular pressure and the arterial pressure was measured by inserting the catheter into the left carotid artery. Following the hemodynamic measurement, the heart was harvested and the right ventricle (RV) and the left ventricle along with septum (LV+S) were separated and weighed, this was was used to calculate the Fulton index [RV/ (LV+S)].

3.2.19 Rat cardiac MRI

Cardiac MRI measurements were performed on a 7.0 T Bruker Pharmascan (Bruker, Ettlingen, Germany), equipped with a 760 mT/m gradient system, using a room temperature 20 mm planar surface ^{1}H receiver-coil and a 72 mm room temperature volume resonator for transmission and the IntraGate^{TM} self-gating tool. The measurement were based on the gradient echo method (repetition time = 6.2 ms; echo time = 1.3 ms; flip angle = 10°; field of view = 45x45 mm; slice thickness = 1.0 mm; matrix = 128 x 128; oversampling = 100; number of frames = 20). The imaging plane was localized using scout images showing the 2- and 4-chamber view of the heart, followed by acquisition in short-axis view, orthogonal on the septum in both scouts. Multiple contiguous short-axis slices consisting of X to Y slices were acquired for complete coverage of the left and right ventricle. Rats were measured under volatile isoflurane (2.0 % in the air with a flow rate of 0.5 L/min) anesthesia; the body temperature was maintained at 37°C by a thermostatically regulated water flow system during the entire imaging protocol. MRI images are analyzed using MASS4Mice digital imaging software (Medis, Leiden, Netherlands).

3.2.20 Tissue processing, embedding and sectioning of Lung

The Isolated lungs were flushed with PBS and the right lobes of the lung were snap-frozen in liquid nitrogen for molecular studies. The left lobe of the lung was fixed in 4% paraformaldehyde for histological analysis and the fixed lobes were then washed in PBS. The fixed left lung lobes were dehydrated using an automatic vacuum dehydrator, the dehydrated tissues were then embedded in paraffin using the embedding station. Following the embedding, 4µm thick sections were made for immunohistochemistry or lung vasculature morphometric analysis.

3.2.21 Lung morphometric analysis

Lung morphometric analysis was performed to measure the degree of vascular remodeling in the lung vasculature. This was performed by measuring the medial wall thickness and muscularization in the vessel in the paraffin-embedded left lung lobe sections.

3.2.21.1 Medial wall thickness measurement of Lung vasculature

To measure the medial wall thickness (MWT), the Weigart-Van Gieson staining was performed. The rat lung sections of 4µm thickness were incubated at 60ᵒC for 1hr. The sections were then deparaffinized by dipping it in xylol for three times of 10mins each, followed by rehydration using a decreasing series of ethanol treatment (99% for 5mins, 99% for 5mins, 80% for 5mins and 70% for 5mins). The slides were then immersed in the Resorcin-Fuchsin solution overnight at RT. The following day, the slides were washed in tap water for 15mins and dipped in distilled water briefly. The slides were then immersed in the freshly prepared Weigert's iron hematoxylin for 5mins and then washed in tap water for 15mins. Subsequently, the slides were stained with Van Gieson solution for 10mins, and the slides were shortly washed with distilled water. The slides were then dehydrated by dipping in the increasing series of ethanol concentration (70% for 5mins, 80% for 5mins, 99% for 5mins and 99% for 5mins), and finally, the slides were mounted using pretex mounting media and coverslip. The MWT of the lung vasculature was measured using the Leica DM6000B microscope and Leica Qwin V3 software. The MWT is calculated based on the distance between the lamina elastic interna and lamina elastic externa using the formula percentage of MWT= (2*medial wall thickness/ external diameter)*100.

3.2.21.2 Muscularization measurement of Lung vasculature

To measure the degree of muscularization, double immunohistological staining was performed against α-SMA and Von-Willebrand factor staining was performed. The rat lung sections of 4µm thickness were incubated at 60ᵒC for 1hr. The sections were then deparaffinized by dipping it in xylol for three times of 10mins each, followed by rehydration using a decreasing series of ethanol treatment (99% for 5mins, 99% for 5mins, 80% for 5mins and 70% for 5mins). The slides were washed for 5mins in distilled water and then peroxidase quenching was performed by treating the slides with 3% H_2O_2-methanol solution for 15mins. The slides were washed thoroughly in distilled water and PBS for each 10mins with shaking. Antigen retrieval was performed by trypsin treatment for 10mins on a 37ᵒC heating block and then the slides were washed three times using PBS for

5mins each. The slides were then incubated with the 10% BSA blocking buffer for 30mins and then slides were washed briefly in PBS for 3mins. The second blocking was performed using the horse serum (Vectastain kit) for 10mins, followed by incubation with the α-SMA primary antibody (the antibody dilutions are shown in appendix table 9.3) for 1hr. The slides are then washed in PBS for 5mins and incubated with the ready-to-use biotinylated secondary antibody for 30mins. Next, the slides were washed three times in PBS and were then treated with Vector Vip Substrate kit for antibody colour development. The time of color development was maintained the same for all the slides and was observed using the Leica DM6000B microscope. After the initial development step, the slides were washed in tap water and was blocked for the next primary antibody staining by incubating in 10%BSA for 30mins followed by ImmPRESS serumblock1 for 20mins. After the blocking, the slides were incubated in the Von-Willebrand primary antibody (the antibody dilutions are shown in appendix table 9.4) for 1hr and were washed three times with PBS. The slides were then incubated in the secondary antibody from the ImmPRESS kit for 30mins and then developed under the microscope using the DAB substrate after the PBS washes. Counterstaining was performed using the Methyl green for 3mins at 60ºC. The slides were then dehydrated by dipping in the increasing series of ethanol concentration (70% for 5mins, 80% for 5mins, 99% for 5mins and 99% for 5mins), and finally, the slides were mounted using pretex mounting media and coverslip. The degree muscularization of the lung vasculature was measured using the Leica DM6000B microscope and Leica Qwin V3 software.

3.2.22 Statistical tests used

All data are expressed as Mean ± Standard Error of Mean (SEM). Statistical comparisons of samples were performed by unpaired student's t-test for comparing two groups or by one-way ANOVA followed by the Dunnet test for multiple comparisons. A difference with $p<0.05$ between the groups was considered significant. All experiments with primary cells were performed in at least three independent biological replicates.

4   Results

4.1   Increased proliferation and apoptotic resistance in IPAH PASMCs

To investigate whether PASMCs that were isolated from IPAH patients have different functional characteristics in comparison to PASMCs isolated from control, both IPAH and donor PASMCs were serum starved for 24hrs and later replenished with the smooth muscle media supplemented with growth factors (PASMC growth media). Proliferation and apoptosis were measured 24hrs after culturing the cells in PASMC growth media. In line with the previous studies, the IPAH PASMCs showed an increased proliferation capacity (Figure 4.1 A) and higher resistance to apoptosis (Figure 4.1 B) in comparison to the donor PASMCs.
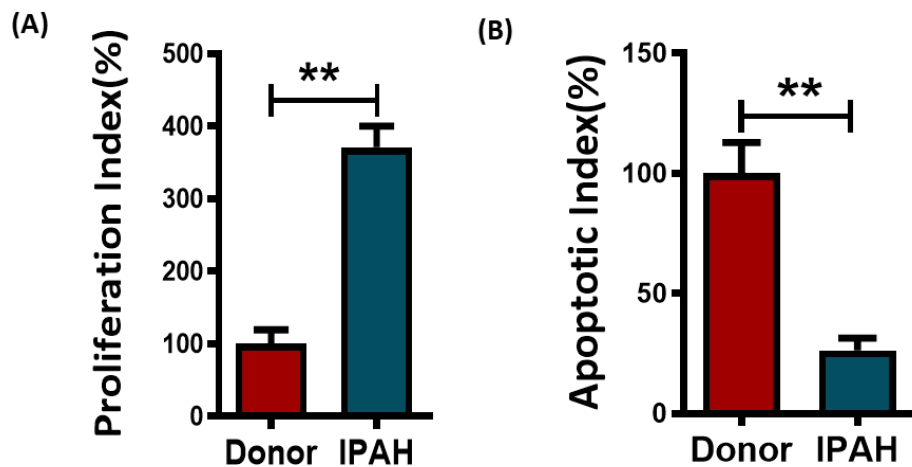
Figure 4.1. Functional characterization of donor and IPAH PASMCs. (A) Measurement of proliferation using BrdU assay in both donor- and IPAH- PASMCs, (n=3). (B) Measurement of apoptosis in both donor- and IPAH- PASMCs using the cell death assay, (n=3). Bars indicate means ± S.E.M. Data are expressed as percentage of donors and were analyzed using the unpaired student t-test. **p <0.01, *vs* Donor PASMCs.

4.2   Decreased intracellular cAMP concentration in IPAH PASMCs

Further to detect whether IPAH PASMCs alter in their intracellular cAMP concentration in contrast to the donor PASMCs, EIA based measurements of the intracellular levels of cAMP was performed from cell lysates. In line with the previous studies, the measurements showed that there is a significant decrease in the intracellular cAMP levels under the disease condition (Figure 4.2 A).
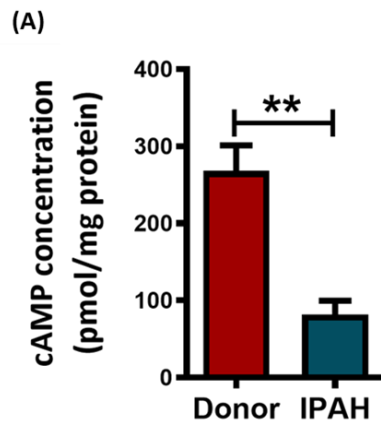
Figure 4.2. Intracellular cAMP measurements of donor- and IPAH- PASMCs. (A) Intracellular cAMP was measured using EIA assay kit in both donor and IPAH PASMCs, (n=4). Bars indicate means ± S.E.M. Data were analyzed using the unpaired student t-test. **$p < 0.01$, *vs* Donor PASMCs.

4.3 ecto-5′-nucleotidase (CD73) expression was downregulated in IPAH PASMCs

As the decrease of cAMP levels in IPAH PASMCs could be due to the imbalance of cAMP synthesis versus cAMP degradation, the regulation of cAMP synthesis modulating enzymes (cAMP ecto-5′-nucleotidase ad adenosine receptors) have been screened. Importantly, from the RNA sequencing data, ecto-5′-nucleotidase (CD73; coding gene NT5E), an enzyme that converts AMP to adenosine, was found downregulated in the IPAH PASMCs (Figure 4.3 A). Further, CD73 downregulation is confirmed at the mRNA level using qRT-PCR (Figure 4.3 B) and also at the protein level using western blot (Figure 4.3 C). These data are in line with the previously available studies [147] showing a reduced adenosine level in the pulmonary circulation of PH patients, suggesting an important role of adenosine signaling in disease progression.
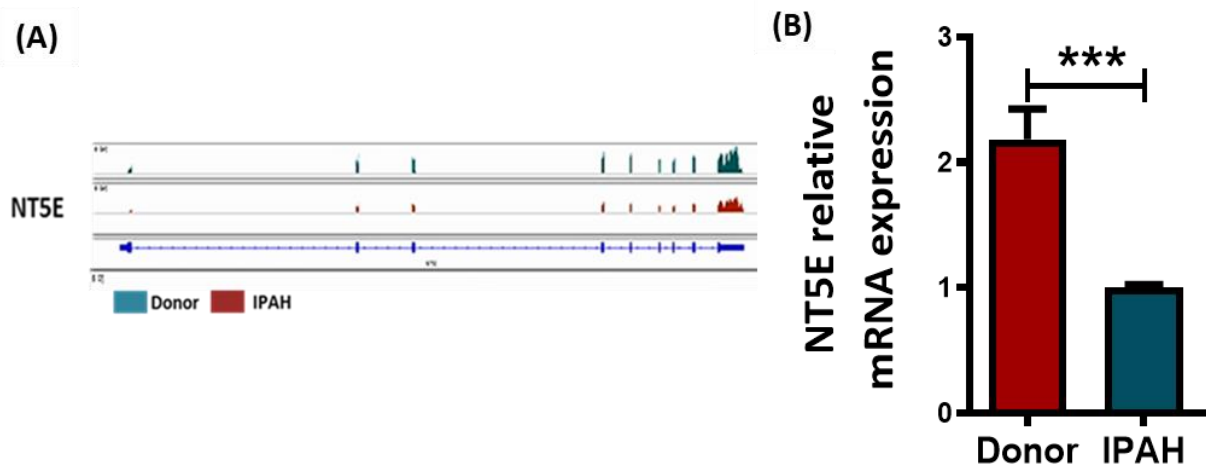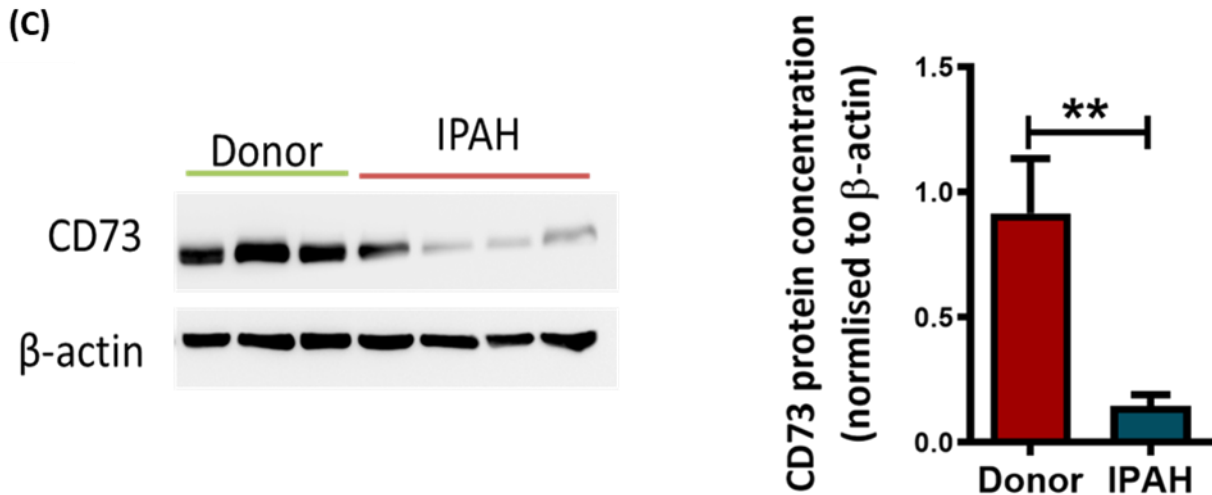
Figure 4.3. Expression analysis of CD73 in donor- and IPAH- PASMCs. (A) Reads of NT5E from RNA sequencing data of donor and IPAH PASMCs. (B) Expression analysis of CD73 using qPCR and (C) western blotting between the donor (n=3) and IPAH (n=4) PASMCs. Bars indicate means ± S.E.M. Data were analyzed using the unpaired student t-test. **p <0.01, ***p <0.001, *vs* Donor PASMCs.

4.4 Adenosine receptor A1 is upregulated at the transcription level in IPAH PASMCs

Similar screening of adenosine receptors from the RNA sequencing data, which mediates extracellular adenosine signaling and subsequently the cAMP signaling, suggests that the peak intensity of adenosine receptor A1 (ADORA1) were higher in IPAH PASMCs as compared to the donor PASMCs (Figure 4.4 A). However, the other adenosine receptors, adenosine receptors A2a (ADORA2a), A2b (ADORA2b), and 3 (ADORA3) were not significantly dysregulated under the disease condition. Further validation with qRT-PCR confirms the significant upregulation of ADORA1 (Figure 4.4 B), but no significant regulation of ADORA2a (Figure 4.4 C) and ADORA2b (Figure 4.4 C) in the IPAH PASMCs at the transcript level. The ADORA3 expression was below the detection level in the qRT-PCR. These results suggest that ADORA1 is upregulated under the disease condition at the transcript level compared to other adenosine receptors.
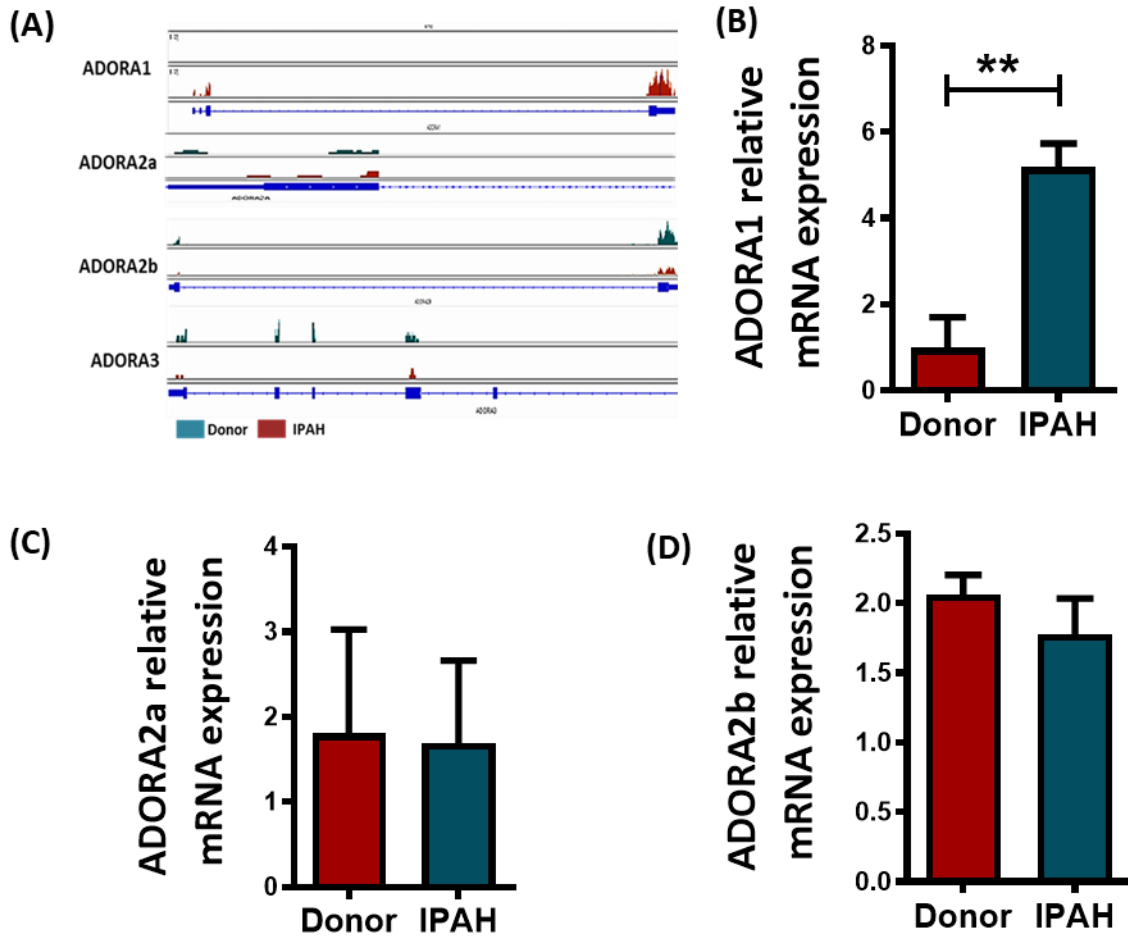
Figure 4.4. Transcriptomic analysis of adenosine receptors in donor- and IPAH- PASMCs. (A) Reads of ADORA1, ADORA2a, ADORA2b, and ADORA3 genes from RNA sequencing data of donor- and IPAH- PASMCs. (B) Expression analysis of ADORA1, (C) ADORA2a, and (D) ADORA2b using qRT-PCR between donor (n=3) and IPAH (n=3) PASMCs. Bars indicate means ± S.E.M. Data were analyzed using the unpaired student t-test. **p <0.01, *vs* Donor PASMCs.

4.5   Adenosine receptor A1 is upregulated at the translational level in IPAH PASMCs

To investigate if the ADORA1 is also upregulated at the translational level, western blotting was performed from the isolated protein from donor- and IPAH- PASMCs and probed using the antibody against ADORA1. As postulated, ADORA1 is upregulated in the IPAH PASMCs compared to the donor PASMCs (Figure 4.5 A). Furthermore, immunofluorescence stainings performed in both donor and IPAH lung tissues detected localization of ADORA1 majorly in medial layer of pulmonary vasculature and an increased immunoreactivity in IPAH pulmonary vasculature (Figure 4.5 B). These results suggest an upregulation of ADORA1 expression in the disease condition and mainly localized in the medial layer of the pulmonary vessel.
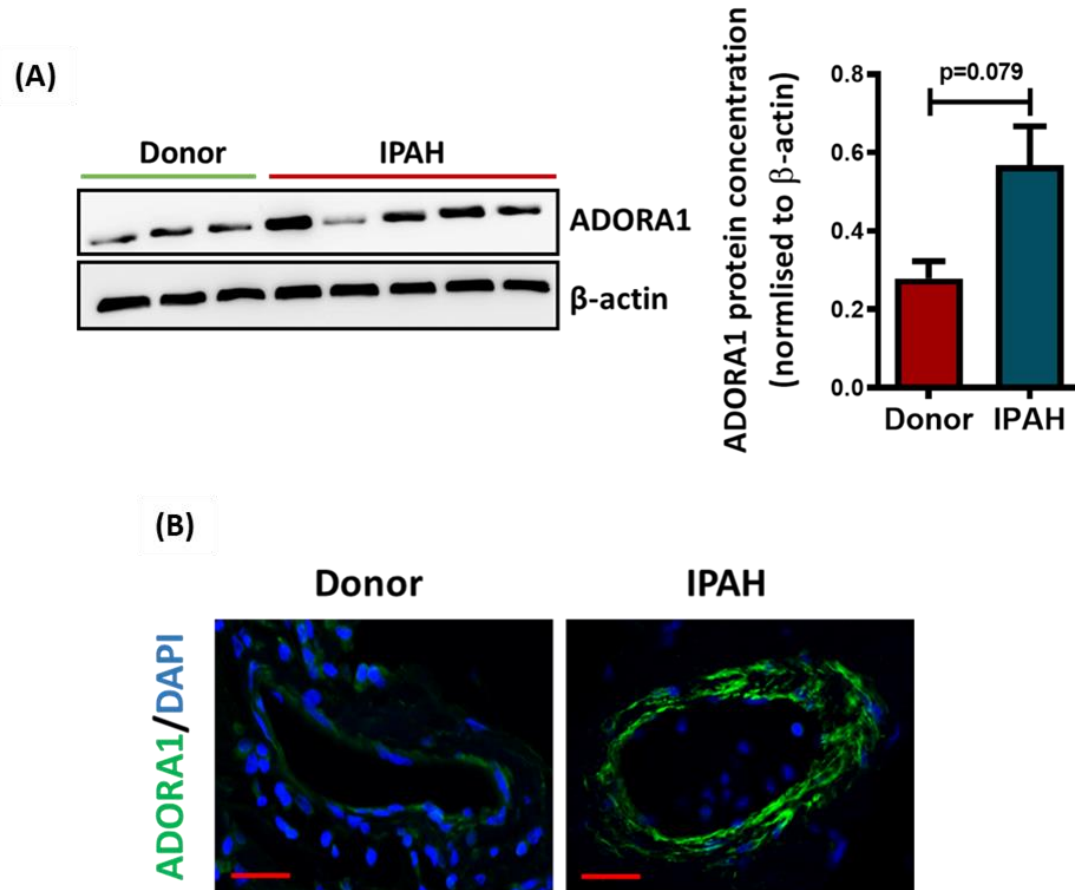
Figure 4.5. Expression analysis of adenosine receptors in donor and IPAH PASMCs. (A) Expression analysis of ADORA1 using western blotting between the donor- (n=3) and IPAH- (n=5) PASMCs. (B) Immunofluorescence staining of ADORA1 in both donor and IPAH lung tissue (n=3) Scale bar=20µm.

4.6   Knockdown of ADORA1 induced apoptosis in donor hPASMCs stimulated with growth factors

To study the functional relevance of ADORA1 under hyperproliferative conditions, the proliferation and apoptosis ability of hPASMCs was measured upon silencing ADORA1 after 72hrs of transfection. As shown in the western blots, knockdown of ADORA1 with specific siRNAs for 48hrs resulted in significant down-regulation of ADORA1 at the protein level (Figure 4.6 A). Knockdown of ADORA1, induced a significant increase in the apoptosis (Figure 4.6 C), but no effect on the proliferation (Figure 4.6 B) ability of donor hPASMCs compared to scramble. Moreover, knockdown of ADORA1 caused an increase in intracellular cAMP levels (Figure 4.6 D), suggesting that silencing ADORA1 induces strong pro-apoptotic effects and increases intracellular cAMP levels in donor hPASMCs.
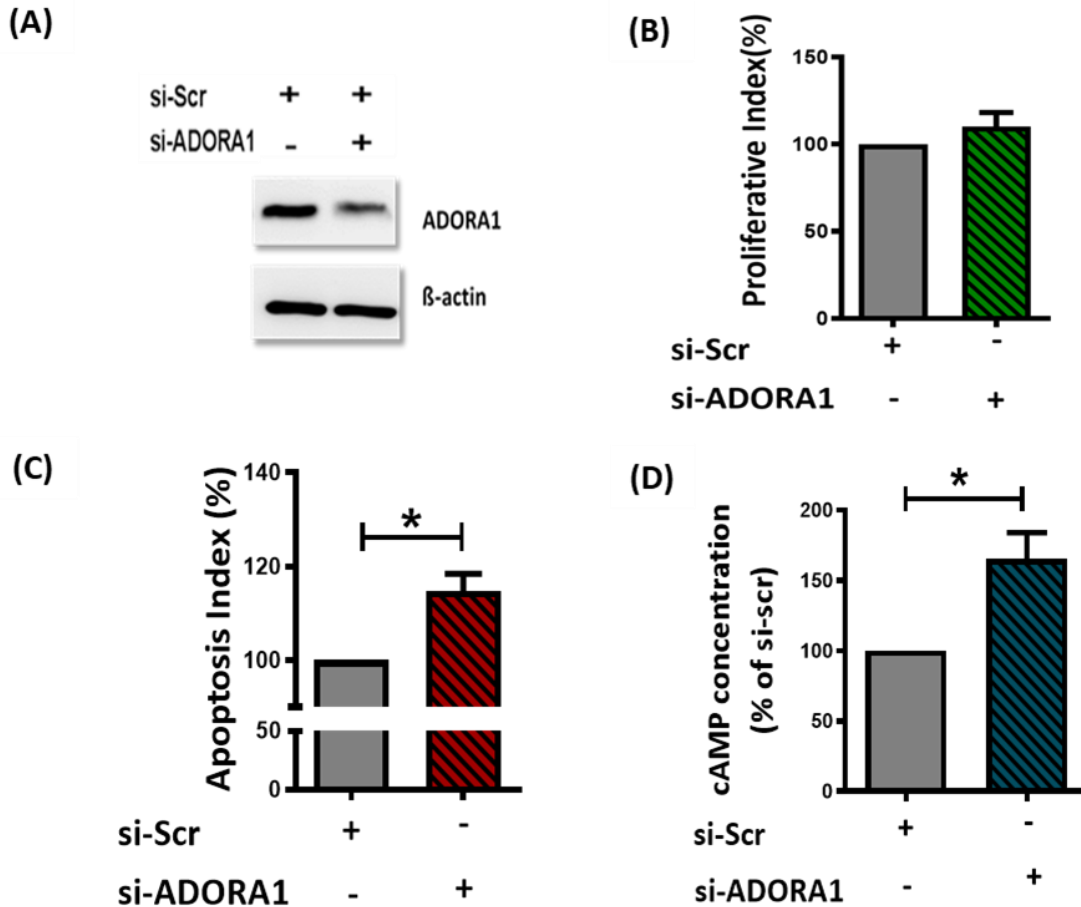
Figure 4.6 Functional effects of ADORA1 silencing in donor hPASMCs stimulated with growth factors. (A) Western blot indicating knockdown efficiency of siRNA targeting ADORA1. (B) Measurement of proliferation using BrdU assay (n=3), (C) measurement of apoptosis using the cell death assay kit (n=3), and (D) intracellular cAMP measurement using cAMP EIA kit (n=3). Bars indicate means ± S.E.M. Data were analyzed using paired t-test. *p <0.05, *vs* si-Scr.

4.7   Pharmacological inhibition of ADORA1 induces pro-apoptotic effect in donor hPASMCs stimulated with growth factors

To substantiate the siRNA mediated effects observed in the donor hPASMCs, pharmacological mediated inhibition of ADORA1 was performed using ADORA1 antagonist in hPASMCs. Prior to the treatment with the inhibitor, the cells were serum starved in 0.1% FCS media for 24hrs. The proliferation and apoptosis assays were performed at 24hrs following the treatment with the antagonist. In line with the previous siRNA results, inhibition of ADORA1 doesn´t exert any significant effects on proliferation (Figure 4.7 A) but induced significant pro-apoptotic effects (Figure 4.7 B) and increased intracellular cAMP levels (Figure 4.7 C) in hPASMCs compared to

vehicle (DMSO)-treated hPASMCs. These results confirm that ADORA1 antagonism by both genetic and pharmacological means, induces the pro-apoptotic effects and increase the intracellular cAMP concentration in donor hPASMCs.
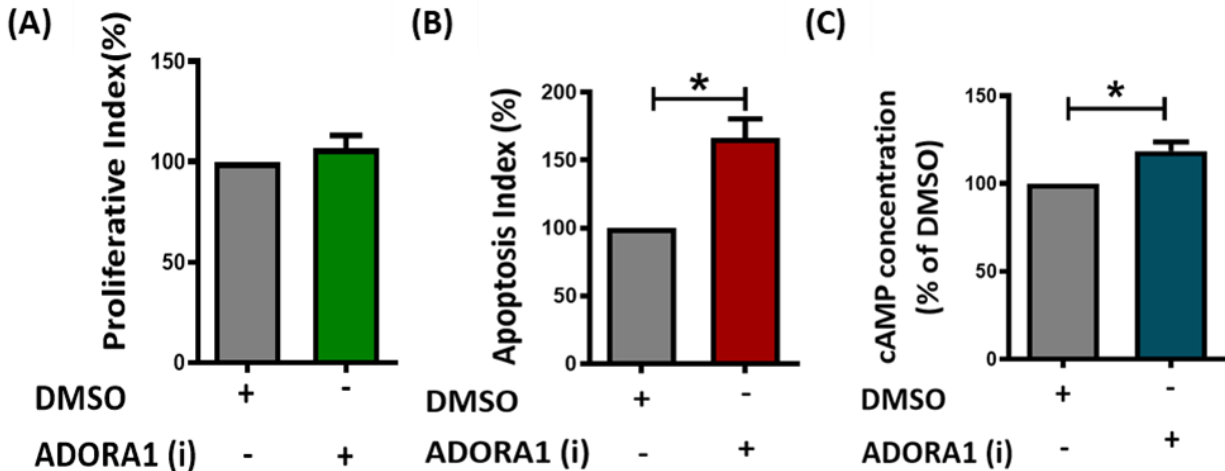
Figure 4.7. Functional effects of ADORA1 antagonist in donor PASMCs stimulated with growth factors. (A) Measurement of proliferation using BrdU assay (n=3), (B) measurement of apoptosis using the cell death assay kit (n=3), and (C) intracellular cAMP measurement using cAMP EIA kit (n=3). Bars indicate means ± S.E.M. Data were analyzed using paired t-test. *p <0.05, *vs* DMSO.

4.8 Inhibition of ADORA1 in IPAH PASMCs didn´t exert any effects on proliferation and apoptosis

To validate the effects of targeting ADORA1 effects under the disease condition, the PASMCs isolated from IPAH patients were treated with siRNA targeting ADORA1 for 72hrs, similar to the donor hPASMCs. Interestingly, neither the knockdown nor pharmacological inhibition of ADORA1 exerted any effects on IPAH PASMCs. They did not induce any anti-proliferative (Figure 4.8 A, D), pro-apoptotic effects (Figure 4.8 B, E), or increase the intracellular cAMP concentration (Figure 4.8 C, F) as observed in the donor hPASMCs. These results suggest that targeting ADORA1 in IPAH PASMCs did not reciprocate any beneficial effects observed in the donor PASMCs.
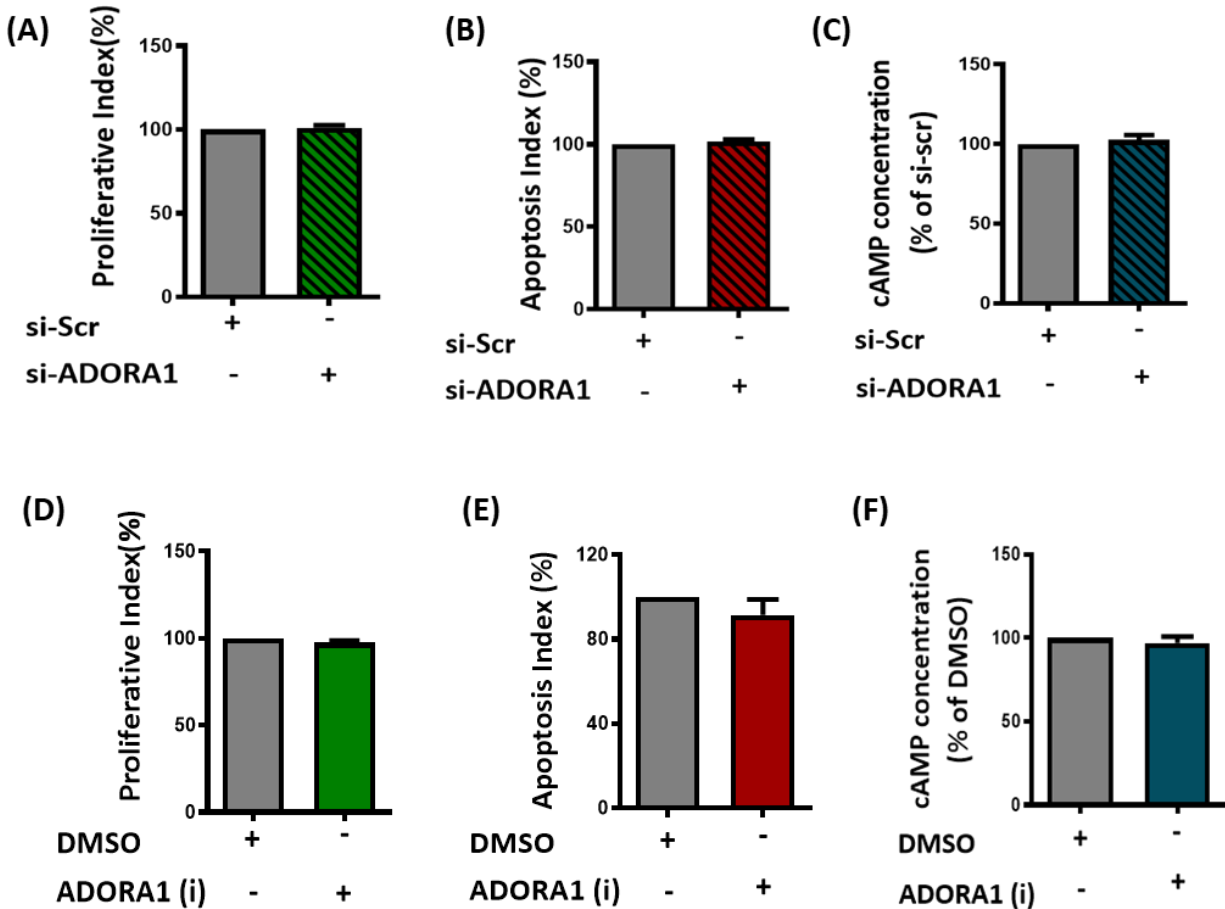
Figure 4.8. Functional effects of ADORA1 inhibition in IPAH PASMCs stimulated with growth factors. (A, D) Measurement of proliferation using BrdU assay (n=3), (B, E) measurement of apoptosis using the cell death assay kit (n=3), and (C, F) intracellular cAMP measurement using cAMP EIA kit (n=3). Bars indicate means ± S.E.M. Data were analyzed using paired t-test.

4.9 ADORA1 co-localizes with cAMP targeting phosphodiesterase 10A (PDE10A) under IPAH condition

The observation that ADORA1 antagonism causes accumulation of intracellular cAMP levels exclusively in donor hPASMCs, but not on IPAH hPASMCs is intriguing and suggest a simultaneous degradation of cAMP produced by ADORA1 in IPAH. To explore this hypothesis, co-localization studies of cAMP targeting PDEs (cAMP-PDEs) and ADORA1 was performed in IPAH PASMCs and IPAH lung tissues. At first, to screen for the cAMP-PDEs co-localizing with ADORA1, immunocytochemistry was performed in IPAH PASMCs. The IPAH PASMCs were cultured in the 8well culture slides for 24hrs in PASMCs growth media. Interestingly, among the cAMP-PDEs (PDE1, PDE3, PDE4, and PDE10A), that were shown to be upregulated in IPAH

[177, 189], PDE10A displays a strongly co-localization with ADORA1 in IPAH PASMCs (Figure 4.9 A, B). In addition, the immunohistochemistry performed in the IPAH patient lung sections confirmed the co-localization of ADORA1 with PDE10 majorly in the medial layer (Figure 4.9 C). The co-localization studies in both IPAH PASMCs and IPAH lung sections suggests that ADORA1 and PDE10A can form a bidirectional cAMP regulatory system.
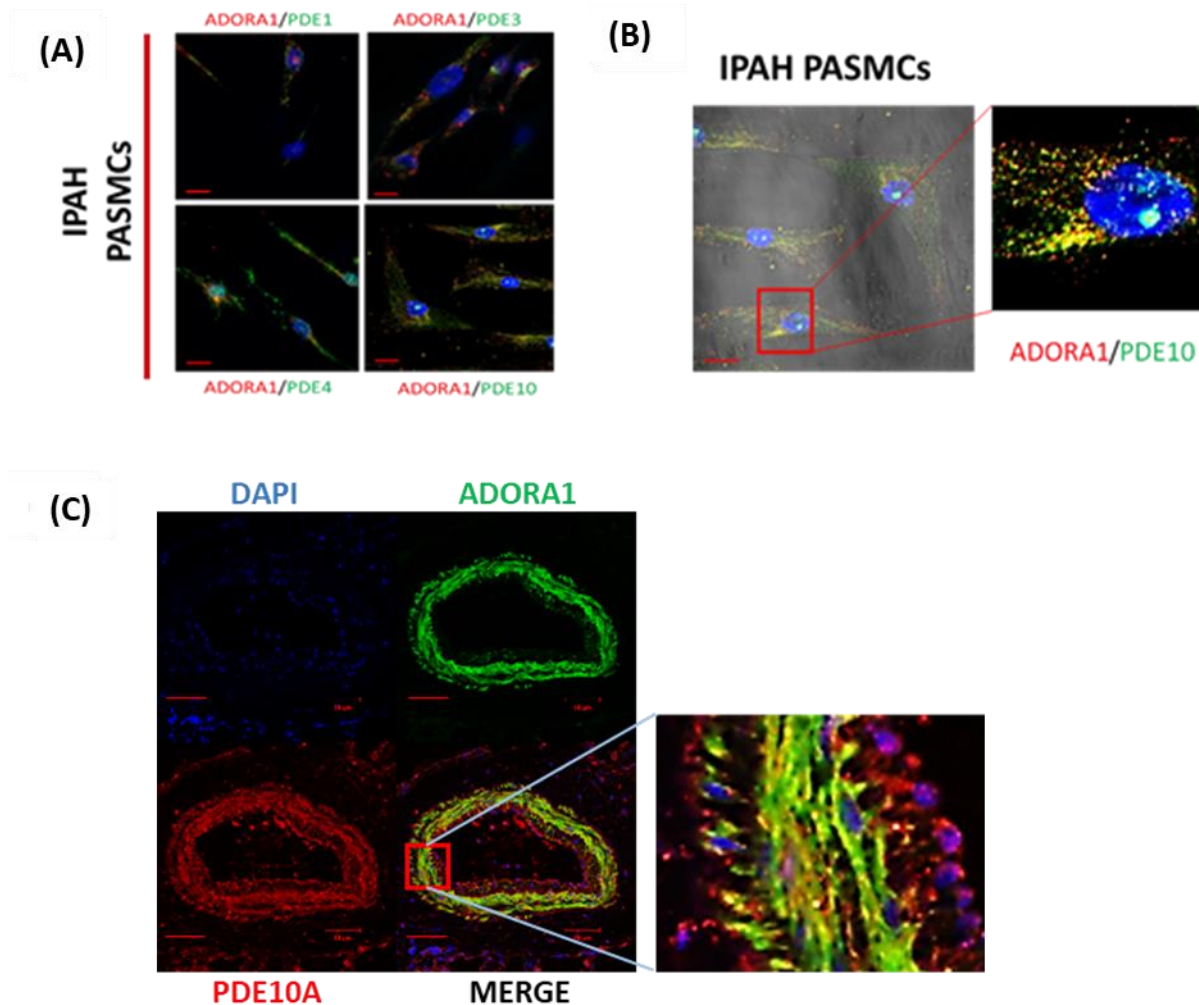
Figure 4.9. Co-localization of ADORA1 and PDE10A in IPAH PASMCs and lung tissues. (A) Immunostaining based screening of cAMP regulating PDEs (PDE1, PDE3, PDE4 and PDE10) co-localization with ADORA1 in IPAH PASMCs (n=3) scale bar= 20µm. (B) Confocal imaging of ADORA1 and PDE10A in IPAH PASMCs (n=3) scale bar= 20µm (C) Dual immunofluorescence staining of ADORA1 and PDE10A in lung tissue from IPAH patients (n=3) scale bar=50µm.

4.10 ADORA1/PDE10A/AKAP5 supercomplex formation in IPAH PASMCs modulates cAMP concentration in the local microenvironment

To investigate if this cAMP regulatory system is observed only under the disease condition, co-immunoprecipitation (Co-IP) and proximity ligation assay (PLA) was performed in both donor and IPAH PASMCs. To perform Co-IPs, the donor- and IPAH- hPASMCs were cultured in the 10 cm dishes using PASMCs growth media. Notably, Co-IP experiments support that notion that PDE10A interacts with ADORA1 exclusively in IPAH PASMCs, but not in the donor PASMCs (Figure 4.10 A). The PLA was performed to validate the Co-IP results, for that the cells were cultured in the 8well chamber slides and cultured in the PASMC growth media. In line with the Co-IP results, the PLA confirms the ADORA1 and PDE10A complex formation under the disease condition (Figure 4.10 B). The PLA also confirms that ADORA1 and PDE10A are in close proximity of less than 400 nm. These results suggest that under the disease condition ADORA1 and PDE10A form a bidirectional regulatory complex to efficiently degrade the cAMP produced by ADORA1. As previous studies have shown that PDE10A can form complex with AKAP5 and thereby modulates the localized cAMP pool [190], we assessed the regulation of AKAP5 and its interaction with ADORA1/PDE10 complex in IPAH disease setting. Strikingly, an increased expression of AKAP5 in IPAH PASMCs compared to donor PASMCs was observed (Figure 4.10 D). Furthermore, Co-IP experiments performed using antibodies against AKAP5 and immunoblotting for AKAP5, ADORA1, and PDE10A (Figure 4.10 E, F) not only confirmed a complex formation with PDE10A, but also supercomplex formation with ADORA1/PDE10A and thereby stringently regulating the cAMP concentration in the local microenvironment.
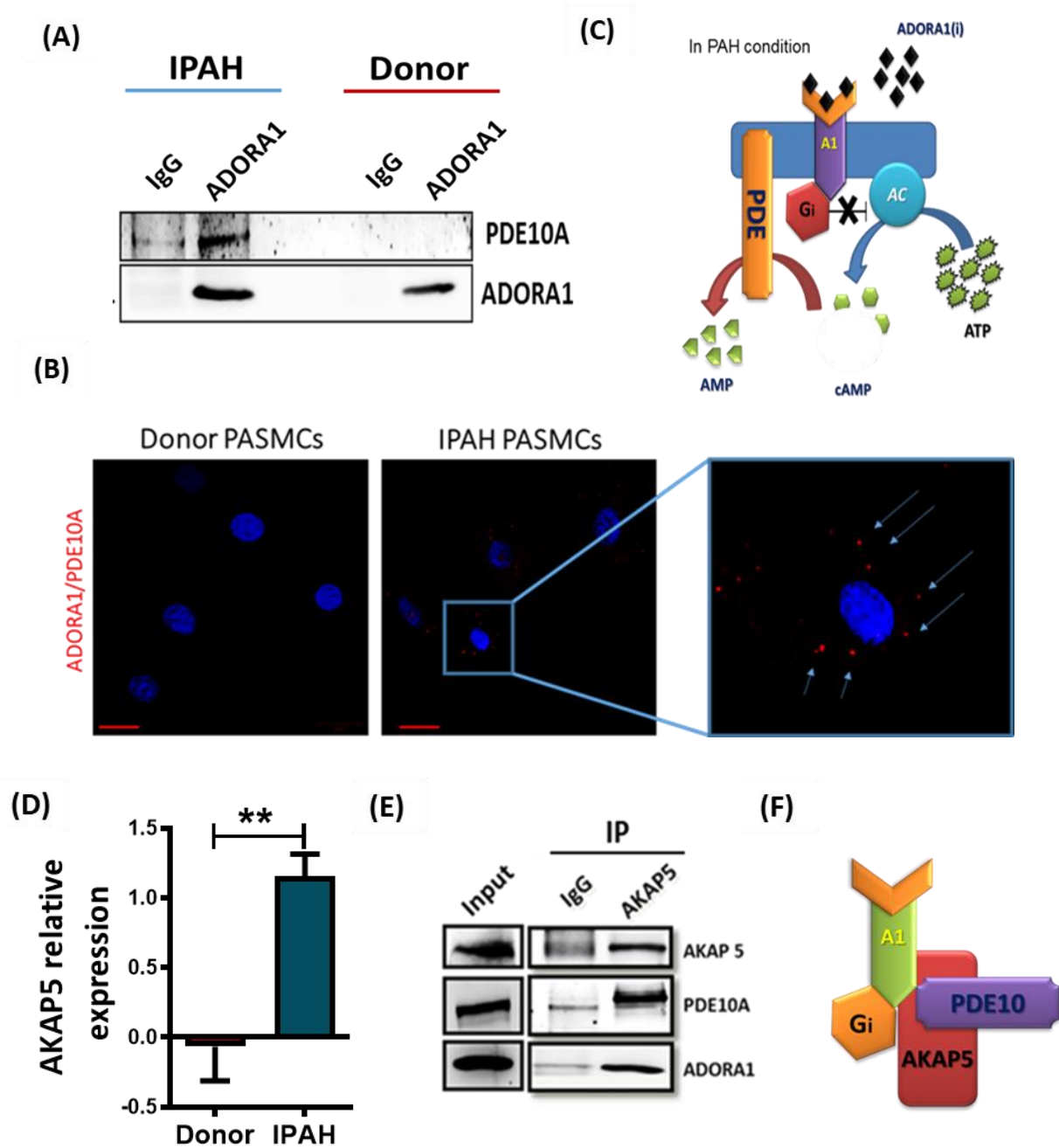
Figure 4.10. ADORA1, PDE10A, and AKAP5 form a supercomplex and regulates the cAMP microenvironment in IPAH PASMCs. (A) Co-IP was performed in IPAH- and donor- PASMCs by pulling down ADORA1 and blotting for both ADORA1 and PDE10A (n=3). (B) Confocal imaging of proximity ligation assay of ADORA1 and PDE10A in IPAH- and donor- PASMCs (n=3) scale bar= 20µm. (C) Proposed mechanism of cAMP regulation by ADORA1 and PDE10A in IPAH PASMCs. (D) AKAP5 expression analysis using qRT-PCR between the donor- (n=3) and IPAH- PASMCs (n=3), (E) Co-IP in IPAH PASMCs by pulling down AKAP5 (n=3), (F) Representative image of the supercomplex. Bars indicate means ± S.E.M. Data were analyzed using the unpaired student t-test. **p <0.01 *vs* Donor.

4.11 Combined knockdown of ADORA1 and PDE10A reverses hyperproliferative and apoptosis-resistant phenotype of IPAH PASMCs

To investigate the functional outcomes of targeting ADORA1/PDE10A complex in IPAH PASMCs, the cells were transfected with a combination of siRNAs targeting both ADORA1 and PDE10A, followed by assessment of proliferation and apoptosis (Figure 4.11 A). Indeed, in line with our assumption, combined knockdown of both, ADORA1 and PDE10A induced strong anti-proliferative (Figure 4.11 B) and pro-apoptotic (Figure 4.11 C) effects in IPAH PASMCs. Moreover, dual inhibition of ADORA1 and PDE10A led to a strong induction of intracellular cAMP concentration (Figure 4.11 D). These results suggest that ADORA1/PDE10A complex plays an important role in regulating the pathological phenotype observed in IPAH conditions.
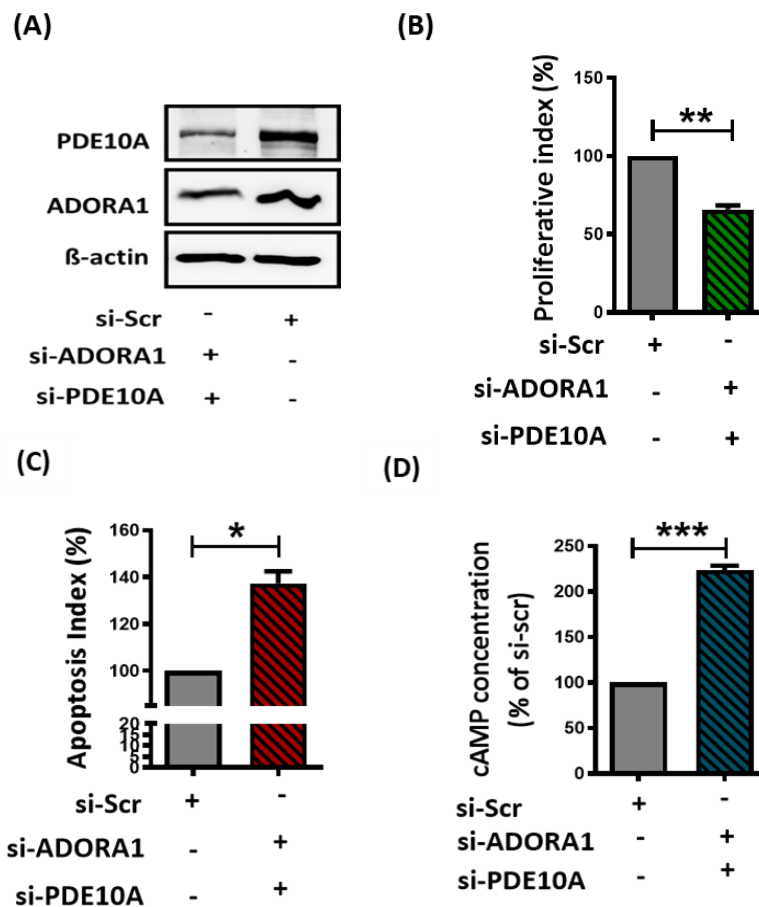
Figure 4.11. Functional effects of silencing ADORA1 and PDE10A in IPAH PASMCs stimulated with growth factors. (A) Western blot indicating knockdown efficiency of siRNAs targeting ADORA1 and PDE10A. (B) Measurement of proliferation using BrdU assay (n=3), (C) measurement of apoptosis using the cell death assay kit

(n=3), and (D) intracellular cAMP measurement using cAMP EIA kit (n=3). Bars indicate means ± S.E.M. Data were analyzed using paired t-test. *p <0.05, **p <0.01, ***p <0.001 *vs* si-Scr.

4.12 Dual inhibition of ADORA1 and PDE10A reverses hyperproliferative and apoptosis-resistant phenotype of IPAH PASMCs

The combined knockdown of ADORA1 and PDE10A reversed the hyperproliferative and apoptosis-resistant phenotype of IPAH PASMCs suggesting the therapeutic potential of this approach. Based on these promising data, we have developed a dual ADORA1 and PDE10A selective inhibitors (here after referred as Dual (i)) by rationale design, in a collaboration with Palobiofarma. To study the influence of dual inhibitor in *ex vivo* cultured diseased cells, IPAH PASMCs were treated with novel dual inhibitor targeting both ADORA1 and PDE10A (Figure 4.12 A), followed by measurements for proliferation, apoptosis, and level of intracellular cAMP. The novel inhibitor reversed the hyperproliferative (Figure 4.12 B) and apoptosis-resistant phenotype (Figure 4.12 C) of IPAH PASMCs as well as increased the intracellular cAMP concentration (Figure 4.12 D) compared to the DMSO control. These results show that targeting ADORA1/PDE10A using the dual inhibitor can be a potential therapeutic option for PH by inducing strong anti-proliferative and pro-apoptotic phenotype.
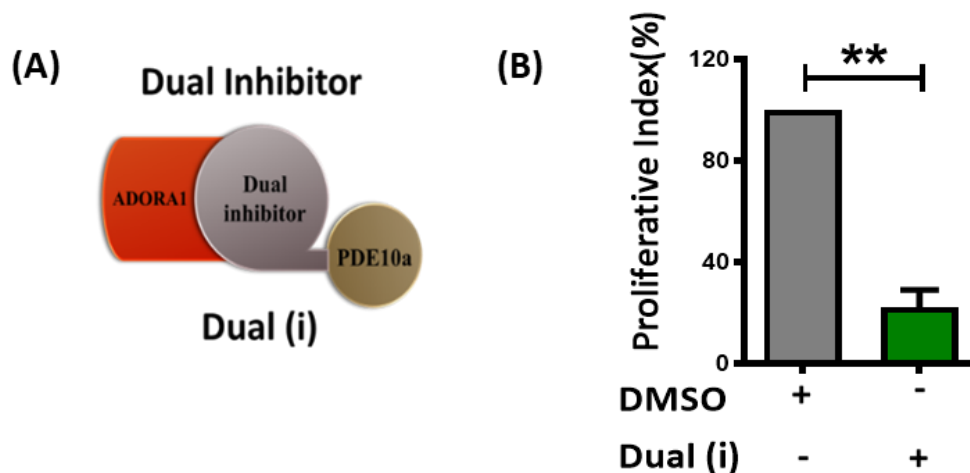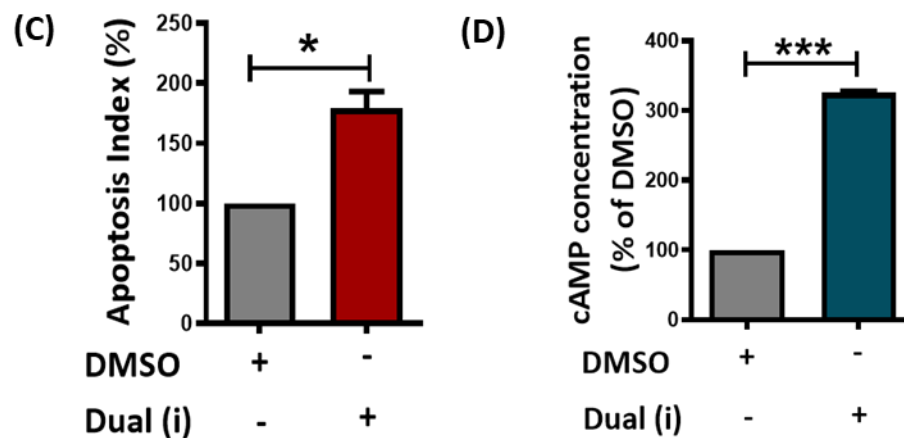
Figure 4.12. Functional effects of Dual inhibitor in IPAH PASMCs stimulated with growth factors. (A) Representative image of dual inhibitor targeting ADORA1and PDE10A. (B) Measurement of proliferation using BrdU assay (n=3), (C) measurement of apoptosis using the cell death assay kit (n=3), and (D) Intracellular cAMP measurement using cAMP EIA kit (n=3). Bars indicate means ± S.E.M. Data were analyzed using paired t-test. *p <0.05, **p <0.01, ***p <0.001 *vs* DMSO.

4.13   Dual inhibitor of ADORA1/PDE10A shows stronger anti-proliferative and pro-apoptotic effects than iloprost and sildenafil

The effect of the novel dual inhibitor was compared in the *in vitro* condition with the functional effects of currently approved PAH therapies such as iloprost and sildenafil. As to the experimental design, IPAH PASMCs were cultured in 96 well and 48 well plates, serum starved for 24hrs, afterwards treated with dual inhibitor, sildenafil, iloprost or vehicle (DMSO) in the presence of PASMC growth media for 24hrs, followed by assessment of proliferation and apoptosis respectively. As shown in Figure 4.13, dual inhibitor treatment caused a significant decrease in the proliferation rate, whereas sildenafil and iloprost have shown mild anti-proliferative effect (Figure 4.13 A). Similarly, pro-apoptotic effects were only observed upon the dual inhibitor treatment (Figure 4.13 B). These results suggest that the novel dual inhibitor can have stronger therapeutic potential compared to the currently approved PAH therapies like iloprost and sildenafil.
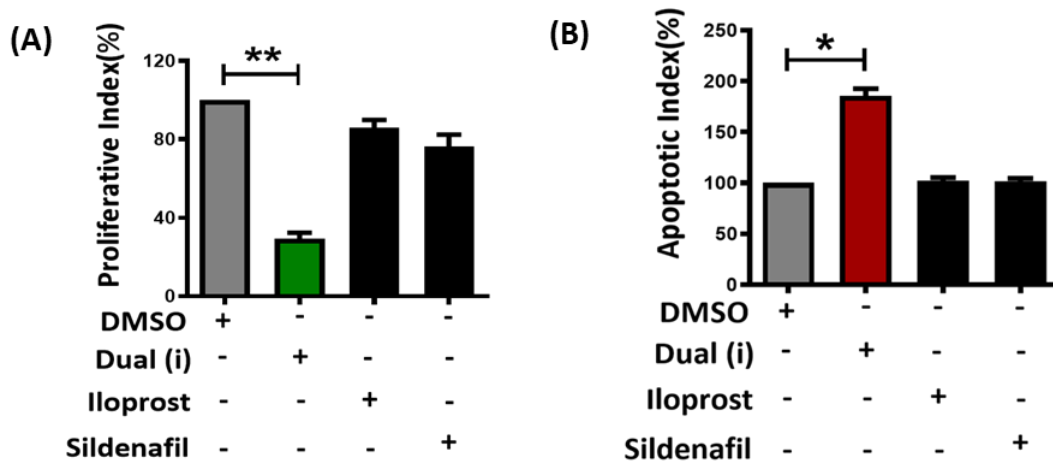
Figure 4.13. Effective reversal of disease phenotype in IPAH PASMCs treated with dual inhibitor compared to iloprost and sildenafil. (A) Measurement of proliferation using BrdU assay (n=3), and (B) measurement of apoptosis using the cell death assay kit (n=3), Bars indicate means ± S.E.M. Data were analyzed using one-way ANOVA with Dunnet's multiple comparison test. $*p < 0.05$, $**p < 0.01$ *vs* DMSO.

4.14 Dual inhibitor of ADORA1/PDE10A augments cAMP downstream signaling

Further to understand the downstream molecular mechanisms mediated by dual inhibitor that subsequently lead to the reversal of PH phenotype *ex vivo*, we evaluated the phosphorylation of CREB (Figure 4.14 D) and regulation of cell cycle regulator, p27 (Figure 4.14 E). Western blotting results demonstrate increased phosphorylation of CREB and an upregulation of p27 upon dual inhibitor treatment compared to control.
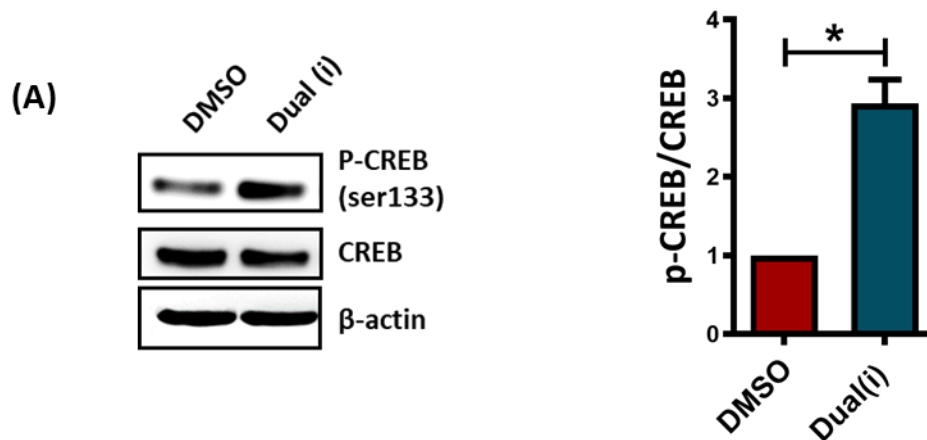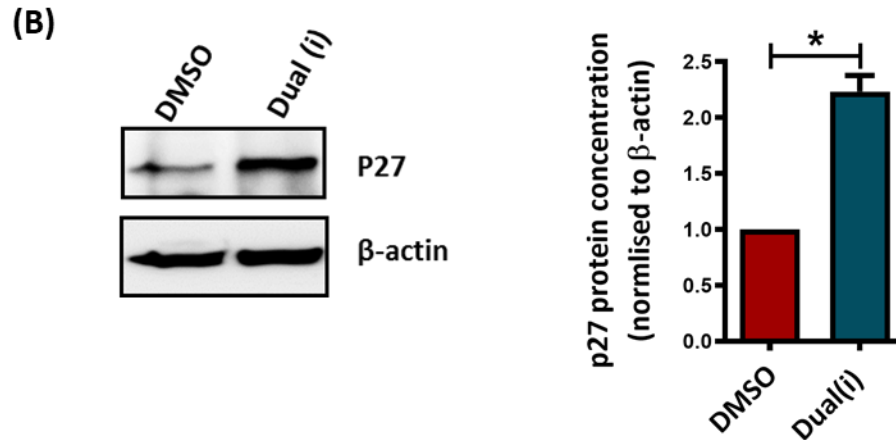
Figure 4.14. Dual inhibitor of ADORA1/PDE10A augments cAMP downstream signaling in IPAH PASMCs. (A) Western blotting of p-CREB, CREB and (B) p27 in IPAH PASMCs treated with dual inhibitor. *p <0.05 *vs* DMSO.

4.15 Dual inhibitor of ADORA1/PDE10A improves survival in MCT-PAH rats

To explore the therapeutic potential of dual inhibitor of ADORA1/PDE10A in *in vivo* settings, two established animal models of PAH that mimic human PAH were employed: Monocrotaline (MCT) induced PAH (here after referred as MCT-PAH) and hypoxia+SU5416 induced PAH (here after referred as SuHx-PAH) rat models [191, 192]. After the establishment of PAH, i.e. 21 days after subcutaneous injection of MCT, the rats were divided randomly into two groups, placebo and treatment groups. Strikingly, dual inhibitor treatment for 14 days (every 2nd day, oral gavage, 10mg/kg body weight) provided 50% more survival advantage compared to the placebo group (Figure 4.15 A). From these results, it was evident that the dual inhibitor has beneficial effects in terms of survival in the MCT-PAH rat model.

(A)
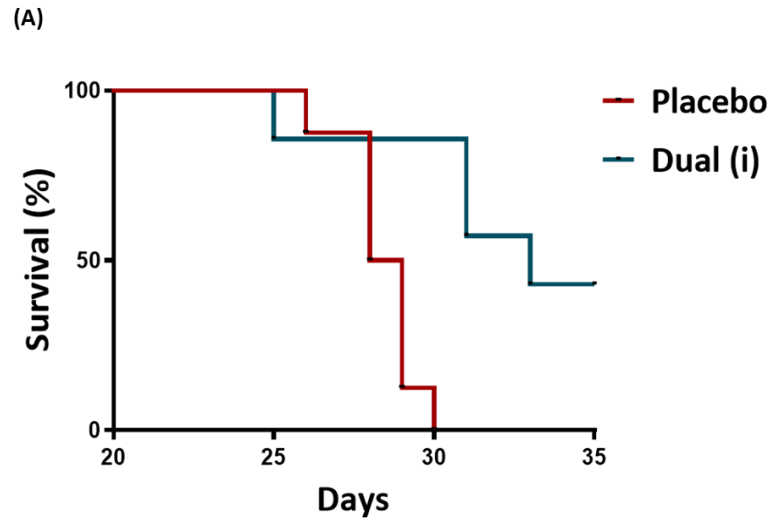
Figure 4.15: Effect of dual inhibitor on the survival of MCT-PAH rats. (A) Survival curve of MCT-PAH rats that were either treated with the dual inhibitor (n=8) or Placebo (n=8) for 14 days after the establishment of PAH.

4.16 Dual inhibitor of ADORA1/PDE10A improves cardiac function in MCT-PAH rats

To study the influence on RV dysfunction, an important predictor and characteristic of PAH [193], cardiac MRI was performed from the rats after 35 days of MCT injection (i.e. after 14 days treatment with dual inhibitor or placebo) (Figure 4.16 A). The images were further analyzed using the Mass4mice software to determine various RV functional parameters like cardiac output (Figure 4.16 B), ejection fraction (Figure 4.16 C), and stroke volume (Figure 4.16 D). Importantly, we have identified that dual inhibitor treatment led to 20% increase in ejection fraction, 100µl increase in stroke volume, and 47000 ml/min increase in the cardiac output compared to the placebo group, suggesting beneficial effects on RV. In accordance, post mortem analysis of RV hypertrophy (assessed as a ratio of RV/left ventricle + septum) was decreased in the treatment group compared to the placebo group (Figure 4.16 E).
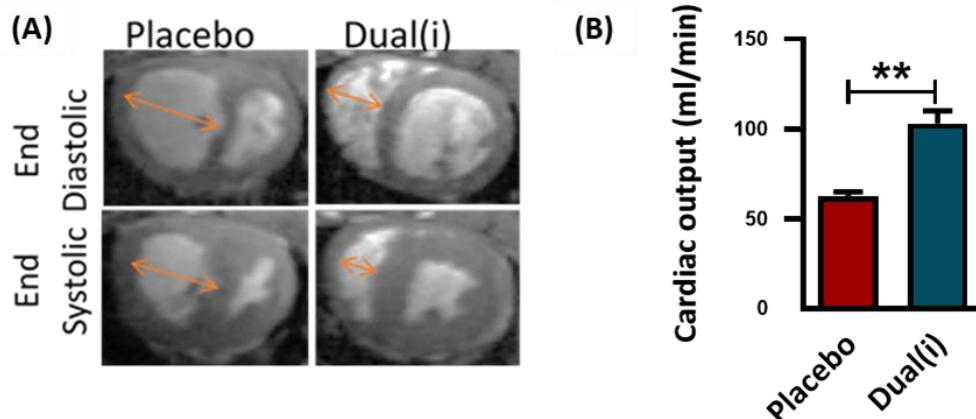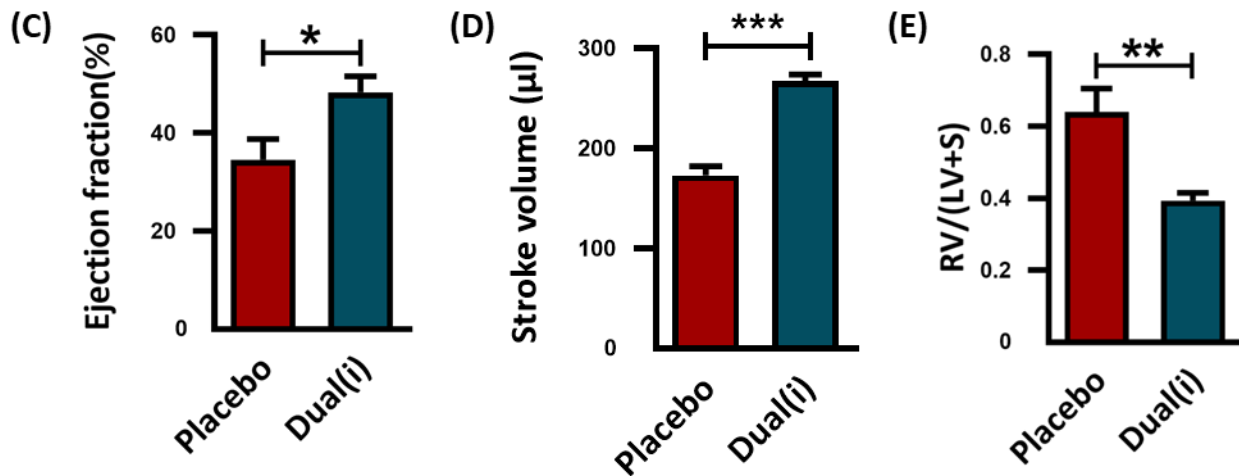
Figure 4.16. Effect of dual inhibitor on the right heart function of MCT-PAH rats. (A) Cardiac MRI image of MCT-PAH rats treated with either Placebo or dual inhibitor. (B) Cardiac output, (C) RV ejection fraction, and (D) RV stroke volume calculations from cardiac MRI from Placebo (n=4) and Dual inhibitor (n=6) treated groups. (E) Fulton index measurement (RV/LV+S) from Placebo (n=4) and Dual inhibitor (n=6) treated groups. Bars indicate means ± S.E.M. Data were analyzed using the unpaired student t-test. *p <0.05, **p <0.01, ***p <0.001 *vs* Placebo.

4.17 Dual inhibitor of ADORA1/PDE10A reduces pulmonary hemodynamic parameters in MCT-PAH rats

Further to study the effects on hemodynamics, one day after MRI, the rats were anaesthetized, followed by hemodynamic measurements using the closed chest right heart catheterization method. The total PVR (TPVR) was calculated from the RV systolic pressure (RVSP) obtained during hemodynamic measurement and the cardiac output obtained from the MRI analysis using the following formula TPVR= (80/3)*(RVSP/CO). Of note, the dual inhibitor treatment reduced the TPVR by 0.02 dyn*s/cm^5 compared to placebo (Figure 4.17 A). However, dual inhibitor didn´t exerted any influence on systemic arterial pressure (SAP) (Figure 4.17 B), suggesting selective pulmonary hemodynamic effects of dual ADORA1/PDE10A inhibitor.
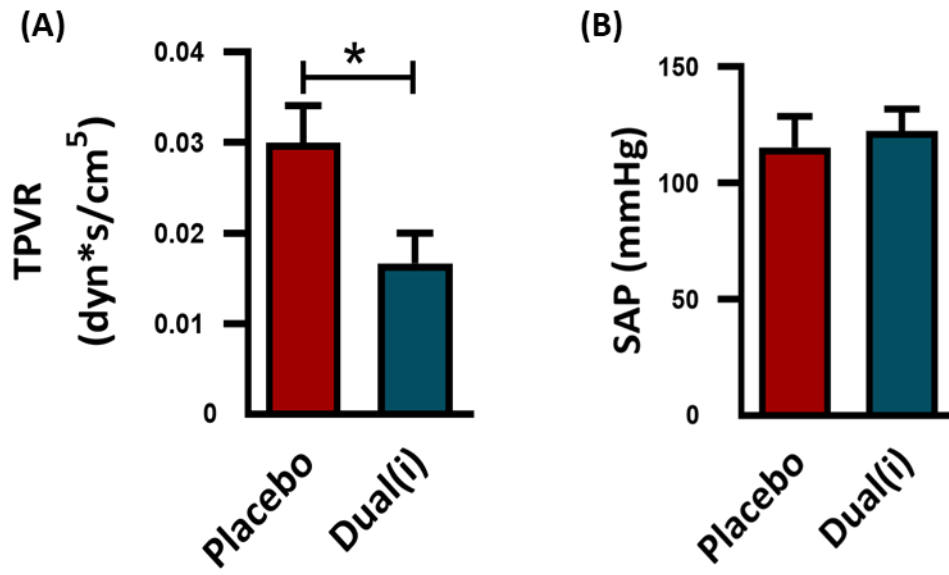
Figure 4.17. Effects of dual inhibitor on hemodynamics of MCT-PAH rats. (A) TPVR as calculated from RVSP and cardiac output, (B) systemic arterial pressure (SAP) measured from placebo (n=4) and dual inhibitor (n=6) treated groups. Bars indicate means ± S.E.M. Data were analyzed using the unpaired student t-test. *p <0.05 *vs* Placebo.

4.18 Dual inhibitor of ADORA1/PDE10A reverses pulmonary vascular remodeling in MCT-PAH rats

As the reduction of pulmonary hemodynamics by dual ADORA1/PDE10A inhibitor can be due to the alterations in pulmonary vascular remodeling, key structural alteration in PH. To assess the influence on pulmonary vascular remodeling, Weigart-Van Gieson staining was performed to determine the changes in medial wall thickness and immunostaining against α-SMA to determine the degree of muscularization in the vessels. The measurements were performed using the Leica go software from 100 vessels from each rat lungs. Elastica van Gieson staining and subsequent quantification demonstrated that a significant reduction of 48% in pulmonary vessels of size 20-50μm diameter, 50% decrease in 51-100μm diameter, with no significant change in >100μm diameter in dual inhibitor treated group compared to placebo group (Figure 4.18 A). Similarly, α-SMA staining and subsequent quantification revealed a significant decrease in fully muscularized pulmonary vessels, and a significant increase in both partially- and non- muscularized pulmonary vessels in dual inhibitor treated group compared to placebo group (Figure 4.18 B). These results demonstrate that dual inhibitor treatment significantly decreases the pulmonary vascular remodeling compared to the placebo treated groups.
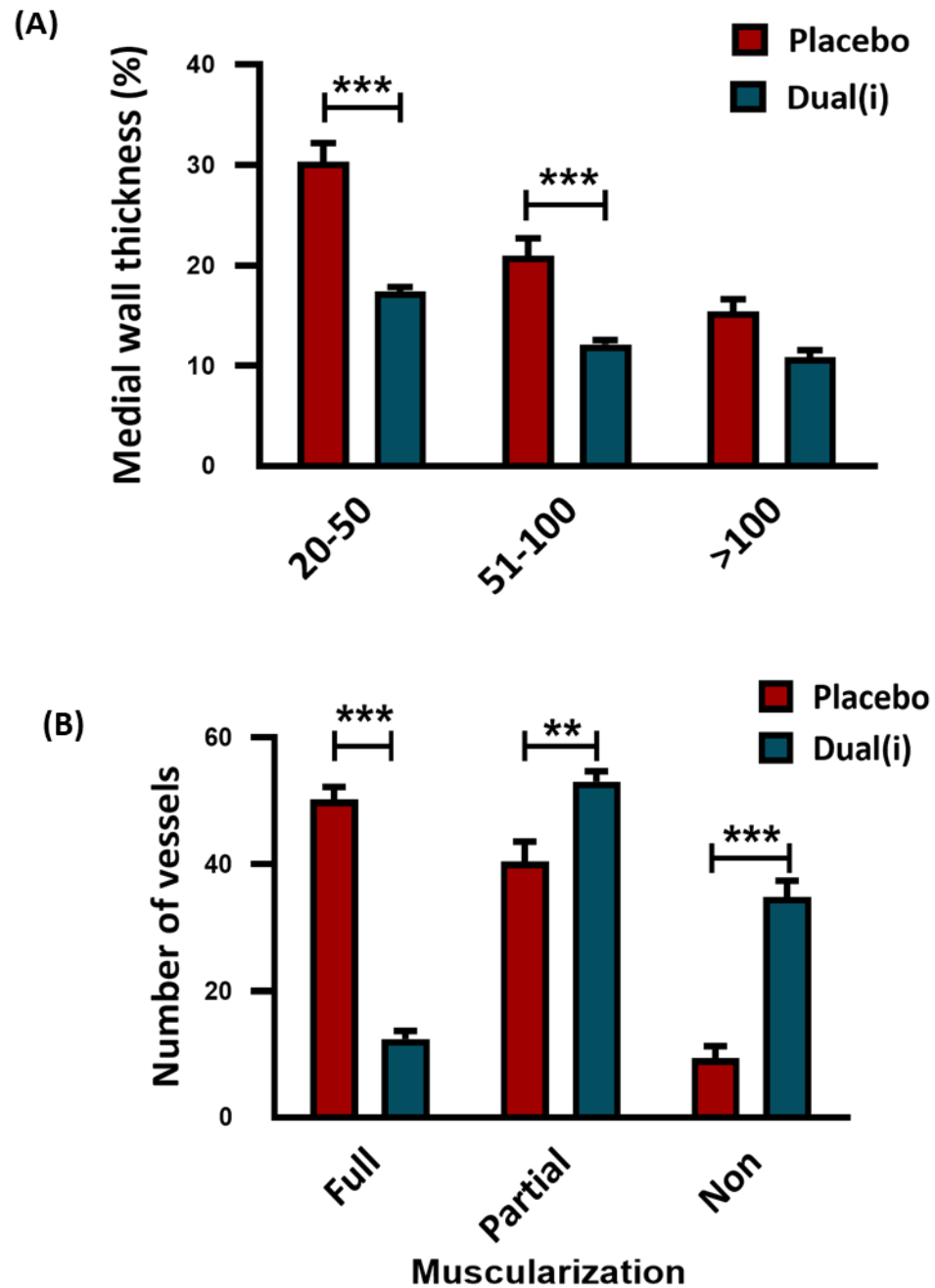
Figure 4.18. Effect of dual inhibitor on pulmonary vascular remodeling in MCT-PAH rats. (A) Medial wall thickness and (B) muscularization of measurements of different size diameter (20-50µm, 51-100µm, <100µm) pulmonary vessels from the lung tissues of placebo (n=4) and dual inhibitor (n=4) treated groups. Bars indicate means ± S.E.M. Data were analyzed using two-way ANOVA with Tukey's multiple comparison. **p <0.01, ***p <0.001 *vs* Placebo.

4.19 Dual inhibitor of ADORA1/PDE10A improves cardiac function in SuHx-PAH rats

The SuHx rats after exposure to 21days of hypoxia were taken for the pretreatment cardiac MRI and then were randomly split into two groups, those that received dual inhibitor or placebo (every 2nd day, oral gavage, 10mg/kg body weight) for 14 days. At the end of treatment protocol, the rats were taken for cardiac MRI for post-treatment measurements (Figure 4.19 A). The images were analyzed using Mass4mice software. The MRI analysis implicate maintenance of RV ejection fraction (Figure 4.19 B) in the dual inhibitor treatment group, whereas a significant decline in the placebo group. On the other hand, stroke volume (Figure 4.19 C) and cardiac output (Figure 4.19 D) have shown a significant increase after the dual inhibitor treatment, wherein the placebo group showed a decline compared to pre-treatment measurement. However, RV hypertrophy is not altered with dual inhibitor treatment compared to the placebo group (Figure 4.19 E). These results show that dual inhibitor has significant beneficial effects on RV function that has been severely impaired in SuHx rats.
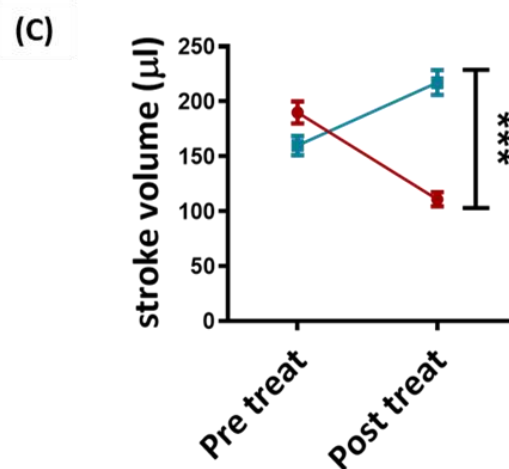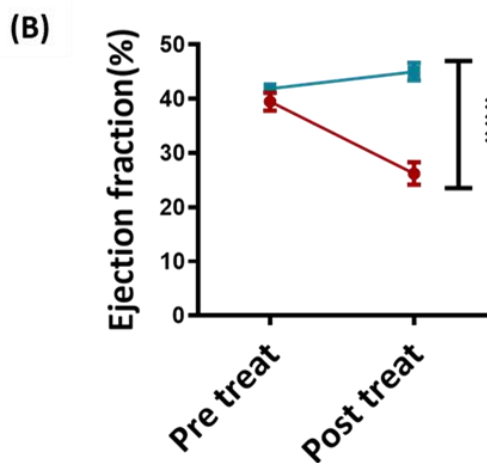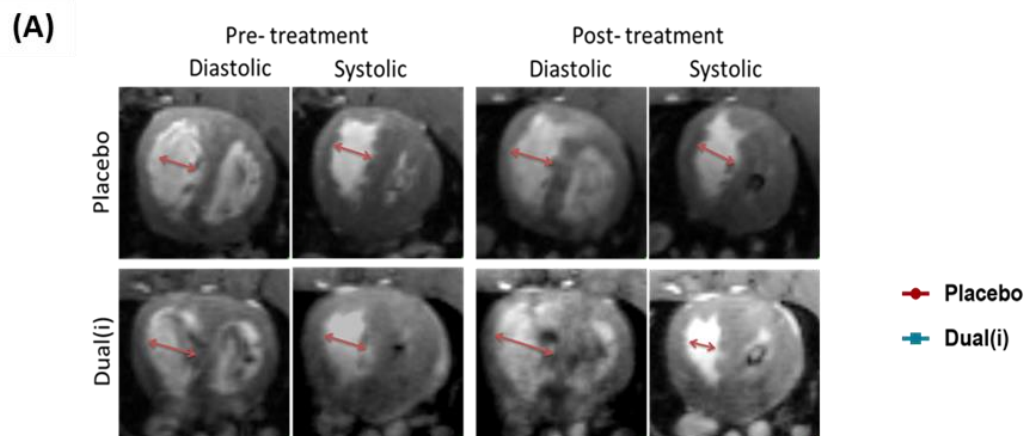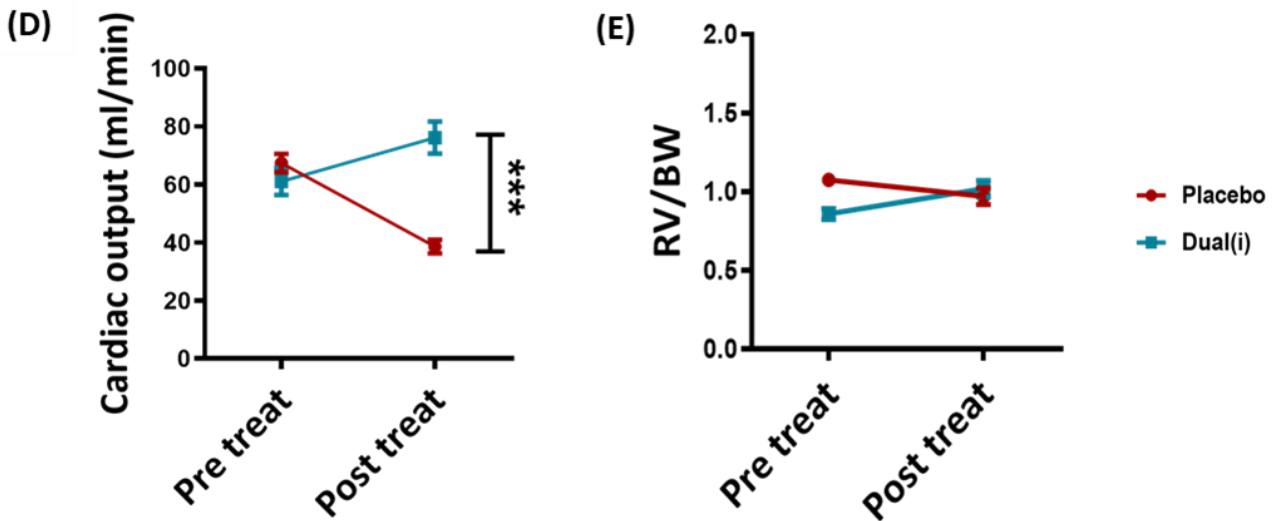
Figure 4.19. Effect of dual inhibitor on the cardiac functioning of SuHx-PAH rat model. (A) Cardiac MRI images of SuHx-PAH rats pre-and post-treatment with placebo or dual inhibitor. (B) RV ejection fraction, (C) RV stroke volume, (D) cardiac output, and (E) Fulton index (RV+LV+S) from cardiac MRI from Placebo (n=6) and dual inhibitor (n=6) treated groups. Bars indicate means $\pm$ S.E.M. Data were analyzed using two-way ANOVA with Tukey's multiple comparison. ***p <0.001 *vs* Placebo.

4.20 Dual inhibitor of ADORA1/PDE10A reduces pulmonary hemodynamic parameters in SuHx-PAH rats

The hemodynamic measurements were performed on rats using the closed chest right heart catheterization method after 35 days of SU5416 injection (i.e. after 14 days treatment with dual inhibitor or placebo). Notably, dual inhibitor treatment significantly reduced TPVR compared to placebo (Figure 4.20 A). However, dual inhibitor treatment didn´t have any influence on the systemic arterial pressure compared to placebo (Figure 4.20 B). These results show that the dual inhibitor treatment has significant therapeutic effects by lowering the total pulmonary vascular resistance.
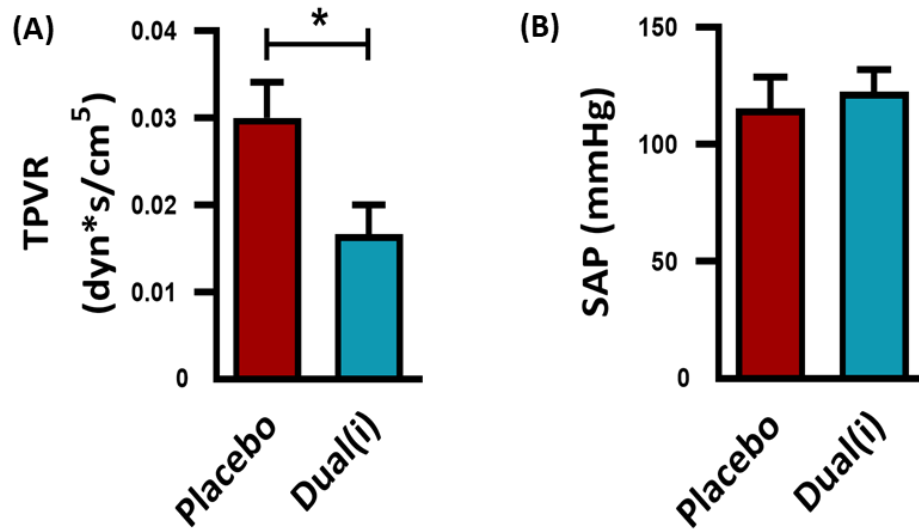
Figure 4.20. Dual inhibitor mediated hemodynamic effects on the SuHx-PAH rat model. (A) TPVR calculated from RVSP and Cardiac output, (B) systemic arterial pressure calculated from placebo (n=6) and Dual inhibitor treated groups (n=6). Bars indicate means ± S.E.M. Data were analyzed using the unpaired student t-test. *p <0.05 *vs* Placebo.

4.21 Dual inhibitor of ADORA1/PDE10A reverses pulmonary vascular remodeling in SuHx-PAH rats

As mentioned above, to assess the influence on pulmonary vascular remodeling, Weigart-Van Gieson staining was performed to determine the changes in medial wall thickness and immunostaining against α-SMA to determine the degree of muscularization in the vessels. Similar to MCT-PAH rats, dual inhibitor treatment caused a significant decrease in the medial wall thickness compared to placebo in all 3 size categories of pulmonary vessels (20-50, 51-100 and > 100 µm diameter) in SuHx rats (Figure 4.21 A). Similarly, dual inhibitor treatment significantly reduced the number of fully muscularized vessels, and an increase in the number of partially muscularized and non-muscularized pulmonary vessels compared to the placebo group (Figure 4.21 B). These results demonstrate that dual inhibitor treatment exerts therapeutic benefits by reducing pulmonary vascular remodeling in SuHx-PAH rats.
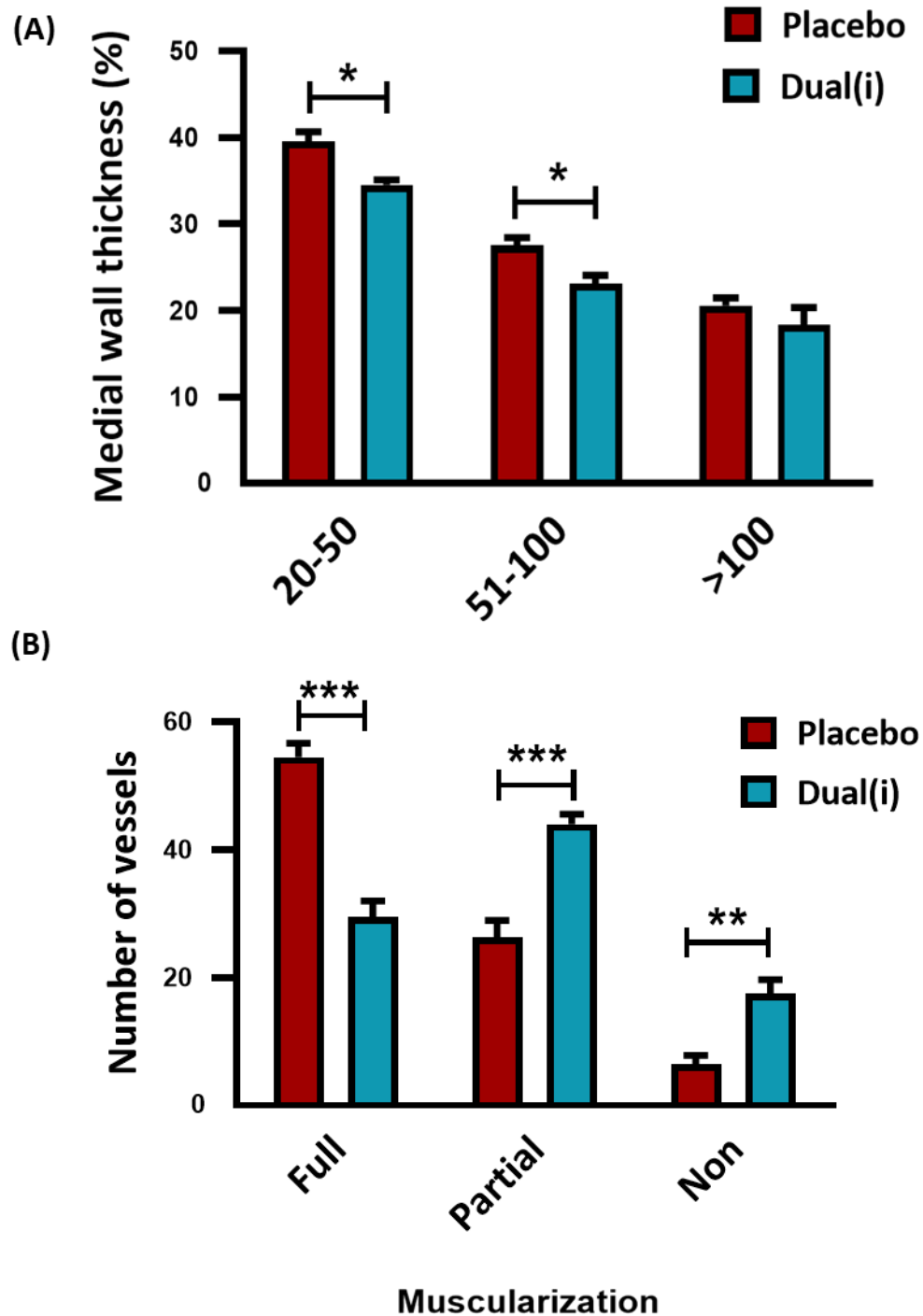
Figure 4.21. Dual inhibitor mediated effects on vascular remodeling in SuHx-PAH rat model. (A) Medial wall thickness measurements in pulmonary vessels, (B) muscularization measurements from placebo (n=4) and Dual inhibitor treated groups (n=4). Bars indicate means ± S.E.M. Data were analyzed using two-way ANOVA with Tukey's multiple comparison. *p <0.05, **p <0.01, ***p <0.001 *vs* Placebo.

5   DISCUSSION

Pulmonary hypertension (PH) is a multifactorial disease mainly characterized by increased pulmonary vascular pressure due to pathological remodeling of vessels, leading to heart failure. The role of dysregulated cAMP/cGMP signaling has been shown to play important role in PH progression by modulating the vascular tone and proliferation of pulmonary vascular cells. Several drugs have been approved for clinical management of PAH (Group 1 PH), an optimal outcome is yet to be achieved. Thus, it is important to investigate novel molecular targets as a therapeutic option for PAH. The major findings of this thesis are 1) decreased intracellular cAMP levels in IPAH PASMCs, 2) upregulation of both, ADORA1 as well as PDE10A resulting in decreased intracellular cAMP levels in IPAH PASMCs, 3) formation of ADORA1/PDE10A complex in AKAP5 microenvironment under the IPAH condition, 4) combined knockdown or dual inhibition of ADORA1/PDE10A by increasing intracellular cAMP concentration reversed pro-proliferative and apoptosis-resistant phenotype of IPAH PASMCs and 5) dual inhibitor of ADORA1/PDE10A reversed pulmonary vascular remodeling, regressed pulmonary hemodynamics and improved right ventricular function in both, MCT- and SuHx- rat models of PAH.

5.1   Dysregulated intracellular cAMP levels in pulmonary hypertension

Previous studies have shown that cAMP plays an important role in vascular homeostasis by maintaining 1) the endothelial barrier function, 2) vasodilation and 3) vascular smooth muscle proliferation [194-196]. The adenylyl cyclase (ACs) synthesizes the cAMP in response to various external stimuli and act as a secondary messenger. The primary messenger molecules dictate the induction or inhibition of cAMP production through various GPCRs [197]. The termination of cAMP signaling is mediated by the phosphodiesterase (PDE) enzymes, which converts cAMP to 5´AMP by hydrolysis [160]. Intracellular cAMP signaling is mediated majorly through the protein kinase A (PKA), exchange proteins activated by cAMP (EPACs), and cyclic nucleotide-gated channels [198, 199]. Vascular smooth muscle cells (VSMC) are specialized vascular cells, which functions by contraction and relaxation to maintain the vascular tone and blood pressure. In healthy vessels, the VSMCs maintain a contractile and low proliferating phenotype and during the vascular injury, the VSMCs converts to a more proliferative phenotype as repair response [200, 201]. A defect in the injury response mechanism leads to sustained proliferative VSMC phenotype resulting in pathological conditions such as atherosclerosis and hypertension [200]. cAMP signaling plays

an important role in maintaining the quiescence state of VSMC and resolution of vascular repair mechanism in the healthy vessels [202]. Several studies have shown that treatment with cAMP elevating agents such as AC activators and PDE inhibitors leads to strong inhibition of VSMCs proliferation both *in vitro* and *in vivo* [196, 203-205]. Notably, we have observed that observed that the PASMCs isolated from the IPAH patients not only maintains a hyperproliferative and anti-apoptotic phenotype (Figure 4.1 A, B), but also have reduced levels of intracellular cAMP levels (Figure 4.2 A) (Figure 5.1). This is in line with previous observations demonstrating the importance of intracellular cAMP in maintaining the VSMC quiescence. Thus, approaches to enhance cAMP levels can have therapeutic benefit in patients with PAH.
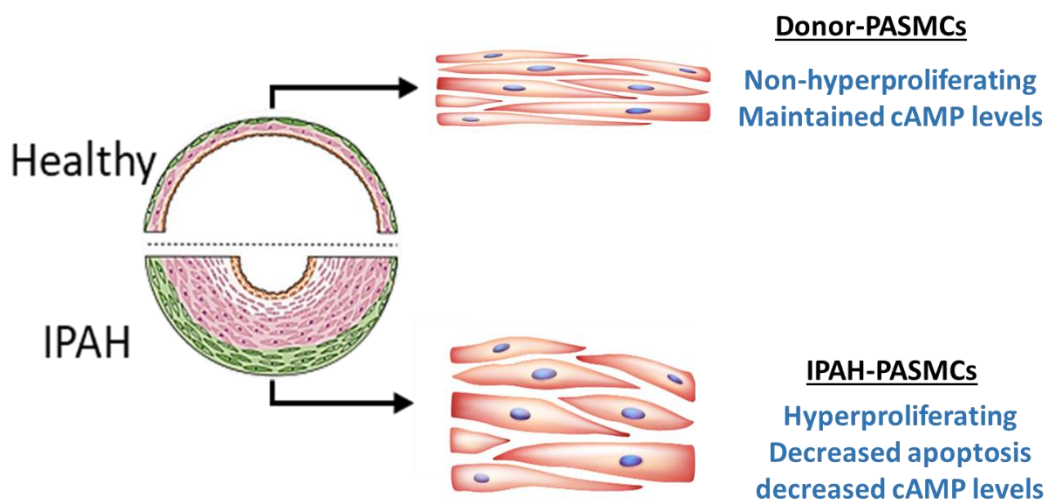
Figure: 5.1. Intracellular cAMP concentration and phenotypical characteristics of Donor and IPAH PASMCs

5.2   Adenosine receptor-mediated regulation of intracellular cAMP levels

Adenosine has been identified as an important modulator of intracellular cAMP levels and actively playing a role in maintaining the VSMC quiescence state [206, 207]. Adenosine is produced by the conversion of ATP by membrane bound enzymes called Ecto-5´-nucleotide (CD73) [208]. The adenosine-cAMP signaling is mainly dictated via the four adenosine receptors (ADOR)-A1, A2a, A2b, and A3. Activation of ADORA1 and ADORA3 decreases the intracellular cAMP levels by inhibiting the AC activity and, ADORA2a and ADORA2b increase the intracellular cAMP activity by activating the AC. Several pharmacological and genetic manipulation studies have shown that adenosine mediated inhibition of VSMC proliferation is mainly via the activation of ADORA2b and ADORA2a [209-213]. Previous studies have shown that pulmonary circulation maintains a higher level of adenosine compared to the systemic circulation, suggesting an important role in

maintaining pulmonary circulation homeostasis. However, of note, reduced levels of circulating adenosine levels were found in PAH patients [147, 214]. Moreover, in animal models of PH, ADORA2a agonists have been shown to play a beneficial role in the reversal of the disease phenotype [215, 216]. In contrast, the activation of ADORA2b has shown to drive vascular remodeling via non-cAMP mediated mechanism in chronic obstructive pulmonary disease- and pulmonary fibrosis- associated PH [156, 217]. All these studies suggest an important role of adenosine-cAMP signaling in maintaining vascular homeostasis under physiological and pathological conditions. In corroboration, the results from this study demonstrate severe deregulation of adenosine-cAMP signaling pathway molecules such as downregulation of CD73 (Figure 4.3 A-C) leading to poor availability of local adenosine for cAMP production and upregulation of ADORA1 (Figure 4.4 A, B and Figure 4.5 A, B) leading to decreased production of cAMP in IPAH patients. These results re-affirm the importance of disrupted cAMP signaling in PH pathobiology and indicates the therapeutic potential of targeting ADORA1 antagonists and/or CD73 agonists. Support, proof, validate, and substantiate, implications, likewise

5.3   *In vitro* effects of inhibiting ADORA1 in donor and IPAH PASMCs

Several cancer studies have shown that inhibiting ADORA1 leads to reduced proliferation and invasion [218, 219]. Similarly, ADORA1 antagonist treatment has been shown to induce apoptosis in breast cancer cells by upregulating p53 expression, while the ADORA1 agonist increased the cell viability and proliferation [220]. ADORA1 is also known to negatively impact the vascular tone [221]. In this study, I have identified that both approaches i.e. gene silencing and pharmacological inhibition of ADORA1 led to accumulation of intracellular cAMP levels and apoptosis induction in donor PASMCs (Figure 4.6 A-D & Figure 4.7 A-C). Astonishingly, these effects mediated by ADORA1 inhibition are selective to healthy/ donor cells, but doesn´t influence neither the phenotypic changes nor intracellular cAMP accumulation in IPAH PASMCs (Figure 4.8 A-F). A study from Fiona Murray *et al* has shown that unlike the donor PASMCs, the induction of intracellular cAMP concentration was severely impaired in the IPAH PASMCs upon treatment with forskolin (AC activator) or beraprost (prostacyclin analog). The intracellular cAMP levels were restored when the IPAH PASMCs were treated with forskolin or beraprost in combination with IBMX (general PDE inhibitor), suggesting a role of PDEs in tightly regulating the cAMP concentration in IPAH PASMCs [222]. Based on this study, I postulated an increased degradation of cAMP via cAMP hydrolyzing PDEs that counteracts the ADORA1 inhibition-mediated cAMP

accumulation in IPAH PASMCs (Figure 5.2). This led me to investigate whether ADORA1 forms a bidirectional regulatory complex with the PDE to tightly regulate intracellular cAMP levels in IPAH PASMCs.
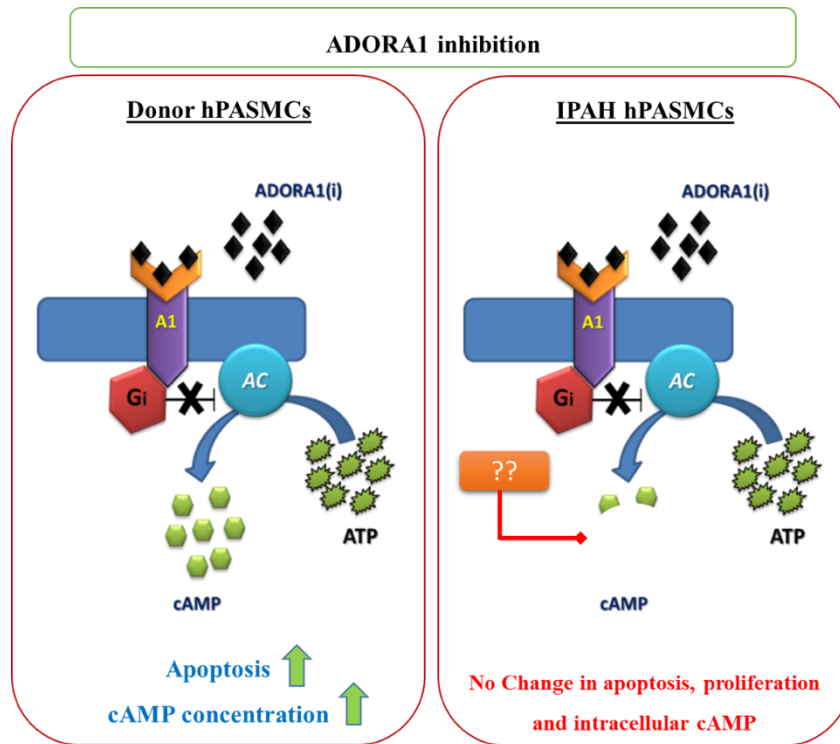
Figure: 5.2. Differential effects of Adenosine receptor A1 (A1) inhibition on Donor and IPAH PASMCs. A1-adenosine receptor A1, AC-adenylyl cyclase, ADORA1 (i) - adenosine receptor A1 inhibitor, ATP-adenosine triphosphate, 3', 5'-cyclic adenosine monophosphate.

The intracellular cyclic nucleotide signaling (cAMP, cGMP) is terminated mainly by PDEs. Studies have shown that activities of both cAMP- and cGMP targeting PDEs were upregulated in PAH condition [171, 222-224]. In the PASMCs isolated from PAH patients, the expression of PDE1, PDE3, PDE4, PDE5, PDE7 and PDE10 was upregulated [177, 189, 225]. The increased activity of these cAMP-PDEs mediate strong cAMP degradation mechanism, studies have shown unless treated with a PDE inhibitor, the cAMP accumulation in PAH-PASMCs was attenuated upon treatment with cAMP enhancing agonist such as forskolin and beraprost [222]. Various studies have shown that PDE is recruited to AC activity regulating receptors to induce tight cAMP regulation and have a localized effect. It was observed in the adult rat ventricular myocytes that

cAMP produced by glucagon receptor (Glu-Rs) stimulation was attenuated by increased PDE4 activity [226]. Inhibition of PDE3 and PDE4 was also found to increase cAMP formation upon stimulation of beta1-adrenergic receptors (beta1-ARs) in ventricular myocytes [226]. In human erythrocytes PDE2 inhibition and not PDE1 inhibition was found to potentiate the cAMP accumulation only upon beta-ARs stimulation but not for cAMP production mediated by IP receptor stimulation [227-229]. In pulmonary vessels, it has been shown that inhibition of PDE3 potentiates the cAMP accumulation mediated by prostacyclin analogs [176, 230]. These studies suggest that specific PDEs are found in close proximity with the G-coupled receptors to tightly regulate spatially and temporarily the cAMP mediated effects (referred as cAMP microdomains). In this study, we investigated whether ADORA1 forms a functional complex with any of the highly expressed cAMP targeting PDEs in IPAH conditions. Indeed, immunostaining and co-immunoprecipitation experiments evidenced co-localization of ADORA1 and PDE10A (Figure 4.9 A-C) and the formation of ADORA1 and PDE10A complex formation exclusively under IPAH condition (Figure 4.10 A-C). These results suggest the existence of a bidirectional regulatory system in IPAH PASMCs and could explain the attenuated effects of ADORA1 inhibition in IPAH PASMCs (Figure 5.3). Furthermore, this also hints that simultaneous targeting of both cAMP regulating enzymes, ADORA1 and PDE10A could accumulate intracellular cAMP even under PAH conditions. In corroboration, combined gene silencing of ADORA1 and PDE10A as well as dual inhibitor of ADORA1/PDE10A strongly induced the intracellular cAMP levels, the anti-proliferative and pro-apoptotic effects in IPAH PASMCs (Figure 4.11 A-D & Figure 4.12 A-D). Sildenafil and iloprost are among the FDA approved drugs for treating PAH patients. Importantly, iloprost is a prostacyclin analogue that elevates cAMP levels by binding to prostacyclin receptor. Notably, head-to-head comparison of dual inhibitor targeting ADORA1 and PDE10A with sildenafil and iloprost demonstrated that dual inhibitor is much more potent and exerts strong anti-proliferative and pro-apoptotic effects in IPAH PASMCs compared to the sildenafil and iloprost treatment *in vitro* (Figure 4.13 A, B). These results also highlight the necessity and therapeutic efficacy of targeting both cAMP synthesis and cAMP degradation (e.g. dual inhibitor of ADORA1/PDE10A) as compared to the targeting of cAMP synthesis alone (iloprost) in the setting of PAH.
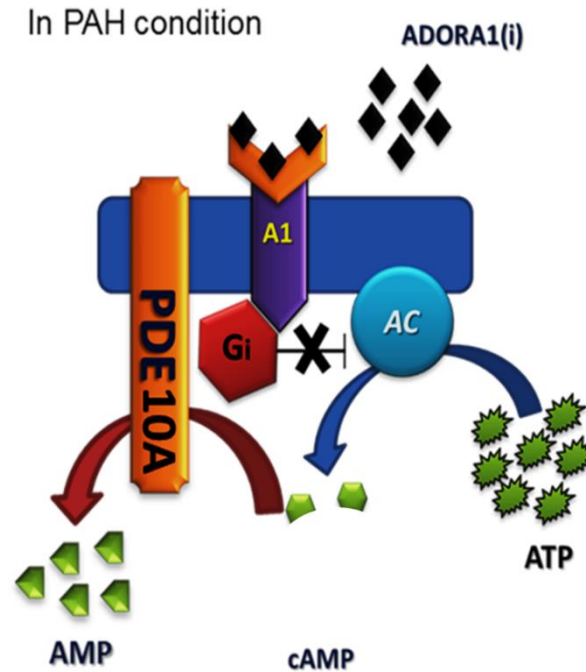
Figure: 5.3. Formation of bi-directional cAMP regulatory complex in IPAH PASMCs. A1-adenosine receptor A1, AC-adenylyl cyclase, ADORA1 (i) - adenosine receptor A1 inhibitor, ATP-adenosine triphosphate, 3', 5'-cyclic adenosine monophosphate, AMP- adenosine monophosphate, PDE10A-phosphodiesteraste 10A

5.4 ADORA1-PDE10A complex regulates the cAMP levels in the AKAP5 (AKAP79/AKAP150) microenvironment

Since the cAMP mediates a cascade of events upon several extracellular signals, it is important to maintain a compartmentalized signaling pattern in the intracellular space to sustain its signaling specificity [99, 231]. Interestingly this is achieved by the formation of multi-protein complexes with the help of large scaffolding proteins called AKAPs. The AKAP often forms a complex with signal transduction and signal-termination enzymes [232]. All AKAPs have been shown to interact with PKAs via the R subunits of PKA [233]. Several AKAPs have been shown to dictate the signal localization to certain subcellular compartments. Gravin (AKAP250) and AKAP18 have been shown to localize in the plasma membrane and DAKAP1 is localized in the mitochondria [95, 97, 234]. Several cAMP signaling modulators and effectors are brought together by the AKAPs as suggested by various studies. In 1995 Coghlan et al. observed AKAP79 to anchor with PKA and protein phosphatase 2B (PP2B), thereby establishing the multivalent paradigm for AKAPs in cAMP signaling [235]. One year later, Faux et al. Identified that PKC is also a part of this complex, thus forming a supercomplex of AKAP79-PKA-PP2B-PKC in the postsynaptic membranes [236,

237]. This supercomplex was found to facilitate the phosphorylation and regulation of various ion channels and N-methyl-D-aspartate receptor (NMDA)-type glutamate receptors, aquaporin water channels [238-240]. It has been also shown that AKAP150 is involved in controlling the vascular tone by modulating the calcium dependent contraction of VSMC [241, 242]. AKAP150 is the key anchoring protein in targeting PKCα to CaV1.2 channels and facilitates the prolonged channel opening [241]. PDE10A has been shown to interact with AKAP150 leading to localization to the synaptic membrane. Furthermore, cAMP effectors such as PKA, NMDA receptor subunits, and postsynaptic density protein 95 are also found as a part of the complex [190]. AKAP79 has shown to also interact with AC5 and AC6 (adenylyl cyclases widely expressed in SMC) and scaffolds to AMPA receptors [243]. In the pulmonary artery, AC5 has been observed to mediate the intracellular cAMP production and plays a role in inhibiting serum induced proliferation of PASMCs [244]. In this study, we found that AKAP5 (AKAP79) expression was upregulated in the IPAH PASMCs (Figure 4.14 A). In this study, employing co-immunoprecipitation, co-localization and proximity ligation assays identified AKAP5 as a scaffold protein that anchors ADORA1 and PDE10A forming a supercomplex of AKAP5-ADORA1-PDE10A that subsequently modulates localized cAMP in IPAH (Figure 4.14 B, C) (Figure 5.4). Previous studies have shown that inducing the cAMP/PKA signaling via the AKAP75 (AKAP5 rat ortholog) microenvironment inhibits the SMC proliferation *in vitro* and *in vivo* via increased p27 expression [245]. In line, our studies also reiterates that induction of cAMP signaling via dual inhibition of ADORA1/PDE10A induces the phosphorylation of CREB, a downstream target of PKA, and increases the levels of p27 expression in IPAH PASMCs (Figure 4.14 D, E). These data suggest that the ADORA1-PDE10A complex is the main modulator of cAMP concentration in the AKAP5 microenvironment.
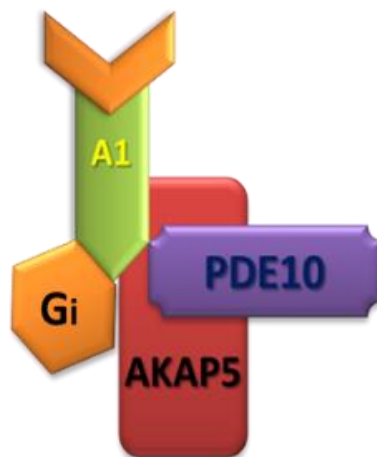
Figure: 5.4. ADORA1/PDE10A forms a bidirectional regulatory complex in the AKAP5 cAMP microenvironment. A1-adenosine receptor A1, PDE10A- phosphodiesterase 10A, AKAP5- A-kinase anchoring protein 5.

5.5 Combination therapy targeting ADORA1-PDE10A in the MCT- and SuHx- PAH rat models

Monocrotaline (MCT) injected rats and rats injected with Su5416 followed by exposure to hypoxia are the two well accepted PAH rat models [193]. The MCT, a toxic alkaloid, is subcutaneously injected into the rats leading to the PAH development characterized by increased medial wall thickening and in turn increasing the pressures in the pulmonary vasculature. This subsequently leads to RV dysfunction and structural changes, yet the pathological resemblance is not exact to the human PAH condition [191, 193]. In the SuHx-PAH rat model, a combination of SU5416, a vascular endothelial growth factor receptor 2 (VEGFR2) inhibitor, and hypobaric hypoxia is used for disease induction. The SuHx rats develop PAH as a result of endothelial cell death in the pulmonary artery followed by the emergence of apoptotic resistant cells. Interestingly the SuHx rat model develops neointima lesions closely resembling the human PAH pathology [192]. This model recapitulates severe PH elements such as elements of inflammation and angio-obliteration leading to RV failure [246]. In this study to observe the dual inhibitor mediated effects in the *in vivo* rat PAH models, we used MCT and SuHx rat models. It was observed that upon treatment with dual inhibitor targeting ADORA1-PDE10A, there was a better survival in the MCT rat PAH model (Figure 4.15 A). In both MCT and the SuHx-PAH models, targeting ADORA1-PDE10 in combination improved the cardiac function such as cardiac output, ejection fraction, and stroke volume (Figure 4.16 C-E & Figure 4.19 B-E). The total pulmonary vascular resistance and

pulmonary vascular remodeling were reduced by targeting the ADORA1-PDE10 in combination in both the experimental models of PAH (Figure 4.17, Figure 4.18, Figure 4.20 & Figure 4.21). These results demonstrated that combined inhibition of ADORA1/PDE10A has the ability to reverse the clinical features of established experimental PAH in vivo and offers a potential therapeutic option for PAH.

5.6   Conclusion

In the thesis, I have shown the intracellular cAMP levels are decreased in the hyperproliferating PASMCs derived from IPAH patients. The CD73 enzyme required for the conversion of ATP to adenosine was found to be down regulated in the IPAH PASMCs. These preliminary results motivated me to investigate the role of novel adenosine-cAMP signaling modulators in PAH. From the screening of adenosine receptors, I found that adenosine receptor A1 (ADORA1) was upregulated in the IPAH patient samples. Astonishingly, I observed that the inhibition of ADORA1 induced anti-apoptotic effects and intracellular cAMP concentration only in the donor PASMCs stimulated with growth factors but not in IPAH PASMCs.

This has led me to investigate whether any of the cAMP targeting PDEs are in close proximity to ADORA1 in IPAH PASMCs. The immunofluorescence staining has revealed that among PDE1, PDE3, PDE4, and PDE10, ADORA1 was in close proximity with PDE10A, which has been previously shown to be upregulated and highly active in the IPAH condition. Furthermore, co-immunoprecipitation, co-localization and proximity ligation assay confirmed that the ADORA1-PDE10A complex is formed exclusively under the disease condition. Targeting ADORA1 and PDE10A in combination using siRNA and inhibitors has been shown to induce strong anti-proliferative and pro-apoptotic effects in IPAH PASMCs, which was not observed with the ADORA1 inhibition alone. The intracellular cAMP levels were also increased with the dual inhibition of ADORA1 and PDE10A in IPAH PASMCs. To further delineate the molecular signaling targeted by the dual inhibition, I investigated if the ADORA1-PDE10A was scaffolded in the AKAP5 complex. Of note, I observed that in IPAH PASMCs ADORA1 and PDE10A were forming a complex with the AKAP5 and possibly regulating the cAMP in that microdomain. Targeting ADORA1-PDE10A induced the cAMP/PKA signaling pathway resulting in the phosphorylation of CREB and upregulation of p27.

Notably, the dual inhibition of ADORA1 and PDE10A improved survival in the MCT-PAH rat model. Especially, dual inhibition of ADORA1 and PDE10A reversed pulmonary vascular

remodeling, regressed pulmonary hemodynamics and improved right ventricular function in both, MCT- and SuHx- rat models of PAH. From these results, I conclude that ADORA1-PDE10A, a bidirectional cAMP regulatory complex found in the AKAP5 microenvironment can be a potential therapeutic target in PAH (Figure 5.5).
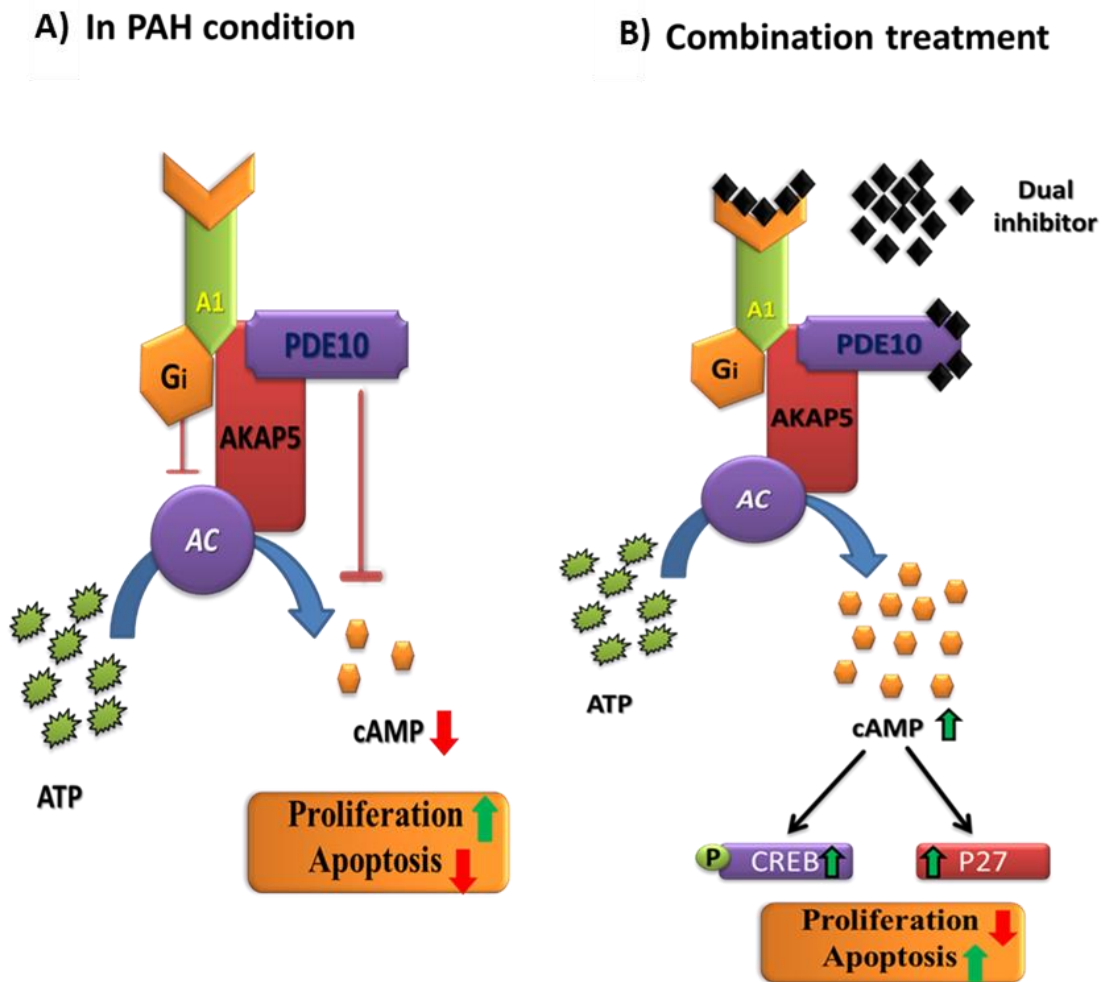
Figure: 5.5. Schematic representation showing the regulation of cAMP by the ADORA1/PDE10A complex in IPAH condition (A) and effect mediated by the combination therapy in IPAH condition (B). A1- adenosine receptor A1, AC- adenylyl cyclase, ATP- adenosine triphosphate, cAMP- 3', 5'-cyclic adenosine monophosphate, PDE10A-phosphodiesteraste 10A, A-kinase anchoring protein 5, p-CREB- phosphorylated cAMP response element binding protein, p27- Cyclin dependent kinase inhibitor 1B protein.

5.7   Future Perspectives

This study highlights the importance of the ADORA1/PDE10A bidirectional cAMP regulatory complex in PAH and targeting them in combination as a novel therapeutic option for treating PAH.

Future perspectives of this project should aim to delineate the downstream signaling effects imparted by the inhibition of ADORA1/PDE10A in PAH and to explore the influence of ADORA1/PDE10A bidirectional cAMP regulatory complex in right heart dysfunction observed in PAH.

5.7.1 Studying the role of ADORA1/PDE10A complex in mediating right ventricular failure in PAH

Previous studies have shown that the expression of ADORA1 was significantly upregulated in the meat-type chicken with acute RV failure and activation of ADORA1 leads to a reduction in the contraction rate [247, 248]. A recent study has shown that PDE10A expression was upregulated in the mouse and human failing hearts, but the expression was relatively low in normal and exercised hearts. Inhibition of PDE10A has also been shown to reduce myocardial hypertrophy, cardiac fibrosis, and dysfunction in the chronic pressure overload model via the transverse aorta constriction (TAC) [249]. From these studies, I hypothesize that the ADORA1/PDE10A complex may contribute to the RV dysfunction observed in the PAH patients. At first, the expression analysis and co-localization studies will be performed in the RV samples available from healthy, compensated, and decompensated patients. As a next step, dual ADORA1/PDE10A inhibitor studies will be performed in pulmonary artery banding (PAB) mice model, a lung independent RV dysfunction model. The results obtained from these experiments can address whether the formation of the ADORA1/PDE10A complex contributes to the progression to RV failure.

5.7.2 Investigating the specific downstream signaling mediated by the inhibition of ADORA1/PDE10A in the AKAP5 microenvironment

The current study has shown that ADORA1/PDE10A interacts with AKAP5 signalosome under the disease condition, it would be interesting to investigate what are the other interacting partners in this complex. A previous study has shown that using the AKAP5 fused to the A Kinase Activity Reporter 2 (AKAR2) biosensor system can detect the cAMP accumulation specifically in the AKAP5 microenvironment [250]. To screen for the novel interacting partners of the ADORA1/PDE10A/AKAP5 signalosome, two-step co-immunoprecipitation followed by mass spectroscopy analysis will be performed in the IPAH PASMCs. The interacting partners will be studied further to delineate their role in the progression of the disease condition.

5.7.3 Investigating the effect of the dual inhibitor on reversing the vascular remodeling using IPAH patients derived precession cut lung slice (PCLS) system

The encouraging results obtained from the dual inhibitor studies performed in the *in vivo* rat PAH models has opened the scope of taking this dual inhibitor for clinical trials. Previous studies have shown that using precession cut lung slices (PCLS) *ex vivo* system it is possible to observe the reversal of vascular remodeling upon treatment with pharmacological inhibitors and genetic inhibition [64, 251] (Figure 5.6). Thus, to complement our *in vivo* rat data, I aim to pharmacologically and genetically target ADORA1/PDE10A in the precession cut lung slices (PCLS) obtained from the IPAH patients and measure the change in the vascular remodeling.

1. PH Lungs
2. Filling low melting Agarose
3. Trimming agarose filled tissue
4. Sectioning using Vibrotome
5. Lung slices of 400µm thickness
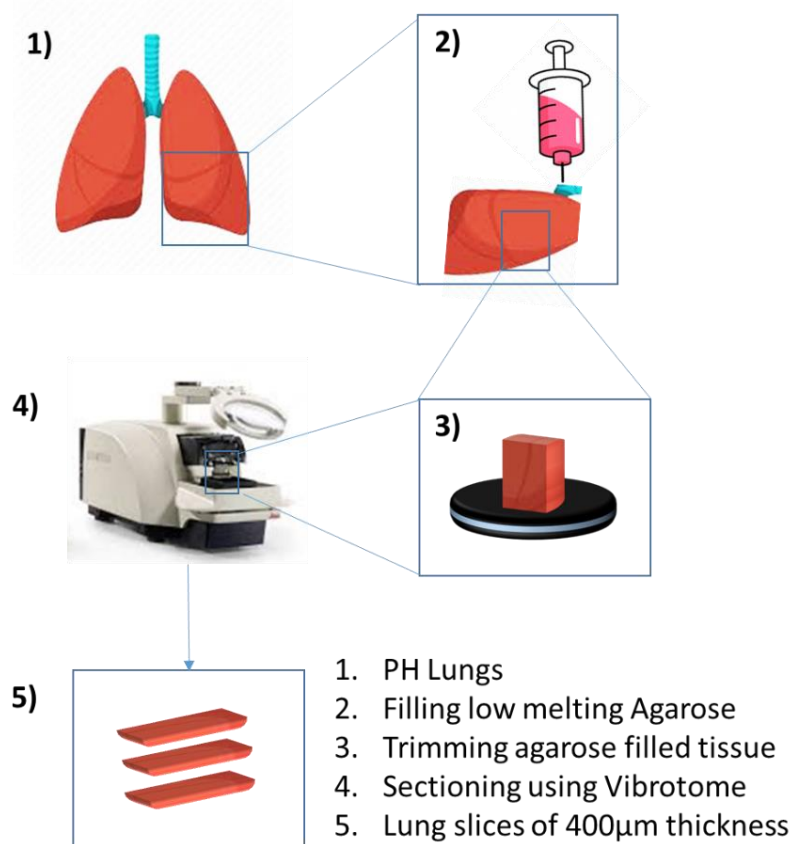
Figure: 5.6. Schematic representation showing the preparation of precession cut lung slices from human lungs

6   SUMMARY

Despite substantial advancements in the treatment of pulmonary arterial hypertension (PAH), obstacles still remain in achieving the optimal outcomes. Various treatments have been developed to target signaling pathways mostly leading to increased intracellular cAMP. The existence of intracellular cAMP microenvironment and various cAMP regulators and effectors as signalosome, adds a different level of complexity to the cAMP signaling. *In vitro* studies were performed majorly in donor and idiopathic PAH (IPAH) human pulmonary artery smooth muscle cells (PASMCs). To study the cAMP complex components, I used co-immunoprecipitation, immunofluorescence staining, and proximity ligation assay. Functional studies include assessment of proliferation and apoptosis in the presence or absence of ADORA1 and/or PDE10A siRNAs and inhibitors. cAMP levels were measured using ELISA kits. *In vivo* studies involve treatment of MCT-PAH and SU5416+Hypoxia-PAH rat models with dual ADORA1/PDE10A inhibitor for 14 days after establishment of PAH. After the treatment protocol, rats are subjected to cardiac MRI, right heart catheterization, and isolated lungs were taken for morphometric analysis. From the expression studies, (Figure 4.19 A) I observed that ADORA1 was highly expressed under the disease condition. Screening for cAMP inhibiting PDEs that can be colocalized with ADORA1, I observed a close proximity of ADORA1 with PDE10A compared to other cAMP targeting PDEs exclusively under PAH setting. PDE10A was also upregulated under the disease condition. From the functional studies, I demonstrate that genetic and pharmacological inhibition of ADORA1 and PDE10A induces pro-apoptotic and anti-proliferative effects in PASMCs isolated from IPAH patient lungs via increased cAMP levels. Impressively, in *in vivo* studies, the dual inhibitor treatment improved survival in the MCT-PAH rats compared to placebo. The hemodynamics and MRI data indicated that dual inhibitor treatment of MCT- and SuHx- rat models of PAH, significantly lowered pulmonary vascular resistance, reduced right ventricular hypertrophy, and improved cardiac performance. The morphometric analysis revealed that the MCT- and SuHx- PAH rats treated with dual inhibitors reversed pulmonary vascular remodeling i.e. reduced medial wall thickness and muscularization compared to the placebo group. In conclusion, these results show that targeting ADORA1/PDE10A signalosome regulated cAMP microenvironment is a promising step towards the development of novel and potent therapeutic strategy in the field of PAH.

7 ZUSAMMENFASSUNG

Trotz erheblicher Fortschritte bei der Behandlung der pulmonalen arteriellen Hypertonie (PAH) bleiben Hindernisse für die Erzielung der optimalen Ergebnisse bestehen. Es wurden verschiedene Behandlungen entwickelt, um auf Signalwege abzuzielen, die hauptsächlich zu einem erhöhten intrazellulären cAMP führen. Die Existenz einer intrazellulären cAMP-Mikroumgebung und verschiedener cAMP-Regulatoren und -Effektoren als Signalosom erhöht die Komplexität der cAMP-Signalübertragung. In-vitro Studien wurden hauptsächlich an glatten Muskelzellen (PASMCs) der menschlichen Lungenarterie von Spendern und IPAH-patienten durchgeführt. Um die cAMP komplexen Komponenten zu untersuchen, verwendete ich Co-Immunpräzipitation, Immunfluoreszenzfärbung und Proximity-Ligationstest. Funktionelle Studien umfassten die Bewertung der Proliferation und Apoptose in Gegenwart oder Abwesenheit von ADORA1- und / oder PDE10A-siRNAs und -Inhibitoren. Der cAMP-Spiegel wurde unter Verwendung von ELISA-Kits gemessen. In-vivo-Studien beinhalteten die Behandlung von MCT-PAH- und SU5416 + Hypoxia-PAH-Rattenmodellen mit dualem ADORA1 / PDE10A-Inhibitor für 14 Tage nach Etablierung von PH. Nach dem Behandlungsprotokoll wurden die Ratten einer Herz-MRT und einer Rechtsherzkatheterisierung unterzogen und die isolierten Lungen wurden zur morphometrischen Analyse entnommen. Aus den Expressionsstudien (Abbildung 4.19 A) ging hervor, dass ADORA1 unter den Krankheitsbedingungen stark exprimiert wurde. Beim Screening auf cAMP-inhibierende PDEs, die mit ADORA1 kolokalisiert sein können, beobachtete ich eine enge Nähe von ADORA1 mit PDE10A im Vergleich zu anderen cAMP-abzielenden-PDEs, ausschließlich mit PAH-Hintergrund. Ebenso war PDE10A unter dem Krankheitszustand hochreguliert. Durch die funktionellen Studien kann ich aufzeigen, dass die genetische und pharmakologische Inhibition von ADORA1 und PDE10A proapoptotische und antiproliferative Wirkungen in PASMCs induziert, die über erhöhte cAMP-Spiegel aus IPAH-Patientenlungen isoliert wurden. Beeindruckenderweise verbesserte in In-vivo Studien die duale Inhibitor-Behandlung das Überleben in MCT-PAH-Ratten im Vergleich zum Placebo. Die Hämodynamik- und MRT-Daten zeigten, dass die duale Inhibitor-Behandlung von MCT- und SuHx-Rattenmodellen mit PAH den Lungengefäßwiderstand signifikant senkte, die rechtsventrikuläre Hypertrophie verringerte und die Herzleistung verbesserte. Die morphometrische Analyse ergab, dass die mit den dualen Inhibitoren behandelten MCT- und SuHx-PAH-Ratten die Umgestaltung der Lungengefäße umkehrten, d. h. die mediale Wandstärke und Muskulatur im Vergleich zur

Placebogruppe verringerten. Zusammenfassend zeigen diese Ergebnisse, dass das Targeting der ADORA1 / PDE10A-Signalosomen-regulierten cAMP-Mikroumgebung ein vielversprechender Schritt zur Entwicklung einer neuen und wirksamen therapeutischen Strategie auf dem Gebiet der pulmonalen Hypertonie ist.

8   REFERENCES

1.   Boyette, L.C. and B. Burns, *Physiology, Pulmonary Circulation*, in *StatPearls*. 2020: Treasure Island (FL).
2.   Townsley, M.I., *Structure and composition of pulmonary arteries, capillaries, and veins.* Compr Physiol, 2012. **2**(1): p. 675-709.
3.   Brinkman, J.E. and S. Sharma, *Physiology, Pulmonary*, in *StatPearls*. 2020: Treasure Island (FL).
4.   Jeffery, T.K. and N.W. Morrell, *Molecular and cellular basis of pulmonary vascular remodeling in pulmonary hypertension.* Prog Cardiovasc Dis, 2002. **45**(3): p. 173-202.
5.   Kolpakov, V., et al., *Effect of mechanical forces on growth and matrix protein synthesis in the in vitro pulmonary artery. Analysis of the role of individual cell types.* Circ Res, 1995. **77**(4): p. 823-31.
6.   Chelladurai, P., W. Seeger, and S.S. Pullamsetti, *Matrix metalloproteinases and their inhibitors in pulmonary hypertension.* Eur Respir J, 2012. **40**(3): p. 766-82.
7.   Marini, T.J., et al., *Pictorial review of the pulmonary vasculature: from arteries to veins.* Insights Imaging, 2018. **9**(6): p. 971-987.
8.   Simonneau, G., et al., *Haemodynamic definitions and updated clinical classification of pulmonary hypertension.* Eur Respir J, 2019. **53**(1).
9.   Rabinovitch, M., *Molecular pathogenesis of pulmonary arterial hypertension.* J Clin Invest, 2012. **122**(12): p. 4306-13.
10.   Dewachter, L., et al., *Angiopoietin/Tie2 pathway influences smooth muscle hyperplasia in idiopathic pulmonary hypertension.* Am J Respir Crit Care Med, 2006. **174**(9): p. 1025-33.
11.   Thompson, K. and M. Rabinovitch, *Exogenous leukocyte and endogenous elastases can mediate mitogenic activity in pulmonary artery smooth muscle cells by release of extracellular-matrix bound basic fibroblast growth factor.* J Cell Physiol, 1996. **166**(3): p. 495-505.
12.   Alastalo, T.P., et al., *Disruption of PPARgamma/beta-catenin-mediated regulation of apelin impairs BMP-induced mouse and human pulmonary arterial EC survival.* J Clin Invest, 2011. **121**(9): p. 3735-46.
13.   Humbert, M., et al., *Pathology and pathobiology of pulmonary hypertension: state of the art and research perspectives.* Eur Respir J, 2019. **53**(1).
14.   Taraseviciene-Stewart, L., et al., *A bradykinin antagonist and a caspase inhibitor prevent severe pulmonary hypertension in a rat model.* Can J Physiol Pharmacol, 2002. **80**(4): p. 269-74.
15.   Liptay, M.J., et al., *Neointimal macrophages colocalize with extracellular matrix gene expression in human atherosclerotic pulmonary arteries.* J Clin Invest, 1993. **91**(2): p. 588-94.
16.   Khan, M., et al., *Physiology, Pulmonary Vasoconstriction*, in *StatPearls*. 2020: Treasure Island (FL).
17.   Mandegar, M., et al., *Cellular and molecular mechanisms of pulmonary vascular remodeling: role in the development of pulmonary hypertension.* Microvasc Res, 2004. **68**(2): p. 75-103.
18.   Huertas, A., et al., *Pulmonary vascular endothelium: the orchestra conductor in respiratory diseases: Highlights from basic research to therapy.* Eur Respir J, 2018. **51**(4).
19.   Dunham-Snary, K.J., et al., *Hypoxic Pulmonary Vasoconstriction: From Molecular Mechanisms to Medicine.* Chest, 2017. **151**(1): p. 181-192.

20. Christman, B.W., et al., *An imbalance between the excretion of thromboxane and prostacyclin metabolites in pulmonary hypertension.* N Engl J Med, 1992. **327**(2): p. 70-5.
21. Lo, C.C.W., S.M. Moosavi, and K.J. Bubb, *The Regulation of Pulmonary Vascular Tone by Neuropeptides and the Implications for Pulmonary Hypertension.* Front Physiol, 2018. **9**: p. 1167.
22. Galie, N., et al., *2015 ESC/ERS Guidelines for the diagnosis and treatment of pulmonary hypertension: The Joint Task Force for the Diagnosis and Treatment of Pulmonary Hypertension of the European Society of Cardiology (ESC) and the European Respiratory Society (ERS): Endorsed by: Association for European Paediatric and Congenital Cardiology (AEPC), International Society for Heart and Lung Transplantation (ISHLT).* Eur Heart J, 2016. **37**(1): p. 67-119.
23. Vonk-Noordegraaf, A., et al., *Right heart adaptation to pulmonary arterial hypertension: physiology and pathobiology.* J Am Coll Cardiol, 2013. **62**(25 Suppl): p. D22-33.
24. Bronicki, R.A. and H.P. Baden, *Pathophysiology of right ventricular failure in pulmonary hypertension.* Pediatr Crit Care Med, 2010. **11**(2 Suppl): p. S15-22.
25. Vonk Noordegraaf, A., et al., *Pathophysiology of the right ventricle and of the pulmonary circulation in pulmonary hypertension: an update.* Eur Respir J, 2019. **53**(1).
26. Frump, A.L., et al., *Emerging role of angiogenesis in adaptive and maladaptive right ventricular remodeling in pulmonary hypertension.* Am J Physiol Lung Cell Mol Physiol, 2018. **314**(3): p. L443-L460.
27. Maarman, G.J., et al., *Novel putative pharmacological therapies to protect the right ventricle in pulmonary hypertension: a review of current literature.* Br J Pharmacol, 2017. **174**(7): p. 497-511.
28. Pullamsetti, S.S., et al., *Transcription factors, transcriptional coregulators, and epigenetic modulation in the control of pulmonary vascular cell phenotype: therapeutic implications for pulmonary hypertension (2015 Grover Conference series).* Pulm Circ, 2016. **6**(4): p. 448-464.
29. Brusselmans, K., et al., *Heterozygous deficiency of hypoxia-inducible factor-2alpha protects mice against pulmonary hypertension and right ventricular dysfunction during prolonged hypoxia.* J Clin Invest, 2003. **111**(10): p. 1519-27.
30. Bonnet, S., et al., *An abnormal mitochondrial-hypoxia inducible factor-1alpha-Kv channel pathway disrupts oxygen sensing and triggers pulmonary arterial hypertension in fawn hooded rats: similarities to human pulmonary arterial hypertension.* Circulation, 2006. **113**(22): p. 2630-41.
31. Masri, F.A., et al., *Hyperproliferative apoptosis-resistant endothelial cells in idiopathic pulmonary arterial hypertension.* Am J Physiol Lung Cell Mol Physiol, 2007. **293**(3): p. L548-54.
32. Li, X., et al., *Notch3 signaling promotes the development of pulmonary arterial hypertension.* Nat Med, 2009. **15**(11): p. 1289-97.
33. Firth, A.L., et al., *Upregulation of Oct-4 isoforms in pulmonary artery smooth muscle cells from patients with pulmonary arterial hypertension.* Am J Physiol Lung Cell Mol Physiol, 2010. **298**(4): p. L548-57.
34. Price, L.C., et al., *Nuclear factor kappa-B is activated in the pulmonary vessels of patients with end-stage idiopathic pulmonary arterial hypertension.* PLoS One, 2013. **8**(10): p. e75415.
35. Ranchoux, B., et al., *Endothelial-to-mesenchymal transition in pulmonary hypertension.* Circulation, 2015. **131**(11): p. 1006-18.

36.   Ghatnekar, A., et al., *Endothelial GATA-6 deficiency promotes pulmonary arterial hypertension.* Am J Pathol, 2013. **182**(6): p. 2391-406.

37.   Ameshima, S., et al., *Peroxisome proliferator-activated receptor gamma (PPARgamma) expression is decreased in pulmonary hypertension and affects endothelial cell growth.* Circ Res, 2003. **92**(10): p. 1162-9.

38.   Savai, R., et al., *Pro-proliferative and inflammatory signaling converge on FoxO1 transcription factor in pulmonary hypertension.* Nat Med, 2014. **20**(11): p. 1289-300.

39.   Mizuno, S., et al., *p53 Gene deficiency promotes hypoxia-induced pulmonary hypertension and vascular remodeling in mice.* Am J Physiol Lung Cell Mol Physiol, 2011. **300**(5): p. L753-61.

40.   Kim, J., et al., *Restoration of impaired endothelial myocyte enhancer factor 2 function rescues pulmonary arterial hypertension.* Circulation, 2015. **131**(2): p. 190-9.

41.   Shatat, M.A., et al., *Endothelial Kruppel-like factor 4 modulates pulmonary arterial hypertension.* Am J Respir Cell Mol Biol, 2014. **50**(3): p. 647-53.

42.   Goldberg, A.D., C.D. Allis, and E. Bernstein, *Epigenetics: a landscape takes shape.* Cell, 2007. **128**(4): p. 635-8.

43.   Trerotola, M., et al., *Epigenetic inheritance and the missing heritability.* Hum Genomics, 2015. **9**: p. 17.

44.   Chelladurai, P., W. Seeger, and S.S. Pullamsetti, *Epigenetic mechanisms in pulmonary arterial hypertension: the need for global perspectives.* Eur Respir Rev, 2016. **25**(140): p. 135-40.

45.   Bonisch, C. and S.B. Hake, *Histone H2A variants in nucleosomes and chromatin: more or less stable?* Nucleic Acids Res, 2012. **40**(21): p. 10719-41.

46.   Archer, S.L., et al., *Epigenetic attenuation of mitochondrial superoxide dismutase 2 in pulmonary arterial hypertension: a basis for excessive cell proliferation and a new therapeutic target.* Circulation, 2010. **121**(24): p. 2661-71.

47.   Cohen, I., et al., *Histone modifiers in cancer: friends or foes?* Genes Cancer, 2011. **2**(6): p. 631-47.

48.   Xu, X.F., et al., *Epigenetic regulation of the endothelial nitric oxide synthase gene in persistent pulmonary hypertension of the newborn rat.* J Hypertens, 2010. **28**(11): p. 2227-35.

49.   Li, M., et al., *Emergence of fibroblasts with a proinflammatory epigenetically altered phenotype in severe hypoxic pulmonary hypertension.* J Immunol, 2011. **187**(5): p. 2711-22.

50.   Humbert, M., et al., *Platelet-derived growth factor expression in primary pulmonary hypertension: comparison of HIV seropositive and HIV seronegative patients.* Eur Respir J, 1998. **11**(3): p. 554-9.

51.   Schermuly, R.T., et al., *Reversal of experimental pulmonary hypertension by PDGF inhibition.* J Clin Invest, 2005. **115**(10): p. 2811-21.

52.   Merklinger, S.L., et al., *Epidermal growth factor receptor blockade mediates smooth muscle cell apoptosis and improves survival in rats with pulmonary hypertension.* Circulation, 2005. **112**(3): p. 423-31.

53.   Sakao, S., et al., *VEGF-R blockade causes endothelial cell apoptosis, expansion of surviving CD34+ precursor cells and transdifferentiation to smooth muscle-like and neuronal-like cells.* FASEB J, 2007. **21**(13): p. 3640-52.

54.   Tuder, R.M., et al., *Expression of angiogenesis-related molecules in plexiform lesions in severe pulmonary hypertension: evidence for a process of disordered angiogenesis.* J Pathol, 2001. **195**(3): p. 367-74.

55.   Jones, P.L., K.N. Cowan, and M. Rabinovitch, *Tenascin-C, proliferation and subendothelial fibronectin in progressive pulmonary vascular disease.* Am J Pathol, 1997. **150**(4): p. 1349-60.

56.   Frost, A.E., et al., *Long-term safety and efficacy of imatinib in pulmonary arterial hypertension.* J Heart Lung Transplant, 2015. **34**(11): p. 1366-75.

57.   Hoeper, M.M., et al., *Imatinib mesylate as add-on therapy for pulmonary arterial hypertension: results of the randomized IMPRES study.* Circulation, 2013. **127**(10): p. 1128-38.

58.   Jusic, A., Y. Devaux, and E.U.-C.C. Action, *Noncoding RNAs in Hypertension.* Hypertension, 2019. **74**(3): p. 477-492.

59.   Bertero, T., et al., *Systems-level regulation of microRNA networks by miR-130/301 promotes pulmonary hypertension.* J Clin Invest, 2014. **124**(8): p. 3514-28.

60.   Bertero, T., et al., *The microRNA-130/301 family controls vasoconstriction in pulmonary hypertension.* J Biol Chem, 2015. **290**(4): p. 2069-85.

61.   Jin, Q., et al., *Long noncoding RNAs: emerging roles in pulmonary hypertension.* Heart Fail Rev, 2020. **25**(5): p. 795-815.

62.   Wang, D., et al., *Long noncoding RNA MALAT1 sponges miR1243p.1/KLF5 to promote pulmonary vascular remodeling and cell cycle progression of pulmonary artery hypertension.* Int J Mol Med, 2019. **44**(3): p. 871-884.

63.   Zhou, S., et al., *Estrogen administration reduces the risk of pulmonary arterial hypertension by modulating the miR-133a signaling pathways in rats.* Gene Ther, 2020. **27**(3-4): p. 113-126.

64.   Zehendner, C.M., et al., *Long Noncoding RNA TYKRIL Plays a Role in Pulmonary Hypertension via the p53-mediated Regulation of PDGFRbeta.* Am J Respir Crit Care Med, 2020. **202**(10): p. 1445-1457.

65.   Sun, Z., et al., *Long Non-Coding RNA MEG3 Downregulation Triggers Human Pulmonary Artery Smooth Muscle Cell Proliferation and Migration via the p53 Signaling Pathway.* Cell Physiol Biochem, 2017. **42**(6): p. 2569-2581.

66.   Josipovic, I., et al., *Long noncoding RNA LISPR1 is required for S1P signaling and endothelial cell function.* J Mol Cell Cardiol, 2018. **116**: p. 57-68.

67.   Gong, J., et al., *Long non-coding RNA CASC2 suppresses pulmonary artery smooth muscle cell proliferation and phenotypic switch in hypoxia-induced pulmonary hypertension.* Respir Res, 2019. **20**(1): p. 53.

68.   Omura, J., et al., *Identification of Long Noncoding RNA H19 as a New Biomarker and Therapeutic Target in Right Ventricular Failure in Pulmonary Arterial Hypertension.* Circulation, 2020. **142**(15): p. 1464-1484.

69.   Sutherland, E.W. and T.W. Rall, *Fractionation and characterization of a cyclic adenine ribonucleotide formed by tissue particles.* J Biol Chem, 1958. **232**(2): p. 1077-91.

70.   McKnight, G.S., *Cyclic AMP second messenger systems.* Curr Opin Cell Biol, 1991. **3**(2): p. 213-7.

71.   Mathiesen, J.M., L. Vedel, and H. Brauner-Osborne, *cAMP biosensors applied in molecular pharmacological studies of G protein-coupled receptors.* Methods Enzymol, 2013. **522**: p. 191-207.

72.	Pierce, K.L., R.T. Premont, and R.J. Lefkowitz, *Seven-transmembrane receptors.* Nat Rev Mol Cell Biol, 2002. **3**(9): p. 639-50.

73.	Savai, R., et al., *Targeting cancer with phosphodiesterase inhibitors.* Expert Opin Investig Drugs, 2010. **19**(1): p. 117-31.

74.	Taylor, S.S., et al., *Structural framework for the protein kinase family.* Annu Rev Cell Biol, 1992. **8**: p. 429-62.

75.	Tasken, K., et al., *Structure, function, and regulation of human cAMP-dependent protein kinases.* Adv Second Messenger Phosphoprotein Res, 1997. **31**: p. 191-204.

76.	Sassone-Corsi, P., *The cyclic AMP pathway.* Cold Spring Harb Perspect Biol, 2012. **4**(12).

77.	Sassone-Corsi, P., *Transcription factors responsive to cAMP.* Annu Rev Cell Dev Biol, 1995. **11**: p. 355-77.

78.	Mayr, B. and M. Montminy, *Transcriptional regulation by the phosphorylation-dependent factor CREB.* Nat Rev Mol Cell Biol, 2001. **2**(8): p. 599-609.

79.	Bos, J.L., *Epac: a new cAMP target and new avenues in cAMP research.* Nat Rev Mol Cell Biol, 2003. **4**(9): p. 733-8.

80.	Zaccolo, M. and T. Pozzan, *CAMP and Ca2+ interplay: a matter of oscillation patterns.* Trends Neurosci, 2003. **26**(2): p. 53-5.

81.	Calebiro, D. and I. Maiellaro, *cAMP signaling microdomains and their observation by optical methods.* Front Cell Neurosci, 2014. **8**: p. 350.

82.	Corbin, J.D., et al., *Compartmentalization of adenosine 3':5'-monophosphate and adenosine 3':5'-monophosphate-dependent protein kinase in heart tissue.* J Biol Chem, 1977. **252**(11): p. 3854-61.

83.	Rybin, V.O., et al., *Differential targeting of beta -adrenergic receptor subtypes and adenylyl cyclase to cardiomyocyte caveolae. A mechanism to functionally regulate the cAMP signaling pathway.* J Biol Chem, 2000. **275**(52): p. 41447-57.

84.	DiPilato, L.M. and J. Zhang, *The role of membrane microdomains in shaping beta2-adrenergic receptor-mediated cAMP dynamics.* Mol Biosyst, 2009. **5**(8): p. 832-7.

85.	Calebiro, D., et al., *Persistent cAMP-signals triggered by internalized G-protein-coupled receptors.* PLoS Biol, 2009. **7**(8): p. e1000172.

86.	Tadevosyan, A., et al., *G protein-coupled receptor signalling in the cardiac nuclear membrane: evidence and possible roles in physiological and pathophysiological function.* J Physiol, 2012. **590**(6): p. 1313-30.

87.	Davare, M.A., et al., *A beta2 adrenergic receptor signaling complex assembled with the Ca2+ channel Cav1.2.* Science, 2001. **293**(5527): p. 98-101.

88.	Esseltine, J.L. and J.D. Scott, *AKAP signaling complexes: pointing towards the next generation of therapeutic targets?* Trends Pharmacol Sci, 2013. **34**(12): p. 648-55.

89.	Tavalin, S.J., et al., *Regulation of GluR1 by the A-kinase anchoring protein 79 (AKAP79) signaling complex shares properties with long-term depression.* J Neurosci, 2002. **22**(8): p. 3044-51.

90.	Dell'Acqua, M.L., et al., *Regulation of neuronal PKA signaling through AKAP targeting dynamics.* Eur J Cell Biol, 2006. **85**(7): p. 627-33.

91.	Dart, C. and M.L. Leyland, *Targeting of an A kinase-anchoring protein, AKAP79, to an inwardly rectifying potassium channel, Kir2.1.* J Biol Chem, 2001. **276**(23): p. 20499-505.

92.	Oliveria, S.F., M.L. Dell'Acqua, and W.A. Sather, *AKAP79/150 anchoring of calcineurin controls neuronal L-type Ca2+ channel activity and nuclear signaling.* Neuron, 2007. **55**(2): p. 261-75.

93. Brandon, N.J., et al., *A-kinase anchoring protein 79/150 facilitates the phosphorylation of GABA(A) receptors by cAMP-dependent protein kinase via selective interaction with receptor beta subunits.* Mol Cell Neurosci, 2003. **22**(1): p. 87-97.

94. Fraser, I.D., et al., *A novel lipid-anchored A-kinase Anchoring Protein facilitates cAMP-responsive membrane events.* EMBO J, 1998. **17**(8): p. 2261-72.

95. Trotter, K.W., et al., *Alternative splicing regulates the subcellular localization of A-kinase anchoring protein 18 isoforms.* J Cell Biol, 1999. **147**(7): p. 1481-92.

96. Dell'Acqua, M.L., et al., *Membrane-targeting sequences on AKAP79 bind phosphatidylinositol-4, 5-bisphosphate.* EMBO J, 1998. **17**(8): p. 2246-60.

97. Huang, L.J., et al., *NH2-Terminal targeting motifs direct dual specificity A-kinase-anchoring protein 1 (D-AKAP1) to either mitochondria or endoplasmic reticulum.* J Cell Biol, 1999. **145**(5): p. 951-9.

98. Gillingham, A.K. and S. Munro, *The PACT domain, a conserved centrosomal targeting motif in the coiled-coil proteins AKAP450 and pericentrin.* EMBO Rep, 2000. **1**(6): p. 524-9.

99. Tasken, K. and E.M. Aandahl, *Localized effects of cAMP mediated by distinct routes of protein kinase A.* Physiol Rev, 2004. **84**(1): p. 137-67.

100. Navedo, M.F. and L.F. Santana, *CaV1.2 sparklets in heart and vascular smooth muscle.* J Mol Cell Cardiol, 2013. **58**: p. 67-76.

101. Mercado, J., et al., *Local control of TRPV4 channels by AKAP150-targeted PKC in arterial smooth muscle.* J Gen Physiol, 2014. **143**(5): p. 559-75.

102. Kwon, H.B., et al., *AKAP12 regulates vascular integrity in zebrafish.* Exp Mol Med, 2012. **44**(3): p. 225-35.

103. Radeva, M.Y., et al., *PKA compartmentalization via AKAP220 and AKAP12 contributes to endothelial barrier regulation.* PLoS One, 2014. **9**(9): p. e106733.

104. Marx, S.O., et al., *Requirement of a macromolecular signaling complex for beta adrenergic receptor modulation of the KCNQ1-KCNE1 potassium channel.* Science, 2002. **295**(5554): p. 496-9.

105. Appert-Collin, A., et al., *The A-kinase anchoring protein (AKAP)-Lbc-signaling complex mediates alpha1 adrenergic receptor-induced cardiomyocyte hypertrophy.* Proc Natl Acad Sci U S A, 2007. **104**(24): p. 10140-5.

106. Dodge-Kafka, K.L., et al., *The protein kinase A anchoring protein mAKAP coordinates two integrated cAMP effector pathways.* Nature, 2005. **437**(7058): p. 574-8.

107. Ercu, M. and E. Klussmann, *Roles of A-Kinase Anchoring Proteins and Phosphodiesterases in the Cardiovascular System.* J Cardiovasc Dev Dis, 2018. **5**(1).

108. Sassi, Y. and J.S. Hulot, *Pulmonary hypertension: novel pathways and emerging therapies inhibitors of cGMP and cAMP metabolism.* Handb Exp Pharmacol, 2013. **218**: p. 513-29.

109. Bisserier, M., N. Pradhan, and L. Hadri, *Current and emerging therapeutic approaches to pulmonary hypertension.* Rev Cardiovasc Med, 2020. **21**(2): p. 163-179.

110. Drury, A.N. and A. Szent-Gyorgyi, *The physiological activity of adenine compounds with especial reference to their action upon the mammalian heart.* J Physiol, 1929. **68**(3): p. 213-37.

111. Eltzschig, H.K., *Extracellular adenosine signaling in molecular medicine.* J Mol Med (Berl), 2013. **91**(2): p. 141-6.

112. Hart, M.L., et al., *Extracellular adenosine production by ecto-5'-nucleotidase protects during murine hepatic ischemic preconditioning.* Gastroenterology, 2008. **135**(5): p. 1739-1750 e3.

113. Kohler, D., et al., *CD39/ectonucleoside triphosphate diphosphohydrolase 1 provides myocardial protection during cardiac ischemia/reperfusion injury.* Circulation, 2007. **116**(16): p. 1784-94.

114. Antonioli, L., et al., *Regulation of enteric functions by adenosine: pathophysiological and pharmacological implications.* Pharmacol Ther, 2008. **120**(3): p. 233-53.

115. Novotny, J., *[Adenosine and its role in physiology].* Cesk Fysiol, 2015. **64**(1): p. 35-44.

116. Fernanda da Rocha Lapa, S.J.M.J., Murilo Luiz Cerutti and Adair Roberto Soares Santos, *Pharmacology of Adenosine Receptors and Their Signaling Role in Immunity and Inflammation*, S.J.T. Gowder, Editor. 2014, IntechOpen.

117. Borea, P.A., et al., *Adenosine as a Multi-Signalling Guardian Angel in Human Diseases: When, Where and How Does it Exert its Protective Effects?* Trends Pharmacol Sci, 2016. **37**(6): p. 419-434.

118. Fredholm, B.B., et al., *Structure and function of adenosine receptors and their genes.* Naunyn Schmiedebergs Arch Pharmacol, 2000. **362**(4-5): p. 364-74.

119. Eltzschig, H.K., *Adenosine: an old drug newly discovered.* Anesthesiology, 2009. **111**(4): p. 904-15.

120. Borea, P.A., et al., *Pharmacology of Adenosine Receptors: The State of the Art.* Physiol Rev, 2018. **98**(3): p. 1591-1625.

121. Bechara, A., K.A. Zito, and D. van der Kooy, *Peripheral receptors mediate the aversive conditioning effects of morphine in the rat.* Pharmacol Biochem Behav, 1987. **28**(2): p. 219-25.

122. Jespers, W., et al., *Structural Mapping of Adenosine Receptor Mutations: Ligand Binding and Signaling Mechanisms.* Trends Pharmacol Sci, 2018. **39**(1): p. 75-89.

123. Peeters, M.C., et al., *The role of the second and third extracellular loops of the adenosine A1 receptor in activation and allosteric modulation.* Biochem Pharmacol, 2012. **84**(1): p. 76-87.

124. Glukhova, A., et al., *Structure of the Adenosine A1 Receptor Reveals the Basis for Subtype Selectivity.* Cell, 2017. **168**(5): p. 867-877 e13.

125. Headrick, J.P., et al., *Cardiovascular adenosine receptors: expression, actions and interactions.* Pharmacol Ther, 2013. **140**(1): p. 92-111.

126. Varani, K., et al., *Biochemical and Pharmacological Role of A1 Adenosine Receptors and Their Modulation as Novel Therapeutic Strategy.* Adv Exp Med Biol, 2017. **1051**: p. 193-232.

127. Biber, K., et al., *Adenosine A1 receptor-mediated activation of phospholipase C in cultured astrocytes depends on the level of receptor expression.* J Neurosci, 1997. **17**(13): p. 4956-64.

128. Schulte, G. and B.B. Fredholm, *Human adenosine A(1), A(2A), A(2B), and A(3) receptors expressed in Chinese hamster ovary cells all mediate the phosphorylation of extracellular-regulated kinase 1/2.* Mol Pharmacol, 2000. **58**(3): p. 477-82.

129. Ansari, H.R., et al., *A(1) adenosine receptor-mediated PKC and p42/p44 MAPK signaling in mouse coronary artery smooth muscle cells.* Am J Physiol Heart Circ Physiol, 2009. **297**(3): p. H1032-9.

130. Gessi, S., et al., *Adenosine modulates HIF-1{alpha}, VEGF, IL-8, and foam cell formation in a human model of hypoxic foam cells.* Arterioscler Thromb Vasc Biol, 2010. **30**(1): p. 90-7.

131. Merighi, S., S. Gessi, and P.A. Borea, *Adenosine Receptors: Structure, Distribution, and Signal Transduction*, in *The Adenosine Receptors*, P.A. Borea, et al., Editors. 2018, Springer International Publishing: Cham. p. 33-57.

132. de Lera Ruiz, M., Y.H. Lim, and J. Zheng, *Adenosine A2A receptor as a drug discovery target.* J Med Chem, 2014. **57**(9): p. 3623-50.

133. Jaakola, V.P. and A.P. Ijzerman, *The crystallographic structure of the human adenosine A2A receptor in a high-affinity antagonist-bound state: implications for GPCR drug screening and design.* Curr Opin Struct Biol, 2010. **20**(4): p. 401-14.

134. Gessi, S., et al., *A(2A) adenosine receptors in human peripheral blood cells.* Br J Pharmacol, 2000. **129**(1): p. 2-11.

135. Preti, D., et al., *History and perspectives of A2A adenosine receptor antagonists as potential therapeutic agents.* Med Res Rev, 2015. **35**(4): p. 790-848.

136. Giambelluca, M.S. and M. Pouliot, *Early tyrosine phosphorylation events following adenosine A2A receptor in human neutrophils: identification of regulated pathways.* J Leukoc Biol, 2017. **102**(3): p. 829-836.

137. Guinzberg, R., et al., *Newly synthesized cAMP is integrated at a membrane protein complex signalosome to ensure receptor response specificity.* FEBS J, 2017. **284**(2): p. 258-276.

138. Beukers, M.W., et al., *Why are A(2B) receptors low-affinity adenosine receptors? Mutation of Asn273 to Tyr increases affinity of human A(2B) receptor for 2-(1-Hexynyl)adenosine.* Mol Pharmacol, 2000. **58**(6): p. 1349-56.

139. Aherne, C.M., E.M. Kewley, and H.K. Eltzschig, *The resurgence of A2B adenosine receptor signaling.* Biochim Biophys Acta, 2011. **1808**(5): p. 1329-39.

140. Schiedel, A.C., et al., *The four cysteine residues in the second extracellular loop of the human adenosine A2B receptor: role in ligand binding and receptor function.* Biochem Pharmacol, 2011. **82**(4): p. 389-99.

141. Seibt, B.F., et al., *The second extracellular loop of GPCRs determines subtype-selectivity and controls efficacy as evidenced by loop exchange study at A2 adenosine receptors.* Biochem Pharmacol, 2013. **85**(9): p. 1317-29.

142. Storme, J., et al., *Molecular dissection of the human A3 adenosine receptor coupling with beta-arrestin2.* Biochem Pharmacol, 2018. **148**: p. 298-307.

143. Janes, K., et al., *A3 adenosine receptor agonist prevents the development of paclitaxel-induced neuropathic pain by modulating spinal glial-restricted redox-dependent signaling pathways.* Pain, 2014. **155**(12): p. 2560-7.

144. Gessi, S., et al., *The A3 adenosine receptor: an enigmatic player in cell biology.* Pharmacol Ther, 2008. **117**(1): p. 123-40.

145. Borea, P.A., et al., *The A3 adenosine receptor: history and perspectives.* Pharmacol Rev, 2015. **67**(1): p. 74-102.

146. Reeves, J.T., B.M. Groves, and E.K. Weir, *Adenosine and selective reduction of pulmonary vascular resistance in primary pulmonary hypertension.* Circulation, 1991. **84**(3): p. 1437-9.

147. Saadjian, A.Y., et al., *Adenosine plasma concentration in pulmonary hypertension.* Cardiovasc Res, 1999. **43**(1): p. 228-36.

148. Shryock, J.C. and L. Belardinelli, *Adenosine and adenosine receptors in the cardiovascular system: biochemistry, physiology, and pharmacology.* Am J Cardiol, 1997. **79**(12A): p. 2-10.

149. Nootens, M., et al., *Comparative acute effects of adenosine and prostacyclin in primary pulmonary hypertension.* Chest, 1995. **107**(1): p. 54-7.

150. Zhong, H., et al., *A(2B) adenosine receptors increase cytokine release by bronchial smooth muscle cells.* Am J Respir Cell Mol Biol, 2004. **30**(1): p. 118-25.

151. Varani, K., et al., *Alteration of adenosine receptors in patients with chronic obstructive pulmonary disease.* Am J Respir Crit Care Med, 2006. **173**(4): p. 398-406.

152. Shang, P., et al., *Absence of the Adenosine A2A Receptor Confers Pulmonary Arterial Hypertension Through RhoA/ROCK Signaling Pathway in Mice.* J Cardiovasc Pharmacol, 2015. **66**(6): p. 569-75.

153. Huang, X., et al., *Salidroside attenuates chronic hypoxia-induced pulmonary hypertension via adenosine A2a receptor related mitochondria-dependent apoptosis pathway.* J Mol Cell Cardiol, 2015. **82**: p. 153-66.

154. Karmouty-Quintana, H., Y. Xia, and M.R. Blackburn, *Adenosine signaling during acute and chronic disease states.* J Mol Med (Berl), 2013. **91**(2): p. 173-81.

155. Karmouty-Quintana, H., et al., *The A2B adenosine receptor modulates pulmonary hypertension associated with interstitial lung disease.* FASEB J, 2012. **26**(6): p. 2546-57.

156. Karmouty-Quintana, H., et al., *Adenosine A2B receptor and hyaluronan modulate pulmonary hypertension associated with chronic obstructive pulmonary disease.* Am J Respir Cell Mol Biol, 2013. **49**(6): p. 1038-47.

157. Hinze, A.V., et al., *Adenosine A(3) receptor-induced proliferation of primary human coronary smooth muscle cells involving the induction of early growth response genes.* J Mol Cell Cardiol, 2012. **53**(5): p. 639-45.

158. Lugnier, C., *Cyclic nucleotide phosphodiesterase (PDE) superfamily: a new target for the development of specific therapeutic agents.* Pharmacol Ther, 2006. **109**(3): p. 366-98.

159. Ahmad, F., E. Degerman, and V.C. Manganiello, *Cyclic nucleotide phosphodiesterase 3 signaling complexes.* Horm Metab Res, 2012. **44**(10): p. 776-85.

160. Francis, S.H., M.A. Blount, and J.D. Corbin, *Mammalian cyclic nucleotide phosphodiesterases: molecular mechanisms and physiological functions.* Physiol Rev, 2011. **91**(2): p. 651-90.

161. Ahmad, F., et al., *Cyclic nucleotide phosphodiesterases: important signaling modulators and therapeutic targets.* Oral Dis, 2015. **21**(1): p. e25-50.

162. Conti, M., *Phosphodiesterases and cyclic nucleotide signaling in endocrine cells.* Mol Endocrinol, 2000. **14**(9): p. 1317-27.

163. Ho, Y.S., L.M. Burden, and J.H. Hurley, *Structure of the GAF domain, a ubiquitous signaling motif and a new class of cyclic GMP receptor.* EMBO J, 2000. **19**(20): p. 5288-99.

164. Zoraghi, R., J.D. Corbin, and S.H. Francis, *Properties and functions of GAF domains in cyclic nucleotide phosphodiesterases and other proteins.* Mol Pharmacol, 2004. **65**(2): p. 267-78.

165. Omori, K. and J. Kotera, *Overview of PDEs and their regulation.* Circ Res, 2007. **100**(3): p. 309-27.

166. Bender, A.T. and J.A. Beavo, *Cyclic nucleotide phosphodiesterases: molecular regulation to clinical use.* Pharmacol Rev, 2006. **58**(3): p. 488-520.

167. Gross-Langenhoff, M., et al., *cAMP is a ligand for the tandem GAF domain of human phosphodiesterase 10 and cGMP for the tandem GAF domain of phosphodiesterase 11.* J Biol Chem, 2006. **281**(5): p. 2841-6.

168. Fujishige, K., et al., *Cloning and characterization of a novel human phosphodiesterase that hydrolyzes both cAMP and cGMP (PDE10A).* J Biol Chem, 1999. **274**(26): p. 18438-45.

169. Kotera, J., et al., *Subcellular localization of cyclic nucleotide phosphodiesterase type 10A variants, and alteration of the localization by cAMP-dependent protein kinase-dependent phosphorylation.* J Biol Chem, 2004. **279**(6): p. 4366-75.

170. Theo Schermuly, R., H. Ardeschir Ghofrani, and N. Weissmann, *Prostanoids and phosphodiesterase inhibitors in experimental pulmonary hypertension.* Curr Top Dev Biol, 2005. **67**: p. 251-84.

171. Maclean, M.R., et al., *Phosphodiesterase isoforms in the pulmonary arterial circulation of the rat: changes in pulmonary hypertension.* J Pharmacol Exp Ther, 1997. **283**(2): p. 619-24.

172. Schermuly, R.T., et al., *Phosphodiesterase 1 upregulation in pulmonary arterial hypertension: target for reverse-remodeling therapy.* Circulation, 2007. **115**(17): p. 2331-9.

173. Kelly, L.E., A. Ohlsson, and P.S. Shah, *Sildenafil for pulmonary hypertension in neonates.* Cochrane Database Syst Rev, 2017. **8**: p. CD005494.

174. Schermuly, R.T., et al., *Chronic sildenafil treatment inhibits monocrotaline-induced pulmonary hypertension in rats.* Am J Respir Crit Care Med, 2004. **169**(1): p. 39-45.

175. Pullamsetti, S., et al., *Inhaled tolafentrine reverses pulmonary vascular remodeling via inhibition of smooth muscle cell migration.* Respir Res, 2005. **6**: p. 128.

176. Phillips, P.G., et al., *cAMP phosphodiesterase inhibitors potentiate effects of prostacyclin analogs in hypoxic pulmonary vascular remodeling.* Am J Physiol Lung Cell Mol Physiol, 2005. **288**(1): p. L103-15.

177. Tian, X., et al., *Phosphodiesterase 10A upregulation contributes to pulmonary vascular remodeling.* PLoS One, 2011. **6**(4): p. e18136.

178. Barst, R.J., et al., *A comparison of continuous intravenous epoprostenol (prostacyclin) with conventional therapy for primary pulmonary hypertension.* N Engl J Med, 1996. **334**(5): p. 296-301.

179. Simonneau, G., et al., *Continuous subcutaneous infusion of treprostinil, a prostacyclin analogue, in patients with pulmonary arterial hypertension: a double-blind, randomized, placebo-controlled trial.* Am J Respir Crit Care Med, 2002. **165**(6): p. 800-4.

180. Olschewski, H., et al., *Inhaled iloprost for severe pulmonary hypertension.* N Engl J Med, 2002. **347**(5): p. 322-9.

181. Sitbon, O., et al., *Selexipag for the Treatment of Pulmonary Arterial Hypertension.* N Engl J Med, 2015. **373**(26): p. 2522-33.

182. O'Callaghan, D.S., et al., *Endothelin receptor antagonists for the treatment of pulmonary arterial hypertension.* Expert Opin Pharmacother, 2011. **12**(10): p. 1585-96.

183. Galie, N., et al., *Ambrisentan for the treatment of pulmonary arterial hypertension: results of the ambrisentan in pulmonary arterial hypertension, randomized, double-blind, placebo-controlled, multicenter, efficacy (ARIES) study 1 and 2.* Circulation, 2008. **117**(23): p. 3010-9.

184. Galie, N., et al., *Tadalafil therapy for pulmonary arterial hypertension.* Circulation, 2009. **119**(22): p. 2894-903.

185. Galie, N., et al., *Sildenafil citrate therapy for pulmonary arterial hypertension.* N Engl J Med, 2005. **353**(20): p. 2148-57.

186. Ghofrani, H.A., et al., *Riociguat for the treatment of pulmonary arterial hypertension.* N Engl J Med, 2013. **369**(4): p. 330-40.

187. Ghofrani, H.A., et al., *Riociguat for the treatment of chronic thromboembolic pulmonary hypertension.* N Engl J Med, 2013. **369**(4): p. 319-29.

188. Hoeper, M.M., et al., *A global view of pulmonary hypertension.* Lancet Respir Med, 2016. **4**(4): p. 306-22.

189. Murray, F., M.R. Maclean, and P.A. Insel, *Role of phosphodiesterases in adult-onset pulmonary arterial hypertension.* Handb Exp Pharmacol, 2011(204): p. 279-305.

190. Russwurm, C., D. Koesling, and M. Russwurm, *Phosphodiesterase 10A Is Tethered to a Synaptic Signaling Complex in Striatum.* J Biol Chem, 2015. **290**(19): p. 11936-47.

191. Maarman, G., et al., *A comprehensive review: the evolution of animal models in pulmonary hypertension research; are we there yet?* Pulm Circ, 2013. **3**(4): p. 739-56.

192. Abe, K., et al., *Formation of plexiform lesions in experimental severe pulmonary arterial hypertension.* Circulation, 2010. **121**(25): p. 2747-54.

193. Gomez-Arroyo, J.G., et al., *The monocrotaline model of pulmonary hypertension in perspective.* Am J Physiol Lung Cell Mol Physiol, 2012. **302**(4): p. L363-9.

194. Patterson, C.E., et al., *Regulation of endothelial barrier function by the cAMP-dependent protein kinase.* Endothelium, 2000. **7**(4): p. 287-308.

195. Morgado, M., et al., *Cyclic nucleotide-dependent relaxation pathways in vascular smooth muscle.* Cell Mol Life Sci, 2012. **69**(2): p. 247-66.

196. Indolfi, C., et al., *Activation of cAMP-PKA signaling in vivo inhibits smooth muscle cell proliferation induced by vascular injury.* Nat Med, 1997. **3**(7): p. 775-9.

197. Roth, B.L. and F.H. Marshall, *NOBEL 2012 Chemistry: Studies of a ubiquitous receptor family.* Nature, 2012. **492**(7427): p. 57.

198. Bos, J.L., *Epac proteins: multi-purpose cAMP targets.* Trends Biochem Sci, 2006. **31**(12): p. 680-6.

199. Matulef, K. and W.N. Zagotta, *Cyclic nucleotide-gated ion channels.* Annu Rev Cell Dev Biol, 2003. **19**: p. 23-44.

200. Gordon, D. and S.M. Schwartz, *Replication of arterial smooth muscle cells in hypertension and atherosclerosis.* Am J Cardiol, 1987. **59**(2): p. 44A-48A.

201. Campbell, J.H. and G.R. Campbell, *Endothelial cell influences on vascular smooth muscle phenotype.* Annu Rev Physiol, 1986. **48**: p. 295-306.

202. Smith, S.A., A.C. Newby, and M. Bond, *Ending Restenosis: Inhibition of Vascular Smooth Muscle Cell Proliferation by cAMP.* Cells, 2019. **8**(11).

203. Wu, Y.J., et al., *Altered S-phase kinase-associated protein-2 levels are a major mediator of cyclic nucleotide-induced inhibition of vascular smooth muscle cell proliferation.* Circ Res, 2006. **98**(9): p. 1141-50.

204. Souness, J.E., G.A. Hassall, and D.P. Parrott, *Inhibition of pig aortic smooth muscle cell DNA synthesis by selective type III and type IV cyclic AMP phosphodiesterase inhibitors.* Biochem Pharmacol, 1992. **44**(5): p. 857-66.

205. Kondo, K., et al., *Milrinone, a phosphodiesterase inhibitor, suppresses intimal thickening after photochemically induced endothelial injury in the mouse femoral artery.* Atherosclerosis, 1999. **142**(1): p. 133-8.

206. Querol-Ferrer, V., et al., *Adenosine receptors, cyclic AMP accumulation, and DNA-synthesis in aortic smooth muscle cell cultures of adult and neonatal rats.* J Cell Physiol, 1992. **151**(3): p. 555-60.

207. Dubey, R.K., et al., *Estradiol inhibits smooth muscle cell growth in part by activating the cAMP-adenosine pathway.* Hypertension, 2000. **35**(1 Pt 2): p. 262-6.

208. Gordon, E.L., et al., *The hydrolysis of extracellular adenine nucleotides by arterial smooth muscle cells. Regulation of adenosine production at the cell surface.* J Biol Chem, 1989. **264**(32): p. 18986-95.

209. Dubey, R.K., et al., *Smooth muscle cell-derived adenosine inhibits cell growth.* Hypertension, 1996. **27**(3 Pt 2): p. 766-73.

210. Dubey, R.K., et al., *Adenosine inhibits growth of rat aortic smooth muscle cells. Possible role of A2b receptor.* Hypertension, 1996. **27**(3 Pt 2): p. 786-93.

211. Wang, Y., et al., *Adenosine A(2A) receptor activation reverses hypoxiainduced rat pulmonary artery smooth muscle cell proliferation via cyclic AMPmediated inhibition of the SDF1CXC4 signaling pathway.* Int J Mol Med, 2018. **42**(1): p. 607-614.

212. Yang, D., et al., *The A2b adenosine receptor protects against vascular injury.* Proc Natl Acad Sci U S A, 2008. **105**(2): p. 792-6.

213. Xu, M.H., et al., *Absence of the adenosine A2A receptor confers pulmonary arterial hypertension and increased pulmonary vascular remodeling in mice.* J Vasc Res, 2011. **48**(2): p. 171-83.

214. Saadjian, A.Y., et al., *Plasma beta-endorphin and adenosine concentration in pulmonary hypertension.* Am J Cardiol, 2000. **85**(7): p. 858-63.

215. Alencar, A.K., et al., *Beneficial effects of a novel agonist of the adenosine A2A receptor on monocrotaline-induced pulmonary hypertension in rats.* Br J Pharmacol, 2013. **169**(5): p. 953-62.

216. Alencar, A.K., et al., *N-acylhydrazone derivative ameliorates monocrotaline-induced pulmonary hypertension through the modulation of adenosine AA2R activity.* Int J Cardiol, 2014. **173**(2): p. 154-62.

217. Karmouty-Quintana, H., et al., *Deletion of ADORA2B from myeloid cells dampens lung fibrosis and pulmonary hypertension.* FASEB J, 2015. **29**(1): p. 50-60.

218. Zhou, Y., et al., *The Adenosine A1 Receptor Antagonist DPCPX Inhibits Tumor Progression via the ERK/JNK Pathway in Renal Cell Carcinoma.* Cell Physiol Biochem, 2017. **43**(2): p. 733-742.

219. Lin, Z., et al., *Adenosine A1 receptor, a target and regulator of estrogen receptoralpha action, mediates the proliferative effects of estradiol in breast cancer.* Oncogene, 2010. **29**(8): p. 1114-22.

220. Dastjerdi, M.N., et al., *The effect of adenosine A1 receptor agonist and antagonist on p53 and caspase 3, 8, and 9 expression and apoptosis rate in MCF-7 breast cancer cell line.* Res Pharm Sci, 2016. **11**(4): p. 303-10.

221. Tawfik, H.E., et al., *Role of A1 adenosine receptors in regulation of vascular tone.* Am J Physiol Heart Circ Physiol, 2005. **288**(3): p. H1411-6.

222. Murray, F., et al., *Expression and activity of cAMP phosphodiesterase isoforms in pulmonary artery smooth muscle cells from patients with pulmonary hypertension: role for PDE1.* Am J Physiol Lung Cell Mol Physiol, 2007. **292**(1): p. L294-303.

223. Wharton, J., et al., *Antiproliferative effects of phosphodiesterase type 5 inhibition in human pulmonary artery cells.* Am J Respir Crit Care Med, 2005. **172**(1): p. 105-13.

224. Pullamsetti, S.S., et al., *cAMP phosphodiesterase inhibitors increases nitric oxide production by modulating dimethylarginine dimethylaminohydrolases.* Circulation, 2011. **123**(11): p. 1194-204.

225. Growcott, E.J., et al., *Phosphodiesterase type 4 expression and anti-proliferative effects in human pulmonary artery smooth muscle cells.* Respir Res, 2006. **7**: p. 9.

226. Rochais, F., et al., *A specific pattern of phosphodiesterases controls the cAMP signals generated by different Gs-coupled receptors in adult rat ventricular myocytes.* Circ Res, 2006. **98**(8): p. 1081-8.

227. Adderley, S.P., et al., *Iloprost- and isoproterenol-induced increases in cAMP are regulated by different phosphodiesterases in erythrocytes of both rabbits and humans.* Am J Physiol Heart Circ Physiol, 2009. **296**(5): p. H1617-24.

228. Hanson, M.S., et al., *Phosphodiesterase 3 is present in rabbit and human erythrocytes and its inhibition potentiates iloprost-induced increases in cAMP.* Am J Physiol Heart Circ Physiol, 2008. **295**(2): p. H786-93.

229. Adderley, S.P., et al., *Regulation of cAMP by phosphodiesterases in erythrocytes.* Pharmacol Rep, 2010. **62**(3): p. 475-82.

230. Fujitani, K., et al., *Clinical evaluation on combined administration of oral prostacyclin analogue beraprost and phosphodiesterase inhibitor cilostazol.* Pharmacol Res, 1995. **31**(2): p. 121-5.

231. Houslay, M.D. and G. Milligan, *Tailoring cAMP-signalling responses through isoform multiplicity.* Trends Biochem Sci, 1997. **22**(6): p. 217-24.

232. Wong, W. and J.D. Scott, *AKAP signalling complexes: focal points in space and time.* Nat Rev Mol Cell Biol, 2004. **5**(12): p. 959-70.

233. Newlon, M.G., et al., *The A-kinase anchoring domain of type IIalpha cAMP-dependent protein kinase is highly helical.* J Biol Chem, 1997. **272**(38): p. 23637-44.

234. Malbon, C.C., J. Tao, and H.Y. Wang, *AKAPs (A-kinase anchoring proteins) and molecules that compose their G-protein-coupled receptor signalling complexes.* Biochem J, 2004. **379**(Pt 1): p. 1-9.

235. Coghlan, V.M., et al., *Association of protein kinase A and protein phosphatase 2B with a common anchoring protein.* Science, 1995. **267**(5194): p. 108-11.

236. Faux, M.C. and J.D. Scott, *Molecular glue: kinase anchoring and scaffold proteins.* Cell, 1996. **85**(1): p. 9-12.

237. Faux, M.C., et al., *Mechanism of A-kinase-anchoring protein 79 (AKAP79) and protein kinase C interaction.* Biochem J, 1999. **343 Pt 2**: p. 443-52.

238. Jo, I., et al., *AQP2 is a substrate for endogenous PP2B activity within an inner medullary AKAP-signaling complex.* Am J Physiol Renal Physiol, 2001. **281**(5): p. F958-65.

239. Fraser, I.D. and J.D. Scott, *Modulation of ion channels: a "current" view of AKAPs.* Neuron, 1999. **23**(3): p. 423-6.

240. Penny, C.J. and M.G. Gold, *Mechanisms for localising calcineurin and CaMKII in dendritic spines.* Cell Signal, 2018. **49**: p. 46-58.

241. Navedo, M.F., et al., *AKAP150 is required for stuttering persistent Ca2+ sparklets and angiotensin II-induced hypertension.* Circ Res, 2008. **102**(2): p. e1-e11.

242. Nystoriak, M.A., et al., *AKAP150 contributes to enhanced vascular tone by facilitating large-conductance Ca2+-activated K+ channel remodeling in hyperglycemia and diabetes mellitus.* Circ Res, 2014. **114**(4): p. 607-15.

243. Efendiev, R., et al., *AKAP79 interacts with multiple adenylyl cyclase (AC) isoforms and scaffolds AC5 and -6 to alpha-amino-3-hydroxyl-5-methyl-4-isoxazole-propionate (AMPA) receptors.* J Biol Chem, 2010. **285**(19): p. 14450-8.

244. Jourdan, K.B., et al., *Characterization of adenylyl cyclase isoforms in rat peripheral pulmonary arteries.* Am J Physiol Lung Cell Mol Physiol, 2001. **280**(6): p. L1359-69.

245. Indolfi, C., et al., *Membrane-bound protein kinase A inhibits smooth muscle cell proliferation in vitro and in vivo by amplifying cAMP-protein kinase A signals.* Circ Res, 2001. **88**(3): p. 319-24.

246. Taraseviciene-Stewart, L., et al., *Inhibition of the VEGF receptor 2 combined with chronic hypoxia causes cell death-dependent pulmonary endothelial cell proliferation and severe pulmonary hypertension.* FASEB J, 2001. **15**(2): p. 427-38.

247. Kamely, M., et al., *Upregulation of SERT and ADORA1 in broilers with acute right ventricular failure.* Res Vet Sci, 2019. **125**: p. 397-400.

248. Koeppen, M., T. Eckle, and H.K. Eltzschig, *Selective deletion of the A1 adenosine receptor abolishes heart-rate slowing effects of intravascular adenosine in vivo.* PLoS One, 2009. **4**(8): p. e6784.

249. Chen, S., et al., *A Novel Role of Cyclic Nucleotide Phosphodiesterase 10A in Pathological Cardiac Remodeling and Dysfunction.* Circulation, 2020. **141**(3): p. 217-233.

250. Kocer, S.S., H.Y. Wang, and C.C. Malbon, *"Shaping" of cell signaling via AKAP-tethered PDE4D: Probing with AKAR2-AKAP5 biosensor.* J Mol Signal, 2012. **7**(1): p. 4.

251. Nickel, N.P., et al., *Elafin Reverses Pulmonary Hypertension via Caveolin-1-Dependent Bone Morphogenetic Protein Signaling.* Am J Respir Crit Care Med, 2015. **191**(11): p. 1273-86.

9 APPENDIX

Table 9 1. Sequence of siRNAs

siRNA	Sequence (5'-3')	Company
SCR_SMARTpool	1) UGGUUUACAUGUCGACUAA 2) UGGUUUACAUGUUGUGUGA 3) UGGUUUACAUGUUUUCUGA 4) UGGUUUACAUGUUUUCCUA	Dharmacon
ADORA1_SMARTpool	1) GGUAGGUGCUGGCCUCAAA 2) GGAGUCUGCUUGUCUUAGA 3) CAAGAUCCCUCUCCGGUAC 4) AUCCAGAAGUUCCGCGUCA	Dharmacon
PDE10A_SMARTpool	1) GAACUAAACAGCUAUAUAG 2) GUAAUUGGUUUGAUGAUGA 3) GAACAAGGAGUUAUAUUCA 4) GCAGAGGCCUUGCCAAACA	Dharmacon

Table 9 2. List of qPCR primers

Gene	Species	Sequences (5'-3')	Annealing Temperature (°C)
B2M	Human	F: AGATGAGTATGCCTGCCGTG R: TCATCCAATCCAAATGCGGC	60
ADORA1	Human	F: GGCAGGTGAGGAAGGGTTTA R: CTGCCTGACTGTTCTGTCCA	60
ADORA2a	Human	F: GCGCAGTATGAGAGGGCTTA R: GAGGCACCCCAGCACTATC	60
ADORA2b	Human	F: ATACCTGGCCATCTGTGTCC R: GAGTCAATCCGATGCCAAAG	60
PBGD	Human	F: CAGGAGTCAGACTGTAGG R: ACTCTCATCTTTGGGCTGTTTTC	58
PDE10A	Human	F: CTCCGACATGGAAGATGGAC R: CCCCCATCTCTTCAACTGTAA	60
AKAP5	Human	F: GACTGCAGCATCAAAGTCCA R: CATCTTTCCGTGAGATGCCT	60
NT5E	Human	F: ACTTCATGAACGCCCTGC R: TTGGAAATTTGGCCTCTTTG	60

Genomic DNA conrol (GAPDH intron)	Human	F: CCCACACACATGCACTTACC R: GCCCACCCCTTCTCTAAGTC	60

Table 9 3. List of Primary antibodies

Antibody	Source	Dilution (WB)	Dilution (IHC/ICC/PLA)	Concentration (IP)	Company
ADORA1	rabbit	1:1000	1:200	10µg	Abcam
	mouse		1:200		Santa Cruz Biotechnology
PDE10A	Goat	1:1000	1:100		Santa Cruz Biotechnology
	Rabbit	1:1000			Abcam
AKAP5	mouse	1:1000	1:200	10 µg	BD Transduction Laboratories™
PDE1	rabbit		1:200		Abcam
PDE3	rabbit		1:200		Abcam
PDE4	rabbit		1:200		Abcam
CD73	mouse	1:1000			Santa Cruz Biotechnology
CREB	rabbit	1:1000			Cell Signaling Technology

P-CREB (Ser 133)	rabbit	1:500			Cell Signaling Technology
p27	rabbit	1:1000			Abcam
a-SMA	mouse	1:700			Sigma Aldrich
Von Willebrand factor	mouse	1:900			Agilent

Table 9 4. List of Secondary antibodies

Antibody	Dilution (WB)	Dilution (IHC/ICC/PLA)	Company
Alex Flour 488 anti-rabbit IgG		1:500	Life Technologies
Alex Flour 568 anti-rabbit IgG		1:500	Life Technologies
Alex Flour 488 anti-mouse IgG		1:500	Life Technologies
Alex Flour 568 anti-mouse IgG		1:500	Life Technologies
Alex Flour 647anti-goat IgG		1:200	Abcam
HRP conjugated anti-rabbit IgG	1:40000		Sigma Aldrich
HRP conjugated anti-mouse IgG	1:30000		Sigma Aldrich
HRP conjugated anti-Goat IgG	1:2000		R&D

RESUME

Der Lebenslauf wurde aus der elektronischen Version der Arbeit entfernt.

The curriculum vitae was removed from the electronic version of the paper.

ERKLARUNG ZUR DISSERTATION

"Hiermit erkläre ich, dass ich die vorliegende Arbeit selbständig und ohne unzulässige Hilfe oder Benutzung anderer als der angegebenen Hilfsmittel angefertigt habe. Alle Textstellen, die wörtlich oder sinngemäß aus veröffentlichten oder nichtveröffentlichten Schriften entnommen sind, und alle Angaben, die auf mündlichen Auskünften beruhen, sind als solche kenntlich gemacht. Bei den von mir durchgeführten und in der Dissertation erwähnten Untersuchungen habe ich die Grundsätze guter wissenschaftlicher Praxis, wie sie in der „Satzung der JustusLiebig-Universität Gießen zur Sicherung guter wissenschaftlicher Praxis" niedergelegt sind, eingehalten sowie ethische, datenschutzrechtliche und tierschutzrechtliche Grundsätze befolgt. Ich versichere, dass Dritte von mir weder unmittelbar noch mittelbar geldwerte Leistungen für Arbeiten erhalten haben, die im Zusammenhang mit dem Inhalt der vorgelegten Dissertation stehen, oder habe diese nachstehend spezifiziert. Die vorgelegte Arbeit wurde weder im Inland noch im Ausland in gleicher oder ähnlicher Form einer anderen Prüfungsbehörde zum Zweck einer Promotion oder eines anderen Prüfungsverfahrens vorgelegt. Alles aus anderen Quellen und von anderen Personen übernommene Material, das in der Arbeit verwendet wurde oder auf das direkt Bezug genommen wird, wurde als solches kenntlich gemacht. Insbesondere wurden alle Personen genannt, die direkt und indirekt an der Entstehung der vorliegenden Arbeit beteiligt waren. Mit der Überprüfung meiner Arbeit durch eine Plagiatserkennungssoftware bzw. ein internetbasiertes Softwareprogramm erkläre ich mich einverstanden"

_____   _____

Ort, Datum   Unterschrift

ACKNOWLEDGEMENTS

I am ever grateful to my parents, **Valasarajan and Bindhu**, for their unconditional love and care without which none of this would be a reality. I would like to thank my best half and my pillar of support **Swathi Veeroju** for always being there for me throughout this journey. Last but not least, I am thankful to my brothers and my ever loving family for their encouragement and support every single day.

Thank you all for your support

Chanil Valasarajan